UNIVERSITY OF TARTU

Faculty of Science and Technology

Institute of Bioengineering

Brayan Stiveen Rodriguez Morales

Molecular Crosstalk at the Endometrium-Embryo Interface

Master's Thesis (30 ECTS)

Curriculum Bioengineering

Supervisor(s):

Senior Researcher, PhD Alberto Sola Leyva

Senior Researcher, PhD Amruta Pathare

Junior Research Fellow, Apostol Apostolov

Tartu 2026

Molecular Crosstalk at the Endometrium-Embryo Interface

Abstract

Embryo implantation relies on tightly regulated molecular interactions between the endometrium and the developing embryo, however the relative contributions of each remain poorly understood. The main objective of this Master Thesis is to understand the molecular and genomic crosstalk between endometrium and embryo duri ng implantation using a human *in vitro* model consisting of endometrial organoids derived from healthy fertile women and blastoids (embryo-like structures). To unravel the maternal and embryonic contributions, *bulk* RNA sequencing was integrated with genotyping, and a workflow was developed to assign the origin of expressed variants. Differential expression analysis identified 264 upregulated and 172 downregulated genes associated with blastoid attachment under hormonally induced conditions. Integration of variant profiles enabled classification of the assignment of gene expression to maternal, embryonic, or shared origin, revealing key pathways related to immune response, cell adhesion, and extracellular matrix remodeling. Consistently origin-assigned genes across donor-derived models were identified from implantation-related interactions. These findings demonstrate that integration of genomic data enhances the resolution of embryo-endometrium crosstalk and provides novel insights into mechanisms underlying implantation success and failure.

Keywords

Human embryo implantation, endometrium, blastoid, RNA sequencing, genotyping.

CERCS: B570 Obstetrics, gynecology, andrology, reproduction, sexuality

Institute name: Celvia CC AS; University of Tartu

Research group: Prof. Andres Salumets Research group

Molekulaarne dialoog endomeetriumi ja embrüo piirialal

Lühikokkuvõte

Embrüo implantatsioon sõltub rangelt reguleeritud molekulaarsetest interaktsioonidest endomeetriumi ja areneva embrüo vahel, kuid nende osapoolte suhteline panus on siiani puudulikult mõistetud. Käesoleva magistritöö peamine eesmärk on uurida endomeetriumi ja embrüo vahelist molekulaarset ja genoomset seotust implantatsiooni ajal, kasutades inimese *in*

vitro mudelit, mis koosneb tervetelt viljakatelt naistelt pärinevatest endomeetriumi organoididest ja blastoididest (embrüolaadsed struktuurid).

Emapoolse ja embrüonaalse panuse eristamiseks integreeriti RNA sekveneerimine genotüüpimisega ja töötati välja töövoog ekspresseeritud variantide päritolu määramiseks. Diferentsiaalse ekspressiooni analüüs tuvastas hormonaalselt indutseeritud tingimustes blastoidi kinnitumisega seotud 264 ülesreguleeritud ja 172 allareguleeritud geeni.

Variantide profiilide integreerimine võimaldas geeniekspressiooni klassifitseerimist emapoolse, embrüonaalse või jagatud päritolu järgi ning tõi esile võtmerajad, mis on seotud immuunvastuse, rakkude adhesiooni ja rakuvälise maatriksi ümberkujunemisega. Implantatsiooniga seotud interaktsioonide põhjal tuvastati doonorilt saadud mudelites järjepidevalt sama päritoluga geene.

Tulemused näitavad, et genoomsete andmete integreerimine parandab embrüo ja endomeetriumi vahelise molekulaarse kommunikatsiooni mõistmist ning annab uusi teadmisi implantatsiooni õnnestumise ja ebaõnnestumise aluseks olevate mehhanismide kohta.

Võtmesõnad:

Inimese embrüo implantatsioon, endomeetrium, blastoid, RNA sekveneerimine, genotüüpimine.

CERCS: B570 Sünnitusabi, günekoloogia, androloogia, paljunemine, seksuaalsus

TABLE OF CONTENTS

TERMS, ABBREVIATIONS AND NOTATIONS **5**

INTRODUCTION **6**

1 LITERATURE REVIEW **9**

1.1 Endometrial preparation and early embryo development *9*

1.2 Endometrial-embryonic crosstalk during implantation *10*

1.3 In vitro implantation *12*

2 THE AIMS OF THE THESIS **15**

2.1 Research question *15*

2.2 General objective *15*

2.3 Specific objectives *15*

3 MATERIALS AND METHODS **16**

3.1 Implantation model *16*

3.2 Differential expression analysis *17*

3.3 DNA global screening array genotyping *19*

3.4 RNA variant calling and imputation *20*

3.5 Origin assignment *21*

3.6 Integration with differential expression analysis *22*

3.7 Biological interpretation *23*

4 RESULTS **25**

4.1 Differentially expressed genes recapitulate the receptive endometrium and implantation. *25*

4.2 Comparable number of variants across RNA and DNA data *28*

4.3 Origin assignment allowed biologically coherent pathways of implantation biology *31*

5 DISCUSSION **33**

SUMMARY **37**

REFERENCES **39**

NON-EXCLUSIVE LICENCE TO REPRODUCE THESIS AND MAKE THESIS PUBLIC **51**

APPENDICES **52**

TERMS, ABBREVIATIONS AND NOTATIONS

ART = Assisted Reproductive Technology

hCG = Human Chorionic Gonadotropin

DGE = Differential Gene Expression

EEO = Epithelial Endometrial Organoid

EB = Endometrial Biopsy

FEP = Functional Enrichment and Pathway

hPSC = Human Pluripotent Stem Cell

IVF = In vitro Fertilization

OFEL = Open-face Endometrial Layer

SNP = Single Nucleotide Polymorphism

WOI = Window of Implantation

INTRODUCTION

Infertility affects millions of individuals worldwide and represents a major challenge in reproductive medicine. Approximately one in five couples experience infertility, with prevalence rates reaching up to 25% in developed countries (Dabbagh Rezaeiye et al., 2022). Male factors are solely responsible in about 10% of cases and affects an estimated 56 million men globally (Jatan et al., 2026; Kikas et al., 2026). However male and female causes contribute equally to infertility cases (T. Li et al., 2026). In addition, natural fecundity in humans is relatively low, with the probability of achieving pregnancy ranging from 15% to 25%, declining markedly with advancing maternal age (Madjunkov et al., 2026). In this context, assisted reproductive technologies (ART) have been developed to overcome these limitations and improve reproductive outcomes.

Advances in the field of ART have provided new opportunities for individuals facing medical, emotional and financial challenges associated with infertility (Graham et al., 2023). Since the first reported birth after *in vitro* fertilization (IVF) and embryo transfer in 1978 (Steptoe & Edwards, 1978), IVF has been used to bypass couples' infertility (van Loendersloot et al., 2010). Between 1997 and 2020, more than 13 million ART treatment cycles resulted in the birth of over 2.6 million infants, highlighting the major clinical impact of these technologies for individuals experiencing fertility complications (Gliozheni et al., 2025). Nevertheless, the average pregnancy rate per ART cycle remains between 30 to 40%, and more than half of women undergoing IVF still fail to conceive (Farzizadeh et al., 2026).

In fact, defective implantation is estimated to account for approximately 75% of pregnancy losses in these clinical scenarios (Conforti et al., 2022). Lai et al. (2022) stated that abnormal expressions of endometrial receptivity and immune regulation are associated with such implantation failure. This therapeutic bottleneck highlights that achieving a successful pregnancy largely depends on efficient embryo implantation, a highly molecular coordinated process that requires embryos with developmental potential and a receptive endometrium (Chen et al., 2022). Ultimately, synchronization and the implantation into the endometrium represent the most finely regulated process that leads to a successful pregnancy.

Recent studies have highlighted the importance of exploring embryo-endometrium molecular crosstalk and developing personalized approaches for predicting implantation success (Bulletti et al., 2025). However, the mechanisms underlying early implantation remain poorly understood, largely because these developmental stages are difficult to access in humans (Siriwardena & Boroviak, 2022). Further investigation of the early molecular interactions

between the embryo and the endometrium is essential for understanding human implantation (Idelevich & Vilella, 2020). Although animal models have contributed substantially to reproductive research, species-specific differences limit the direct translation of these findings to human implantation biology (Dutta & Sengupta, 2018; Fischer et al., 2012). Consequently, human *in vitro* models have become increasingly important for studying implantation events under ethically acceptable conditions (Siriwardena & Boroviak, 2022).

To investigate these physiological processes, *in vitro* models have become indispensable tools. For instance, while key mechanisms have been described, researchers like Buck et al. (2012) elucidated that the endometrium loses intercellular junctions and desmosomes in preparation for trophoblast invasion, while emphasizing the need to validate this concept *in vitro* human endometrial epithelial cells. Through these *in vitro* models, studies have successfully highlighted the cell-to-cell communication occurring through direct contact, secretion and uptake of soluble chemical factors, and exchange of extracellular vesicles (Moreno et al., 2023). In these systems, Weimar et al. (2012) showed that decidualized endometrial stromal cells respond to embryo quality; in response to a low-quality embryo, endometrium downregulates the production of key pro-implantation cytokines thus inhibiting its migratory response. Meanwhile, trophoblast-like-cell derived extracellular vesicles induce distinct transcriptomic changes in endometrial cells, leading to extracellular matrix remodeling and G protein-coupled receptor-mediated signaling (Godakumara et al., 2021). To systematically validate and examine these delicate communication pathways, the International Society for Stem Cell Research recognizes the implementation of these advanced *in vitro* platforms as robust and ethical alternatives for human embryo research (Clark et al., 2021).

In alignment with these ethical frameworks, endometrial organoid cultures have been developed to recapitulate the molecular and functional characteristics of the endometrium. These organoids represent a reliable, chemically defined, long-term culture of endometrial glands that recapitulates the molecular and functional characteristics of their cells of origin (Turco et al., 2017). Simultaneously, to represent the embryonic counterpart without ethical constraints, blastoid models resembling the human blastocyst have been established; these structures efficiently generate lineage-specific cell types according to the pace and sequence of blastocyst development and produce cells that transcriptionally reflect the blastocyst (Heidari Khoei et al., 2023).

Blastoid studies during implantation have revealed diverse gene expression patterns, including genes involved in trophoblast migration and extracellular remodeling (L. Yu et al., 2023). David et al. (2023) stated that blastoids may improve IVF outcomes by enabling a better understanding

of the molecular regulation of the blastocyst-endometrium interactions. By leveraging both systems, contemporary research has successfully combined these components; specifically, blastoids attach to a hormonally stimulated open-face endometrial layer (OFEL) recapitulating aspects of embryo implantation and post-implantation development, while representing an ethical opportunity (Heidari Khoei et al., 2023). Integrated embryo models offer new opportunities to visualize dynamic developmental events and to investigate the underlying molecular mechanisms through experimental intervention (Thowfeequ et al., 2025). Furthermore, these systems are well-suited for live-cell imaging and genetic analyses, enabling the dissection of the contributions of different cellular components during the implantation period (Rugg-Gunn et al., 2023). Although several pathways and genes involved in this molecular crosstalk have been identified, it remains unclear whether their origin is the blastocyst, the endometrium, or both (Yang, 2025). Future progress in implantation research will require collaborative interdisciplinary efforts aimed to develop integrated models that refine current theories of lineage specification.

In summary, there is a need to dissect maternal and embryonic contributions during implantation using *in vitro* models. In this study, early interactions between blastoids and endometrial epithelial cells will be investigated through genomic analysis of a 2D monolayer OFEL human implantation model. Furthermore, DNA array genotyping will be used to assign the cellular origin of differentially expressed genes, enabling the identification of single nucleotides polymorphisms (SNPs) and the discrimination of maternal and embryonic contributions during implantation-like events.

1 LITERATURE REVIEW

1.1 Endometrial preparation and early embryo development

Embryo implantation is a precisely coordinated process during which the blastocyst apposes, attaches and invades the endometrium, the inner layer of the uterus, enabling embryo growth and development. Understanding the molecular crosstalk of maternal-embryonic interface is fundamental for understanding human reproduction, as it may help identify causes of infertility and minimize adverse maternal and neonatal outcomes during pregnancy (Moreno et al., 2023).

During the normal menstrual cycle, the development of a competent follicle, ovulation, and shedding of the endometrial lining occur at regular intervals in the absence of pregnancy. During the luteal phase, the corpus luteum secretes progesterone and small amounts of estradiol under the influence of luteinizing hormone (Itriyeva, 2022). Meanwhile, the endometrium differentiates from a proliferative to a secretory lining, establishing the conditions necessary for a potential pregnancy and characterizing the secretory phase. Progesterone promotes the development of complex glands, increases glycogen accumulation as energy source, and increases the surface area of the spiral arteries (Thiyagarajan et al., 2026). The remodeled endometrium is therefore prepared for implantation during a period known as the window of implantation (WOI). The WOI allows blastocyst attachment and initiates the final stages of stromal decidualization, which regulate trophoblast invasion and the subsequent placentation. During early pregnancy, progesterone levels remain elevated, playing a pivotal role in maintaining decidualization during the first week (Moreno et al., 2023).

Endometrial receptivity is primarily regulated by the ovarian hormones estrogen and progesterone, which activate crucial downstream signaling pathways including focal adhesion, cAMP signaling, and RAP1 signaling to establish a receptive uterine environment (S.-L. Yu et al., 2021). This highly regulated receptive state defines the WOI, which lasts approximately 6 to 10 days after ovulation (Keleş et al., 2023). Understanding the precise timing and molecular signature of the endometrial WOI is critical for optimizing embryo transfer in clinical settings. Accordingly, transcriptomic approaches have enabled comparative analyses between receptive and non-receptive endometria, providing molecular markers to identify structural variations in receptivity (Poh et al., 2023).

Human blastocyst development proceeds in a highly regulated temporal and sequential manner. A functionally developed blastocyst is formed 6-7 days after fertilization, and comprises three distinct cell lineages: trophectoderm, epiblast and hypoblast (Rossant & Tam, 2022). During the first 4 days, the trophectoderm is established and subsequently develops into an epithelial

cyst containing a fluid-filled cavity, while the inner cell mass forms a cluster of cells localized to one side of the trophectoderm (Radley et al., 2023).

Next, the inner cell mass differentiates into the epiblast and hypoblast. Based on their spatial relationship to the epiblast, the trophectoderm segregates into polar and mural regions, establishing the embryonic-abembryonic axis (Radley et al., 2023). This axis organizes the cellular functions required for implantation. Its formation involves signaling from the epiblast that promotes the local maturation of the polar trophectoderm, which subsequently acquires the capacity to adhere to the uterine lining (Kagawa et al., 2022).

1.2 Endometrial-embryonic crosstalk during implantation

The reproductive process can be viewed as a coordinated sequence of endocrine and cellular events initiated when granulosa cells increase estrogen production to a critical threshold, thereby inducing a surge in luteinizing hormone (LH). This surge activates a complex molecular cascade that drives ovulation and completes the final stages of oocyte maturation during each menstrual cycle (Moreno et al., 2023). With advancing maternal age, defects progressively accumulate in the molecular machinery responsible for chromosome cohesion, leading to abnormal chromosomal segregation. This process is considered a major contributor to the increased incidence of aneuploidy in oocytes from women of advanced maternal age, with these abnormalities subsequently transmitted to daughter cells during cell division.

Embryo implantation rates vary widely with female age. While younger women exhibit implantation rates close to 60%, women older than 42 years old show embryo implantation rates of approximately 25% (Bulletti et al., 2025). Age, however, is not the only determinant of implantation success, as the endometrial immunophenotype plays a key role in regulating proliferation, maturation, and differentiation processes required to achieve endometrial receptivity (Anoshko et al., 2023).

To fully characterize this receptive state beyond morphology, high-throughput molecular tools have become indispensable. Microarray-based transcriptomic studies have consistently demonstrated that the endometrial receptivity can be molecularly subclassified into phase-specific profiles (Ruiz-Alonso et al., 2012). In 2011, the endometrial receptivity array was first introduced as a tool to define the specific transcriptomic signature of the human endometrium (Díaz-Gimeno et al., 2011). The transcriptomic analysis focusses on 238 genes, together with a computational predictor, to assess the receptivity status of an endometrial sample and to determine the personalized WOI for a given patient (Rubin et al., 2023). Building upon these findings, subsequent RNA-seq elucidated the transcriptome comparison of pre-receptive and

receptive human endometrium showcasing genes that may have significance during implantation (Hu et al., 2014). Ultimately, these efforts identified an endometrial receptivity meta-signature of the endometrium composes 57 genes associated to immune response and complement cascade, and highlight the involvement of exosomes (Altmäe et al., 2017).

Further expanding on this temporal regulation, Wang et al. (2020) showed that the WOI is characterized by an abrupt and strong transcriptomic activation in unciliated epithelia, followed by a continuous transition of stromal fibroblasts. Biomarkers of receptivity have therefore been used to study endometrial receptivity in a targeted manner, highlighting the role of the endometrium in the optimization of IVF procedures (Opuchlik et al., 2025). The transcriptomic signature of the endometrial WOI has linked genes involved in cell cycle regulation, extracellular matrix remodeling, vascular development, differentiation, metabolism, and immune responses to early pregnancy loss during the late receptive signature (Díaz-Gimeno et al., 2017).

Embryo development requires the tightly coordinated regulation of meiotic division, the acquisition of oocyte cytoplasmic competence to support early embryonic development, successful fertilization, and pronuclei syngamy (Moreno et al., 2023). Prior to implantation, both the trophectoderm and the uterine luminal epithelium secrete a diverse array of signaling molecules that prime the outer blastocyst layer for adhesion and invasion. At the same time, embryonic secretions enhance endometrium receptivity and promote decidualization (Siriwardena & Boroviak, 2022). Cytokines, for example, play a central role in embryo-maternal communication, mediating bidirectional signaling between the embryo and the endometrium. These cytokines are expressed together with extracellular matrix proteins and endothelial-derived factors that may contribute to the recruitment of immune cells (Marečková et al., 2024).

Among these embryonic secretions, human chorionic gonadotropin (hCG) serves as the primary and earliest signal targeted at the maternal environment. In normal pregnancies, blood levels of hCG increase exponentially following successful implantation, making this hormone widely utilized to diagnose pregnancy and monitor early pregnancy loss (Skogler et al., 2023). Beyond its diagnostic value, hCG supports the maintenance of the corpus luteum, which in turn sustains the progesterone production required to preserve the endometrium during early pregnancy. Multiple forms of hCG are present in both serum and urine, making the hormone readily detectable through standard urine-based pregnancy tests (Betz & Fane, 2026).

At the cellular level, the response of endometrial epithelial cells to embryonic hCG and prostaglandins is mediated through the LH/CG receptor and the MAPK signaling pathway. In

addition, while cAMP production is absent in endometrial epithelial cells, it actively occurs in stromal cells. These findings suggest that the endometrial epithelial cells act as mediators of the stromal response to embryonic hCG (Su & Fazleabas, 2015). Decidualization occurs as part of this coordinated response, involving the sequential reprogramming of processes related to extracellular matrix organization, cell adhesion, cytoskeletal organization, signal transduction, metabolism, stress responses, cell cycle progression, differentiation, and apoptosis (Gellersen et al., 2007).

Following this biochemical preparation, the physical phase of early embryonic attachment begins, driven by signaling molecules that induce coordinated structural and functional adjustments in both the embryo and the endometrium. For instance, the WNT signaling plays a vital role in regulating endometrial remodeling during these initial phases (Tepekoy et al., 2015). Historically, much of our foundational knowledge regarding these uterine interactions and trophoblast invasion has relied on animal models, particularly non-human primates and mice (Su & Fazleabas, 2015). Although these comparative approaches have contributed substantially to understanding general reproductive biology, species-specific variations in placentation, uterine anatomy, and developmental timing severely limit the direct translation of animal findings to human implantation physiology (Su & Fazleabas, 2015). Crucially, while mammalian animal models typically display highly efficient implantation rates, humans present a uniquely low natural fecundity, with clinical implantation rates for euploid embryos averaging only 50-65% (Moreno et al., 2023). This biological discrepancy underscores that comparative animal literature cannot fully resolve the molecular complexities of the human maternal-fetal interface, emphasizing the critical need to develop human-centric *in vitro* systems capable of modeling these dynamics.

1.3 In vitro implantation

To establish these human-centric systems, researchers have focused on developing accurate cellular counterparts for both the embryo and the maternal endometrium. Human blastocyst-like structures, known as blastoids, are transcriptionally similar to human blastocysts and therefore serve as valuable models for studying early human development and implantation processes (Kagawa et al., 2022). These structures generate the three canonical embryonic lineages with nearly 90% efficiency, making them among the closest *in vitro* models to the human embryo (Luijkx et al., 2022). While *in vitro* embryo models enable meaningful comparisons that recapitulate aspects of early embryogenesis, it is important to note that blastoid models lack organismal developmental potential and do not result from fertilization;

nonetheless, they provide important opportunities for studying blastocyst formation and implantation mechanisms (Liu & Polo, 2024).

To overcome the limitations of traditional, non-polarized platforms, modern bioengineering approaches have driven the development of complex three-dimensional (3D) *in vitro* culture systems that accurately recapitulate multiple uterine compartments, including luminal, glandular, and stromal components (Song et al., 2026). Recent structural advancements have demonstrated that these advanced 3D configurations efficiently support human embryo adhesion, initial trophoblast invasion, and early lineage differentiation within a highly controlled environment (Molè et al., 2026; Song et al., 2026). By integrating single-cell RNA sequencing and ligand-receptor interaction analyses, these high-fidelity models have begun to map key signaling pathways governing cellular migration, extracellular matrix remodeling, and pro-survival crosstalk during post-implantation-like stages, including early placental development (Molè et al., 2026; Song et al., 2026). Consequently, these multi-compartment systems offer unprecedented opportunities to analyze the spatiotemporal regulation of human reproduction while addressing the ethical constraints associated with native tissue research.

The clinical imperative to understand these processes is underscored by studies on embryo implantation which have demonstrated that targeting DNA variants associated with recurrent implantation failure during IVF procedures can result in successful fertilization and development of chromosomally normal blastocysts (Capalbo et al., 2021; Sang et al., 2018). To map these crucial genetic factors, characterizing the cellular communication within these platforms has been heavily accelerated by high-throughput technologies. Multi-omic sequencing methods have paved the way for deciphering highly complex yet precisely coordinated epigenomic reprogramming events, as well as their impact on gene expression during early human embryonic development (L. Li et al., 2018). For instance, integrative transcriptomic analyses of epithelial and stromal cells isolated from pre-receptive and receptive endometrial samples, combined with trophectoderm transcriptomic data, have revealed complex embryo-maternal signaling networks governing cellular adhesion, immune signaling, and tissue remodeling (Koel et al., 2022). In particular, protein-protein interaction network analyses identified integrins, galectins, osteopontin, and basigin as central nodes in this embryo-maternal communication, highlighting their potential roles in blastocyst adhesion and implantation initiation. Collectively, these findings support the concept that successful implantation depends on the highly coordinated and specific molecular communication between the endometrial and embryonic compartments.

Despite the morphological accuracy achieved by these contemporary 3D co-culture platforms, deciphering their transcriptomic profiles introduces a significant technical bottleneck. When performing *bulk* RNA sequencing (*bulk* RNA-seq) on a shared interface containing both endometrial cells and embryo-like structures, the raw data inevitably represents a mixed transcriptomic pool. Standard computational pipelines often struggle to establish whether specific gene expression variations originate from the maternal host tissue or the attaching embryonic structure (Yang, 2025). To resolve this analytical limitation, the integration of genomic DNA variant profiling (genotyping) with transcriptomic variation (RNA variant calling) emerges as a critical methodology to definitively assign the cellular origin of gene expression via single-nucleotide polymorphisms (SNPs). Developing a robust bioinformatic workflow to isolate these individual genetic outputs is essential to clarify the bidirectional molecular dynamics that dictate successful human embryo implantation.

2 THE AIMS OF THE THESIS

2.1 Research question

1. How does hormonal stimulation of the endometrium influence transcriptomic profiles in an *in vitro* embryo implantation model?
2. Can integrated genomic and RNA-seq variant analysis be used to infer the cellular origin of expressed genes?

2.2 General objective

To characterize early implantation-like interactions by integrating DNA- and RNA-based variation profiles from blastoid and endometrial epithelial cells on an implantation model, enabling the distinction of maternal and embryonic molecular contributions during implantation.

2.3 Specific objectives

- To generate and curate SNP profiles from genomic DNA obtained from endometrial epithelial organoids, endometrial biopsies (EB), and embryonic stem cells.
- To identify and annotate SNPs present in expressed genes by performing variant calling analysis using RNA-seq data from the implantation model.
- To integrate SNP information from DNA and RNA to distinguish maternal and embryonic gene expression contributions during implantation-like interactions.
- To determine genes and molecular pathways associated with implantation-like interactions *in vitro* through differential expression and functional enrichment analyses.

3 MATERIALS AND METHODS

The study was conducted in three main stages (Figure 1). First, differential gene expression (DGE) analysis on *bulk*-RNA data was performed. Second, SNP genotyping was executed on the samples that originated the model. Then, variants from RNA-data were called and imputed to be comparable with DNA variants. Third, DNA and RNA variation profiles were merged to have origin assigned variants and their corresponding effects. Once SNPs were origin-assigned, the output was linked to the differentially expressed genes, and the subsequent genes were analyzed in relation to the implantation model.

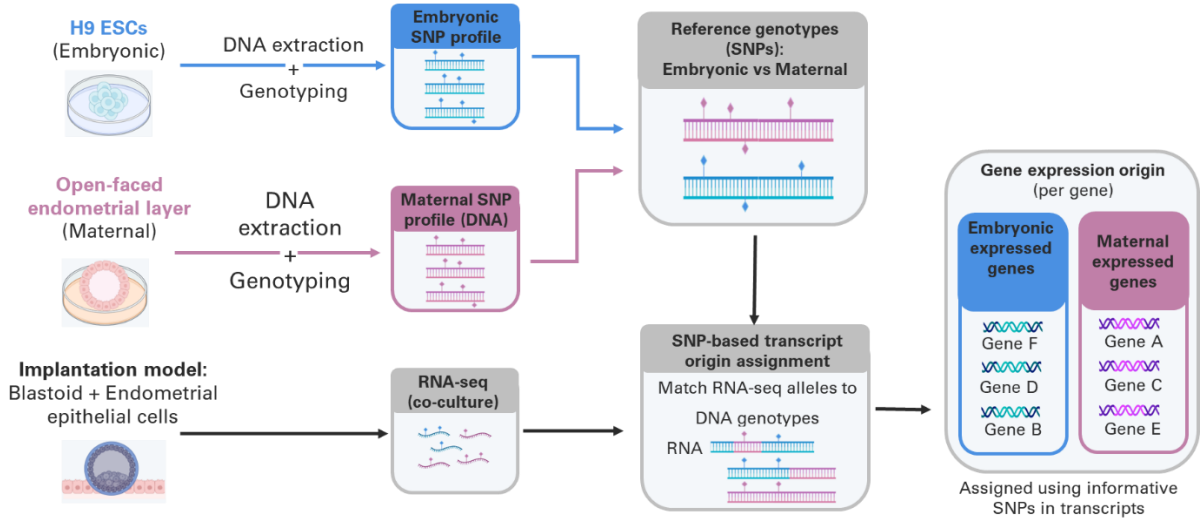

Figure 1. **Schematic representation of the workflow of the study.** DNA was extracted from the human embryonic stem cells (H9 ESCs) and open-faced endometrial layer used in the implantation model, blue and purple, respectively. Genotyping builds an embryonic or maternal profile for origin assignment. RNA variants are called and integrated with the SNPs from genotype profile to distinguish gene expression origin of the *in vitro* implantation model.

3.1 Implantation model

The implantation model was previously developed in Celvia following the protocol by Turco et al. (2017). Two healthy donor-derived endometrial epithelial organoids (EEOs) were thawed and expanded in a drop of Matrigel and cultured at 37 °C in expansion media for up to 10 days before passaging as previously described by Lavogina et al. (2026). EEOs were dissociated into single cells and seeded in a 2D monolayer to form the OFEL. EEOs were separated with Dispase (100 mg/ml) followed by centrifugation after one hour of incubation. Mixture was washed with Advanced DMEM / F12 and resuspended in dissociation solution (TrypLE, N-acetylcysteine, Y-27632) under incubation at optimal temperature for 15 minutes and pipetting until cells were

dissociated to single cells. Afterwards, centrifugation was done and cells were counted before seeding in 96 well-plate with 3% Matrigel diluted in Advanced DMEM / F12. To achieve receptive endometrium, OFEL was treated with 10nM estrogen E2, 1 μM progesterone P4, 250 μM cAMP and 10 μM XAV-939 for 6 days.

Blastoids were generated as previously established by Kagawa et al. (2022). Briefly, naïve H9 stem cells were cultured in 6-well plates in a modified N2B27 medium "PXGL" and then aggregated in AggreWell plates and cultured in "PALLY" medium (Kagawa et al., 2022). The blastoids were acquired for this project 6 days after their aggregation, corresponding to blastocyst-like structures.

Attachment assay was done by transferring 5 blastoids per well as described previously by Heidari Khoei et al. (2023). After two days the evaluation of attachment was assessed by the percentage of attached structures versus the number of structures that were transferred. RNA was extracted using miRNeasy Tissue / Cells Advanced Micro kit (Qiagen) and concentration was quantified using Nanodrop (ThermoFisher, USA). The library for *bulk* RNA sequencing was prepared using TrueSeq Stranded mRNA kit (Illumina, USA) and sequenced on NextSeq 1000 (Illumina, USA) using single-end 80bp settings and replicates.

3.2 Differential expression analysis

The bioinformatic pipeline was designed to process and untangle the mixed transcriptomic data from the co-culture interface (Figure 2). RNA-seq analysis was performed in Galaxy EU where reads were quality checked, aligned to a reference genome, used to perform DGE analysis and downstream gene set enrichment analysis (G.-Y. Lee et al., 2024). The workflow starts with quality and adapter trimming using Trim Galore, then the output is fed into FastQC and HISAT2 with single-end options. FastQC reads quality reports and together with MultiQC, which aggregates results into a single report, a HTML report was displayed for understanding the quality of the data. The FASTQ file was aligned to the human reference genome GRCh38, gencode v43, using HISAT2. RNA-seq reads generated from the alignment as SAM files are count for genomic features with the GTF annotation file taking only exons corresponding to the same reference genome. The tabular output containing the counted reads per gene is used on DESeq2 to estimate the variance-mean dependence in count data and test for differential expression based on a model using the negative binomial distribution. The final output of the workflow is two tabular files, one containing the statistical analysis on reads, another containing the normalized counts of reads, and a pdf file with PCA plot, sample-to-sample distance heatmap, dispersion estimates and MA-plot.

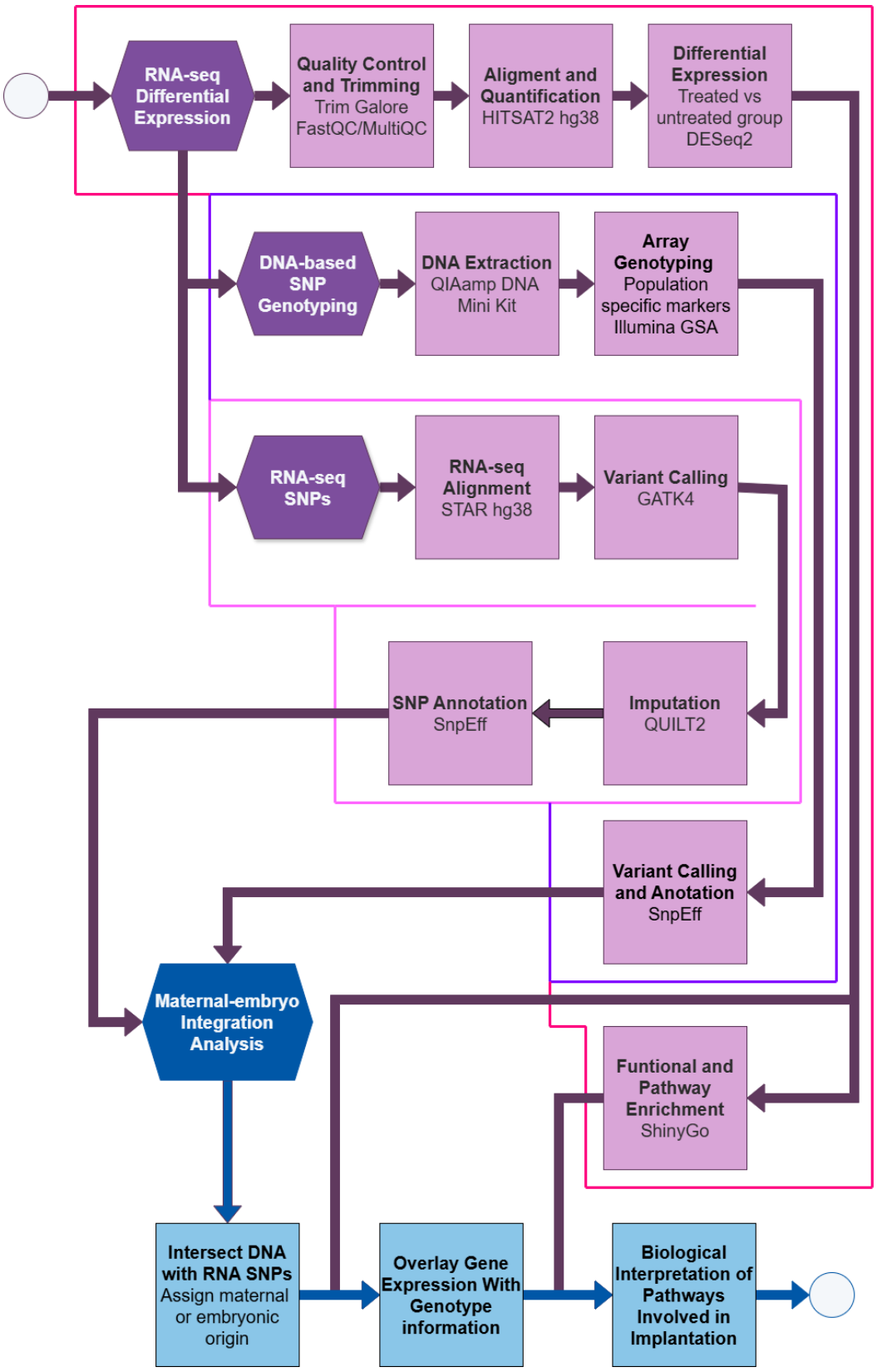

Figure 2. **Descriptive workflow of the study**. Pink and purple represent the first scaffold of the integration for the differential expression analysis, global screening array genotyping and annotation and variant calling from the implantation model, from top to bottom

correspondingly. Light blue and blue represent the integration of the pink/purple part of the workflow from origin assignment, overlay with gene expression and biological interpretation.

Next step in the DGE analysis is gathering the list of upregulated and downregulated genes. To achieve this, output tabular files were analyzed in Python with Pandas. First, differentially expressed genes were recognized for those with an adjusted p-value below 0.05. Second, upregulated genes were filtered with log2 Fold Change higher or equal to 1 and downregulated with lower or equal to -1. The list of up and downregulated genes was recognized in the normalized tabular file and exported. Lastly, the list of upregulated and downregulated genes was consulted for functional enrichment and pathway (FEP) analysis in ShinyGO v0.85.1 with minimum pathway size of 15 and false discovery rate cutoff of 0.05 for KEGG, Go Molecular Function, Cellular component and Go Biological process databases (Ge et al., 2020). Heat map of the downregulated and upregulated genes of the implantation model was generated using ClustVis (Metsalu & Vilo, 2015). Volcano plot was generated with matplotlib.pyplot.scatter using the tabular file from DESeq2.

3.3 DNA global screening array genotyping

DGE elucidated differentially expressed genes following blastoid implantation on the invitro model. To distinguish the maternal or embryonic contributions during implantation DNA was extracted to build the variation profile (Figure 2). Five samples were gathered for building the origin-assignment scaffold of the embryo implantation model. It was considered: (i) the endometrial biopsies from donors EB_89 and EB_93, which were used to generate the donor-derived EEOs and subsequently the OFELs; (ii) the OFELs generated from both donors; and (iii) H9 human embryonic stem cells, which were used to generate blastoids. First, samples were thawed at room temperature, EB were chopped, and following the QIAamp DNA protocol for isolation of genomic DNA from Tissues using the QIAamp DNA Mini kit (Qiagen) DNA was extracted. Next, concentration was measured using Nanodrop (ThermoFisher, USA) and desired concentration for sequencing, 50 ng/µl, was established. DNA was sent to sequencing to Tartu University Institute of Genomics.

Sequencing was carried out with Infinium Global Screening Array-24 v3.0 BeadChip (Illumina, USA) with custom add-on content of 50,000 markers from exons, Illumina multi-disease part, plus 7,000 Estonian population-specific markers; in total, 700,000 markers. Since the EB that were the source of the implantation model come from Estonian women, the targeted genotyping

with Estonian population markers improves quality of variant detection and downstream analysis.

Once sequencing was completed, the data was gathered as a GenomeStudio project, data was visualized in GenomeStudio v2.0 (Illumina, USA). Initial data exploration was assessed with Pandas Python library. The project folder works with variant information files and an accompanying pedigree file. Those files were handled with PLINK v1.9.0-b.7.11 64-bit to write the common variant call format .vcf. PLINK tool was used first for reading the ped and map files, that wrote the binary files bed, bim and fam. Next, variants that possessed call rate higher than 95% were conserved, function --geno 0.05, this will keep the variants where the SNP is called in at least four samples. Additionally, it was kept biallelic SNPs using --biallelic-only strict function that deletes multiallelic and ambiguous cases. Finally, calls reported to be on chromosome 0 were excluded with --chr 1-22 X Y XY MT and exported as the common variant call format using --recode vcf.

Insertions and deletions were removed using Galaxy EU bcftools view –include REF~"^[ACGT]$" && (ALT == "." || ALT~"^[ACGT]$"). This filtering allows to have the four nucleotides on the REF column, and to have the four nucleotides and the point indicator for same as REF in the ALT column. Subsequently, annotation on DNA variants was performed using SnpEff v.5.2 with the reference genome GRCh38.86, the output format was a VCF annotated on variants.

To check if the files recapitulate the clustering of the DGE analysis principal component analysis was performed on data. Therefore, tokenization of genotypes was done in Python by developing an algorithm that takes the VCF file and recognizes the alleles as the string nucleotides forming the genotypes from the REF/ALT format. First, file is read and processed with pandas. Next, unique possible genotypes were identified and tokenized to integers. Tokenization process recognized 12 possible configurations that exclude CT, TC, GT and TG. Additionally, chromosome labeling was changed to follow the GENCODE format. Finally, principal component analysis was completed using sklearn.decomposition.PCA. Ellipses that grouped the PCA were draw with matplotlib.patches.Ellipse using the eigen values and vectors from the trained PCA.

3.4 RNA variant calling and imputation

For the purpose of calling implantation variants, a variant calling workflow was implemented in collaboration with Dr. Tarmo Puurand (Das et al., 2016). The FASTQ files from the implantation model were used to implement the variant calling. First, reads were aligned to the

human reference genome GRCh38, gencode v43, using STAR (Dobin et al., 2013). The resulting BAM files were subsequently processed with GATK v4.2.6.1 for variant calling using HaplotypeCaller (Van der Auwera & O'Connor, 2020), producing VCF files containing candidate variants. Variants were emitted only at polymorphic sites and filtered using a minimum Phred-scaled confidence threshold of 30 to ensure high-confidence calls. Only reads with mapping quality higher or equal to 20 were considered during genotyping, and a diploid model was assumed. A conservative indel model was applied to reduce false-positive insertion and deletion calls. Variants identified from RNA-seq data were then compared with DNA-derived variants.

Owing to the limited number of overlapping SNPs between the RNA- and DNA-derived variant datasets, genotype imputation was performed to increase variant comparability. Imputation was performed on binary files using QUIlT2 which can impute both mother and fetal genome from low coverage reads using cfDNA NIPT data (Z. Li et al., 2025). Imputation was done according to the documentation on GitHub for diploid imputation '--method=diploid' by splitting the genome and reference genome hg38 from1000 genomes into chunks and subsequent imputation with 12 threads. After that, variant files for every chunk were joined with bcftools concat --ligate v1.22+htslib-1.22.1, the variant files were displayed by chromosome. Finally, variants files after imputation were annotated with SnpEff v.5.4 with the reference genome GRCh38.86 enabling gene-level mapping of variants.

3.5 Origin assignment

Origin assignment workflow (Figure 2) was implemented using Linux for Windows (WSL), Ubuntu, bcftools v1.21, Miniconda v25.11.1, bash v5.2.21(1)-release (x86_64-pc-linux-gnu), Awk v5.2.1, VIM v9.1.697 and R v 4.5.2. The workflow suggested by the supervisors of this Master Thesis starts by checking for biallelic SNPs on both DNA and implantation variants with bcftools view -i 'TYPE="snp" && n_alt=1 && strlen(REF)=1 && strlen(ALT)=1', as illustrated on Figure 3. At the same time, the SNPs were counted to verify the amount of SNP filtered. Then, the columns relevant for the integration analysis were extracted with bcftools query -s 'Sample' -f '%CHROM\t%POS\t%REF\t%ALT\t[%GT]\ n' and exported as a tab separated file. This was performed to the OFEL and blastoid genotypes from the VCF files; in the case of the implantation variant file, it was performed by extracting also the ANN from the INFO column. Chosen genotypes were from the blastoid, donor-derived EEO and the corresponding donor-derived implantation model from the non-hormonal treatment for each chromosome file.

Since variants were imputed, the resulting genotype files are expected to be consistent across samples from the same donor, regardless of the hormonal or nor-hormonal conditions. These variant files represent underlying genomic variation and are therefore independent of gene expression or experimental treatment. Consequently, it was assumed that selecting a single sample per donor would preserve the same genotype information required for the origin-assignment task. Importantly, the purpose of the implantation variant files is to determine the origin of SNPs, with annotations being linked to the variant itself rather than to the specific sample.

Imputed files change the notation of genotype from '/' to '|', because when variants are phased the common notation in VCF files is the vertical bar symbol. Hence it was necessary to change all the genotypes to meet the standard slash with VIM :%s#|#/#, which searches and replace, and saving in place. At the same time, the chromosomes of the endometrium and blastoid files were renamed to meet the same format of implantation variant files with awk '{print "chr" $1 "\t" $2 "\t" $3 "\t" $4 "\t" $5}'. Finally, headers are added manually to all the files with VIM having into account that they must be the same.

On RStudio origin assignment was implemented, first by reading the tabular files as data frames. Second, by opposite homozygosity SNPs were merged by position, filtered to homozygosity ('0/0' or '1/1') and non-equal genotypes on the blastoid and endometrium columns, assigned as 'EMBRYO' when the genotype of the model matched the blastoid genotype, as 'ENDOMETRIUM' when genotype of the model matched the endometrium genotype, or as 'BOTH' otherwise. And third, by extracting the gene and impact information from the INFO column. Finally, the output file is exported as a tabular file having the chromosome, position, genotype information from the model, endometrium and blastoid columns, and the information of the genes and impacts. Libraries used were readr, dplyr, tidyverse and base libraries from R. The workflow was iterated through all the chromosomes' files and the donor samples' files, and later merged in Python for downstream analysis.

3.6 Integration with differential expression analysis

Considering the list of upregulated and downregulated genes from the DGE analysis, annotation from the origin assignment was matched with relevant genes (Figure 2). A series of functions were implemented in Python with Pandas, NumPy, matplotlib, matplotlib_venn and base Python libraries. First, all the files from each chromosome corresponding to the donor-related embryo implantation model were merged into a single file. Second, individual genes from each SNP and impact annotations were extracted. If a gene had a match in the differentially expressed

genes list, the gene was reported. Matched genes were displayed in two tabular formats: (i) full SNP information, and (ii) SNPs only displaying the gene annotation match.

Owing that SNPs had only one matched gene, gene annotations were flattened from the second file. Previous steps were iterated by donor-derived embryo implantation model and by the corresponding upregulated and downregulated genes. Subsequently, Venn diagrams were plotted for the downregulated and upregulated matched genes for each donor-derived implantation model grouping them by origin assignment. Next, genes that had SNPs with the same origin were reported for further analysis. In the Venn diagram those genes were exclusively in one group category. Finally, those genes possessing only one origin assignation were matched between the donor-derived files and the list of genes was reported for in depth biological interpretation. The same list was used to match the genes from the normalized counts of reads in the DGE analysis to plot the heatmap of the origin assigned genes in ClustVis (Metsalu & Vilo, 2015).

3.7 Biological interpretation

Genes with single origin based on SNP analysis and shared between the two donor-derived implantation models were retrieved and further investigated using databases such as NCBI and UniProt, as well as relevant literature identified through keyword-based searches. These genes were subsequently integrated into FEP analysis to determine the biological pathways in which the origin-assigned genes are involved (Figure 2). The Python library Pandas was used to import data from ShinyGO, concatenate results from the upregulated and downregulated genes sets, and match genes with assigned origins that were shared between the two donor-derived models.

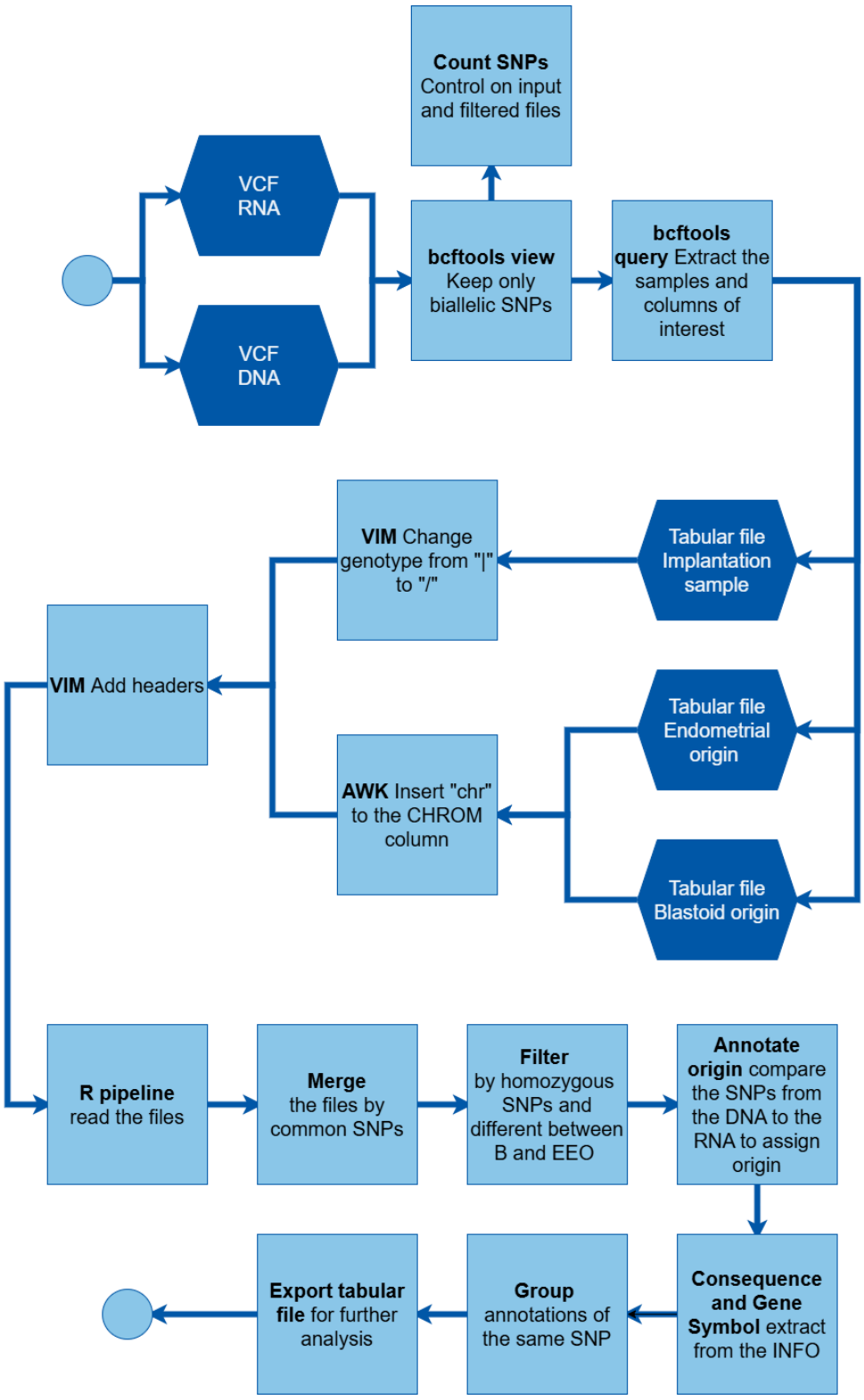

Figure 3. Descriptive origin assignment workflow from DNA and RNA annotated variants. On top is the workflow in bash and on bottom is the workflow in R.

4 RESULTS

4.1 Differentially expressed genes recapitulate the receptive endometrium and implantation.

Quality assessment demonstrated consistently high sequencing performance across all samples, with mean per-base quality scores exceeding Q30 throughout the read length (Supplementary Figure 1), supporting high-confidence downstream analyses. GC content distribution was centered around 53%, consistent with expected human transcriptomic profiles. Although elevated duplication levels were detected (Supplementary Figure 1C), this pattern is characteristic of RNA-seq datasets enriched for highly expressed transcripts rather than technical bias. Adapter contamination remained negligible (<0.29%), indicating high library integrity and effective preprocessing (Andrews, 2023).

Principal component analysis demonstrated a clear segregation of samples according to blastoid attachment status and hormonal treatment conditions, indicating that both implantation competence and endometrial hormonal exposure are major drivers of transcriptional variation in the embryo implantation model (Figure 4A). Additionally, donor-specific transcriptional variation contributed substantially to sample segregation along the x-axis, accounting for a high proportion of the explained variance. Elliptical clustering based on eigenvalues further supported the close grouping of hormonally treated and untreated samples according to blastoid attachment status, reinforcing the strong transcriptional association between implantation outcome and endometrial condition.

Heatmap analysis of sample-to-sample distances (Figure 4B) demonstrated hierarchical clustering primarily driven by technical replicates, followed by donor-derived OFEL origin and blastoid attachment status. Dispersion estimates (Figure 4C) showed relationship between mean normalized expression and dispersion, with gene estimates shrinking towards the fitted trend. Conta, the MA-plot (Figure 4D) revealed a symmetric distribution of logarithmic fold changes around zero where significatively differentially expressed genes were highlighted (Love et al., 2014).

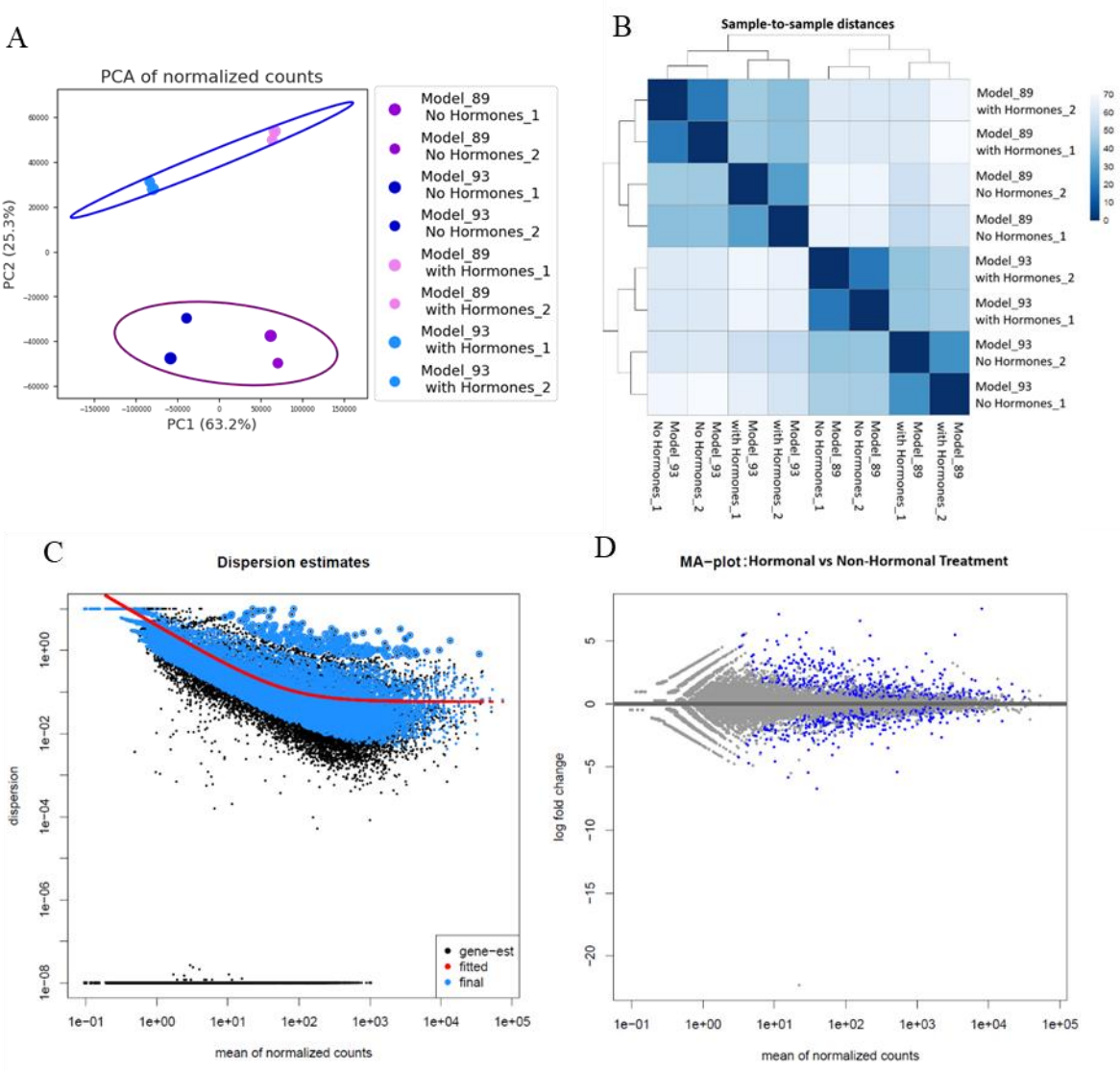

Figure 4. **Differential gene expression analysis overview under hormonally induced co-culture conditions.**. A. Principal component analysis of normalized counts. Blue versus pink tones relate to the donor samples that were used to generate the open-faced endometrial layer. Dark blue and purple illustrate non-hormonal treatment, and pink and light blue illustrate hormonal treatment of the implantation model. B. Heatmap of sample-to-sample distances with hierarchical clustering. C Dispersion estimates plotted against mean normalized counts for all genes. Red line stands for the adjusted tendency, black dotes represent the estimated dispersion of a gene, and blue dots are adjusted with shrinkage genes. D. Log fold change of differentially expressed genes versus mean expression. Each dot is a gene where genes closer to 0 are not differentially expressed, differentially expressed genes are in gray, and significatively differentially expressed genes are blue.

Differential expression analysis revealed 264 upregulated genes and 172 downregulated genes in the implantation model (Supplementary Table 1-2 and Figure 5). Upregulated relevant pathways were associated with IL-17 signaling, cytokines receptors, hormones biosynthesis, activities of steroids, hormones, response to stimulus such as lipopolysaccharides and lipids, and leukocyte migration (Supplementary Figure 2). Downregulated genes were associated with calcium signaling, transforming growth factor-beta, phospholipase activities, antiporter activity, cell adhesion binding proteins, epithelium and tissue development, structure morphogenesis, and developmental induction. Cellular component analysis indicated enrichment at the plasma membrane, endoplasmic reticulum lumen, basal cellular region, and cell surface. (Supplementary Figure 3). The *in vitro* implantation model upregulated *CGB3*, *CGB7* and *CGB8* which encode different beta subunits of the hCG.

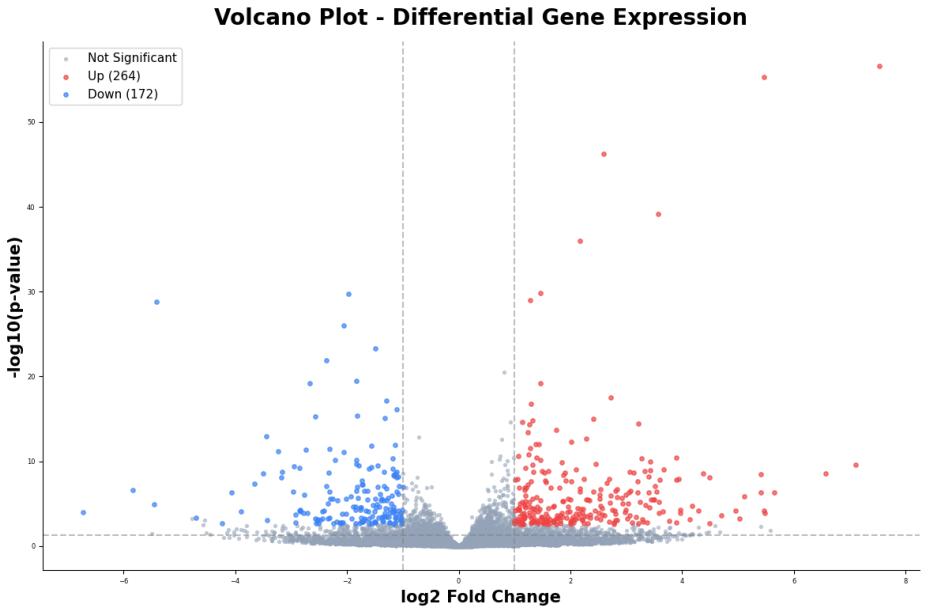

Figure 5. **Volcano plot of the results from the differential expression analysis (DEA).** Red accounts for upregulated differentially expressed genes and blue accounts for downregulated differentially expressed genes.

The top ten upregulated and downregulated genes are shown in Figure 6. These genes are involved in pathways related to response to stimulus, inflammatory responses, secretion, response to other organisms, cell differentiation and development. *DKK1* is downregulated resulting in the potentially reflecting modulation of WNT signaling activity associated with endometrial receptivity. In addition, the downregulation of *SEMA3E, TMEM255A*, and *ANKRD1* may reflect transcriptional remodeling of pathways involved in cellular

differentiation and tissue morphogenesis during blastoid attachment (Supplementary Figure 3D). Several differentially expressed genes, including *CYP1A1, CYP1B1, IL36A, HP*, and *PGLYRP4*, were associated with immune-related processes and hormone response pathways, supporting the involvement of inflammatory and endocrine signaling during blastoid–endometrial interaction (Supplementary Figure 2A, B and D). The heatmap illustrates the sample-to-sample similarities first between the hormonal treatment and second by the donor demonstrating the expression differences when the blastoid attaches to the OFEL. Consequently, it lays the foundation of the downstream analysis.

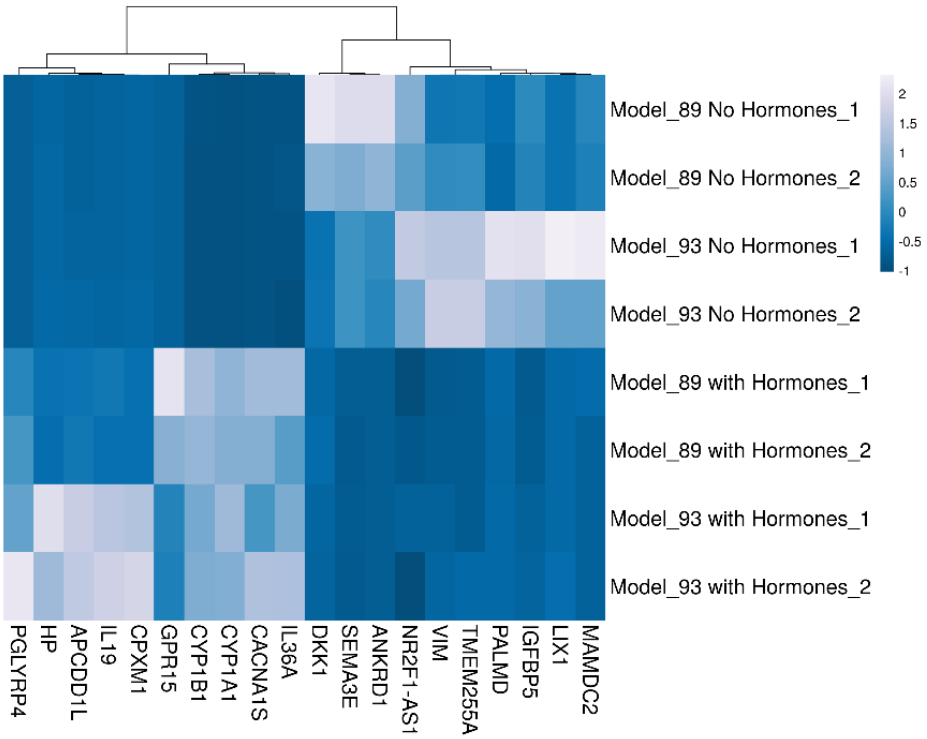

Figure 6. Heatmap of the top ten upregulated and downregulated genes in the implantation model in-vitro.

4.2 Comparable number of variants across RNA and DNA data

DGE analysis revealed genes involved in blastoid attachment to hormonally treated OFEL. Considering that these results come from bulk-RNA sequence data, it was relevant to understand whether these contributions came from the endometrium or rather from the blastoid. To distinguish maternal and embryonic contributions, variants identified from *bulk RNA-seq* data were compared with DNA genotyping profiles obtained from the individual components of the in vitro implantation model. This integrative approach enabled the identification of informative SNPs that could be used to infer the origin of differentially expressed transcripts.

DNA variant profiles were generated from the two donor-derived EEOs, the corresponding donor EB from which the organoids were established, and the H9 cell line used for blastoid generation. Global Screening Array (GSA) genotyping identified high-density SNP profiles across all samples. Genotyping data were visualized and processed with GenomeStudio where 777,016 variants were detected across chromosomes 1-22, X, Y and MT. Genotype calling and clustering were automatically performed using Illumina's GenCall algorithm, which assigns confidence scores to each SNP (Illumina Inc, 2016). On GenomeStudio it was found that there were SNPs labeled as "no-calls" that corresponded to low prediction support. Low quality statistics of SNP call score, normalized theta-value for the sample, normalized R-value for the sample produced empty genotypes labeling (Illumina Inc, 2010). Across all five samples, the 50th percentile SNP call score exceeded 77%. After quality filtering, 745,645 variants were exported in Variant Call Format (VCF).

A total of 730,296 variants passed quality filtering after removal of indels while retaining reference-matching ALT entries. Variant annotation using SnpEff and Ensembl revealed that SnpEff produced a higher number of annotated variants (281,906) compared to Ensembl (265,166) and was therefore selected for downstream analyses. Annotation structure analysis showed that functional information is stored within the INFO field, specifically under the ANN annotation level, which contains multilayered information separated by delimiters. Individual variants frequently displayed multiple predicted functional effects, with a maximum of 129 effects identified for a single SNP (rs4852424) in a blastoid-derived sample. These annotations include allele-specific information, gene identifiers, predicted functional consequences, and impact scores, organized in a hierarchical pipe-separated format. PCA analysis of SNP profiles showed close clustering between donor EB and their corresponding EEO samples, while the blastoid clustered separately from the endometrial samples (Figure 7). These results demonstrate that SNP information distinguishes embryonic and endometrial origins.

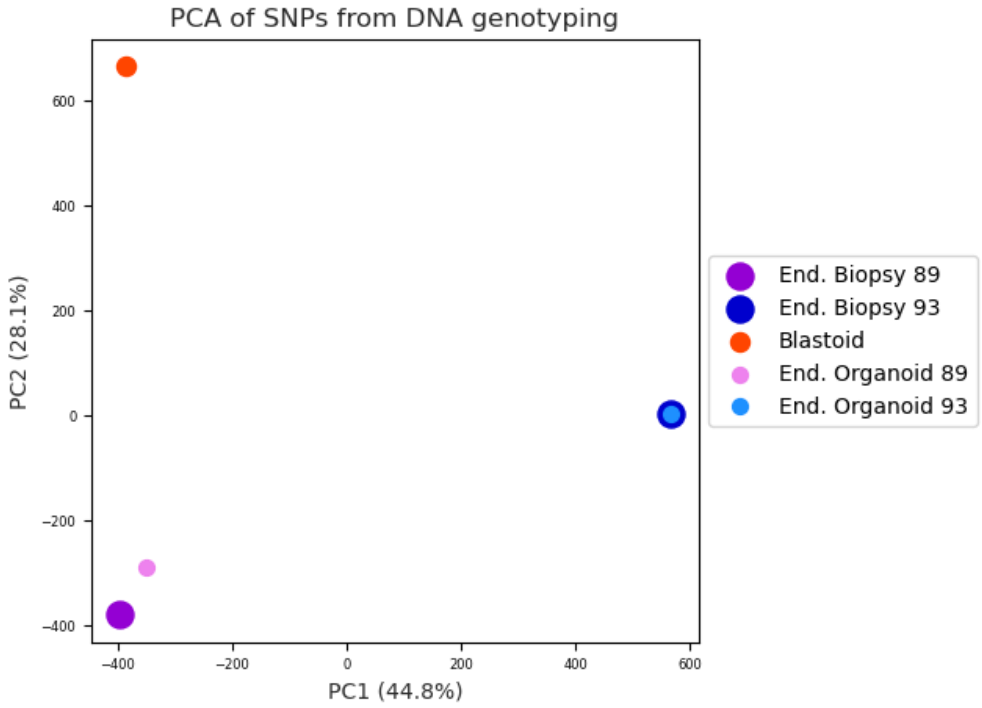

Figure 7. **Principal component analysis (PCA) of the DNA variant profile.** Pink and purple are from donor 89, light blue and dark blue are from donor 93, and blastoid is orange-red. Bigger circles (purple and dark blue) are from the endometrium biopsy (EB) of each donor. Smaller circles (pink and light blue) are from the endometrial epithelial organoids (EEOs) that originated the implantation model.

In parallel, variant calling from the *bulk* RNA-seq datasets identified between 21,000 and 27,000 variants per sample, substantially fewer than those detected in the DNA genotyping datasets, resulting in limited overlap between RNA- and DNA-derived SNPs. To increase the number of comparable variants, genotype imputation was performed on the RNA-seq-derived variant calls using QUILT2.

Imputation substantially increased the number of comparable SNPs across samples, generating between one and six million SNPs per chromosome. Following concatenation and annotation of the imputed VCF files, the implantation workflow produced a total of 97,627,917 comparable annotated SNP records for downstream analyses.

4.3 Origin assignment allowed biologically coherent pathways of implantation biology

To perform origin assignment, RNA- and DNA-derived variant datasets were harmonized following imputation and filtering. Because RNA imputation generated exclusively biallelic variants, matching SNP sets were retained across samples after filtering. In the DNA datasets, filtering for biallelic SNPs reduced the number of variants from approximately 730,296 to 281,906 due to the exclusion of variants lacking alternative allele calls.

Origin assignment in the donor 93-derived implantation model identified 871 embryo, 2,040 both and 3,006 endometrial corresponding to a total of 5,917 annotated variants with assigned origin. Similarly, donor 89-derived implantation model origin assignment determined 1,057 embryo, 2,201 both and 2,845 endometrium SNPs for a total of 6,103 origin assigned annotated variants. Origin assignment per chromosome output ranged from 100 to 400 SNPs.

Origin-assigned annotated SNPs were subsequently compared with differentially expressed genes identified in the DGE analysis. In the donor 93-derived model, 31 downregulated and 44 upregulated genes matched origin-assigned variants (Figure 8C-D), whereas the donor 89-derived model showed matches for 39 downregulated and 36 upregulated genes (Figure 8A-B).

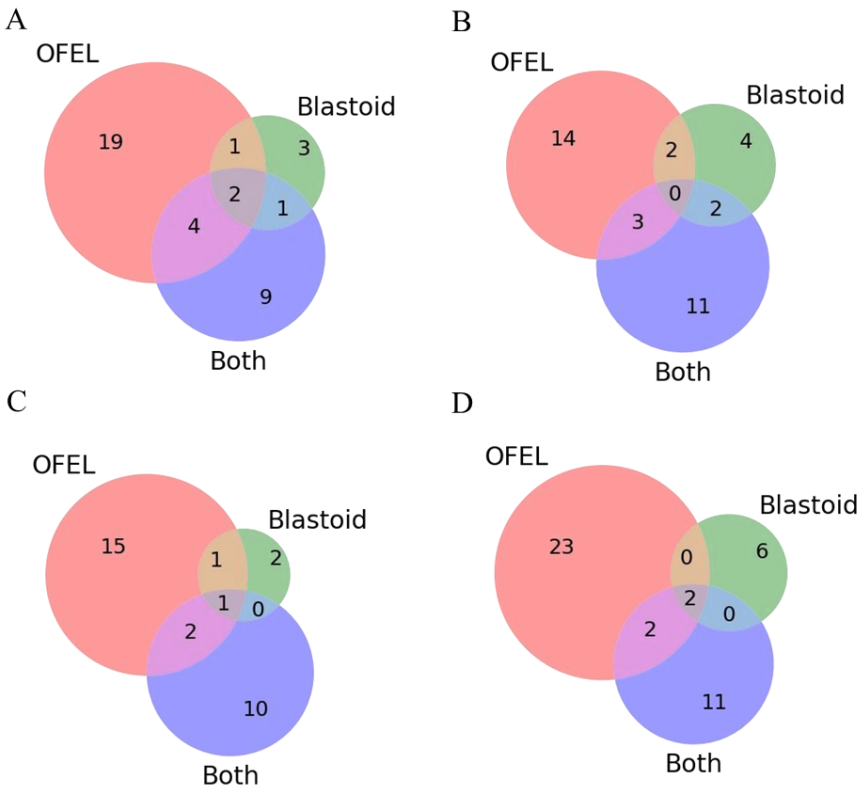

Figure 8. **Venn diagrams of origin assigned differential expressed genes on implantation *in vitro* origin assigned.** A. Venn diagram of downregulated genes with origin assigned from

SNPs integration for donor 89. B. Venn diagram of upregulated genes with origin assigned from SNPs integration for donor 89. C. Venn diagram of downregulated genes with origin assigned from SNPs integration for donor 93. D. Venn diagram of upregulated genes with origin assigned from SNPs integration for donor 93.

Venn diagrams illustrated that there were genes which according to some SNPs annotations might belong to more than one origin classification, intersection of groups in Figure 8. Hence it was considered the origin assigned genes that had the same origin classification. Model from donor 89 distinguished 31 downregulated and 29 upregulated genes, whereas model from donor 93 remarked 27 downregulated and 40 upregulated genes. Next, it was sought for the genes that were in common between the two donor-derived models highlighting the 11 downregulated and 12 upregulated genes at table 1 and table 2.

Endometrium	**Blastoid**	**Both**
CDCA7L	*VIM*	*SLC9A2*
CHN2		*ARL4C*
ADAMTS14		*PDE7B*
NT5DC3		*SDC2*
BCAM		
ELFN2		

Table 1. Shared downregulated differentially expressed genes with origin assigned from the implantation models.

Endometrium	**Blastoid**	**Both**
SELL	*SLC7A11*	*ADD2*
LINC01320	*GPR32*	*ADAMTS20*
IRAK3		*GJB6*
NQO1		*SCUBE1*
TRPV2		
NOS2		

Table 2. Shared upregulated differentially expressed genes with origin assigned from the implantation models.

Most of the genes were found in implantation related reports, however *ARL4C* could only be associated with endometrium or ovarian cancer studies. Additionally, data from FEP analysis was used to detect the pathways from differentially expressed origin assigned genes. 623 pathways from the four databases were associated with the origin assigned genes. Unlike NOS2, *SLC7A11* and *IRAK3* which had 118, 80 and 79 associated pathways, *LINC01320*, *CDCA7L* and *ARL4C* were not associated with any pathway (Supplementary Table 3).

5 DISCUSSION

In this study, integration of transcriptomic profiling with SNP-based origin assigned enabled the characterization of the embryo-endometrium crosstalk following implantation. The combined analysis allowed us to identify the endometrium as the principal transcriptional regulator, suggesting that maternal tissues play a dominant regulatory role during implantation. At the same time, several genes exhibited shared origin, highlighting the coordinated nature endometrium and blastocyst communication. These findings revealed that embryo implantation is supported by highly coordinated signaling networks involving endometrial receptivity, extracellular matrix remodeling, immune modulation and cell survival processes.

Several differentially expressed and origin assigned genes suggest that endometrial receptivity is actively regulated during embryo implantation. Downregulation of *DKK1* indicates a shift from the mid-secretory endometrial profile, consistent with the modulation of the WNT signaling pathway (Marečková et al., 2024). In parallel, markers of endometrial receptivity were upregulated such as *SOD2* as part of the hormonal treatment to mimic the WOI (Poh et al., 2023). Identification of endometrial-origin genes associated with receptivity, including *SELL* and *LINC0130*, supports the establishment of an environment permissive for embryo adhesion and endometrial maturation. *SELL* has been widely associated with cell adhesion processes during implantation (Genbacev et al., 2003; Margarit et al., 2009), whereas *LINC01320* has been linked to the window of implantation and receptive endometrial states (Fernando et al., 2024; Suhorutshenko et al., 2018). Additionally, downregulation of *CHN2* and *ELFN2* in the endometrium suggests that suppression of pathways associated with proliferative or pathological endometrial states may contribute to successful implantation-like events (Y. Dong et al., 2022; Nguyen, 2024; Sponchiado, 2019). The coordinated regulation of insulin-like growth factor-binding proteins further supports active embryo-maternal signaling during decidualization and endometrial remodeling (Damario et al., 1998). Altogether, these findings indicate that the receptive endometrium is not a static hormonal state, but rather a transcriptionally dynamic environment that actively adapts to embryonic presence.

Extracellular matrix remodeling and adhesion-related pathways emerged as major components of embryo-endometrial communication during implantation. Differential expression of *SERPIN* family members, including *SERPINA1*, *SERPINB5*, and *SERPINB7*, supports active regulation of extracellular matrix organization, epithelial proliferation, and inflammatory signaling associated with blastoid attachment. Previous implantation models have demonstrated that knockdown of cell-cell adhesion-related genes compromises trophectoderm attachment (Koel et al., 2022), reinforcing the importance of coordinated extracellular interactions during

implantation. In parallel, opposite regulation of *ADAMTS* family members suggests dynamic remodeling of the endometrial microenvironment. While *ADAMTS14* was downregulated in the endometrium, potentially facilitating placentation (S.-Y. Lee et al., 2014), *ADAMTS20* was upregulated in both embryonic and maternal compartments and was associated with pathways related to cell differentiation, signaling, and survival. . Additionally, downregulation of *BCAM* and *VIM* suggests cellular and structural adaptations associated with epithelial remodeling and early trophoblast interaction (Shibata et al., 2024; Tinning et al., 2025). Together, these transcriptional changes indicate that successful implantation requires tightly coordinated regulation of adhesion and extracellular remodeling pathways to establish a permissive environment for blastocyst attachment and invasion.

Immune and inflammatory signaling pathways were strongly associated with coordinated embryo-endometrial communication during implantation. Joint expression of *GPR32* in both maternal and embryonic compartments suggests the activation of pro-resolving signaling mechanisms involved in maintaining immune homeostasis during implantation-like events. *GPR32*-mediated pathways have been associated with resolvin signaling, which attenuates excessive pro-inflammatory cytokine production while promoting anti-inflammatory responses necessary for pregnancy establishment (Sousa et al., 2025). In parallel, endometrial expression of *TRPV2* and *IRAK3* supports the involvement of innate immune regulatory pathways linked to Toll-like receptor and NOD-like receptor signaling. These pathways converge on MAPK and NF-κB signaling cascades, which regulate inflammatory responses, cellular stress adaptation, and tissue remodeling during implantation (Almeida-da-Silva et al., 2023; Rodriguez et al., 2006). Consistently, several *MAPK*-associated genes were downregulated, suggesting controlled modulation of inflammatory signaling rather than generalized immune activation. The coordinated regulation of *IL6*-associated pathways and *NOS2* further supports the establishment of a permissive inflammatory environment that promotes prostaglandin synthesis, vascular remodeling, decidualization, and maintenance of uterine homeostasis (Kuracinova et al., 2025; Salleh, 2014; Voros et al., 2025). Together, these findings indicate that successful implantation depends on tightly regulated immune modulation that balances inflammatory activation with maternal tolerance toward the developing embryo.

Genes associated with oxidative stress regulation, cellular survival, and developmental support further highlighted the coordinated nature of embryo-endometrial interactions during implantation. Joint upregulation of *SLC7A11* in both maternal and embryonic compartments suggests the activation of anti-ferroptotic mechanisms that promote cellular survival, adhesion, and expansion during implantation-like events (L. Dong et al., 2025). *SLC7A11*-mediated

cysteine transport has been associated with the reduction of oxidative stress, inflammation, and apoptosis, supporting a favorable microenvironment for early embryonic development (Lofthouse et al., 2021). In parallel, endometrial upregulation of *NQO1* and implantation-associated expression of *TP53* family members indicate activation of protective pathways involved in genomic stability and stress adaptation (Atiomo et al., 2017; Price et al., 2010). These pathways may contribute to maintaining cellular integrity while supporting embryo development during early implantation stages. Additionally, blastoid upregulation of *SCUBE1* suggests participation in developmental and placentation-associated processes, potentially linked to vascular adaptation and epithelial differentiation (Kizildemir et al., 2026; Xavier et al., 2009; Zhuang et al., 2010). Coordinated expression of *GJB6* by the endometrium further supports the establishment of intercellular communication pathways associated with embryo development and tissue homeostasis (Salilew-Wondim et al., 2010). Together, these findings indicate that implantation signaling involves not only immune and structural regulation, but also active maintenance of cellular viability and developmental competence in both embryonic and maternal compartments.

Integration of SNP-based origin assignment with transcriptomic profiling provided an additional layer of biological interpretation for embryo–endometrial communication during implantation. Overall, the endometrium displayed a more transcriptionally active profile than the blastoid, supporting the concept that maternal tissues play a dominant role in regulating receptivity, extracellular remodeling, immune modulation, and tissue homeostasis during implantation-like events. In contrast, embryonic contributions were more restricted and were primarily associated with signaling pathways involved in developmental support and immune communication. Interestingly, several genes exhibited shared expression patterns between maternal and embryonic compartments, suggesting the existence of coordinated and bidirectional signaling networks rather than strictly compartmentalized responses. This convergence was particularly evident in pathways associated with extracellular remodeling, inflammatory regulation, and cellular survival. Importantly, the integration of differential expression analysis with SNP-based origin assignment enabled the distinction of maternal and embryonic transcriptional contributions within a shared *in vitro* implantation environment, supporting the biological relevance of the implantation model.

Despite the biological coherence of the identified pathways, several methodological limitations should be considered. SNP-based origin assignment depended on the overlap between transcript-derived variants and genotyped variants, which restricted the number of informative SNPs available for maternal or embryonic classification. In addition, the use of *bulk* RNA

sequencing limited the cellular resolution of the analysis and may have masked cell type-specific transcriptional dynamics during implantation. The *in vitro* implantation model also cannot fully reproduce the spatial and temporal complexity of human implantation in vivo, particularly regarding vascularization, immune cell recruitment, and long-term trophoblast invasion. Furthermore, although blastoids represent highly valuable experimental systems, they do not fully recapitulate all developmental properties of human embryos. Nevertheless, the integration of transcriptomics with SNP-based origin assignment generated biologically consistent patterns that aligned with known implantation-associated mechanisms. Future studies integrating single-cell transcriptomics, spatial omics, deeper sequencing approaches, and functional perturbation assays could provide higher-resolution characterization of embryo-maternal signaling and further clarify lineage-specific contributions during implantation.

In summary, the present study supports the concept that early implantation is driven by highly coordinated molecular communication between maternal and embryonic compartments. Integration of differential expression analysis with SNP-based origin assignment revealed that the endometrium acts as the dominant regulatory environment during implantation-like events, orchestrating pathways associated with receptivity, extracellular remodeling, immune modulation, and tissue homeostasis. At the same time, the blastoid contributed signaling programs linked to developmental support and embryo–maternal communication. The identification of shared transcriptional responses between both compartments further highlights the bidirectional and dynamic nature of implantation biology. Overall, the findings demonstrate that combining *in vitro* implantation models with integrative multi-omic approaches can provide valuable insight into the molecular mechanisms underlying human implantation while preserving the ethical advantages of stem cell-derived embryo models. These approaches may contribute to future advances in reproductive medicine, implantation research, and the understanding of early pregnancy establishment.

SUMMARY

Embryo implantation is a highly coordinated process requiring precise molecular communication between the endometrium and the developing embryo. Despite advances in assisted reproductive technologies, there is limited understanding of early embryo–maternal interactions. In this study, the molecular crosstalk was investigated during implantation using an *in vitro* model based on an open-face endometrial layer co-cultured with human blastoids.

In vitro implantation unraveled the metabolic pathways of human early implantation of the blastocyst to the first layer of the endometrium. Differential gene expression analysis identified 264 upregulated and 172 downregulated genes associated with blastoid attachment under hormonally induced conditions. In parallel, high-density SNP profiles were generated from genomic DNA, while RNA-derived variants were called and imputed to increase resolution. Integration of differentially expressed genes with genomic variants profiles allowed the recognition of 23 genes relevant to implantation-like events.

Communication during the implantation involves the signaling of cytokines where *SELL* and *IRAK3* have important roles. *IRAK3* acts in response to the hCG signaling and is involved in many pathways from which the endometrium relaxes the immune response. As part of this signaling pathway interlekin-6 seems to play a pivotal role where *IRAK3* and *NOS2* enhance the secretion of prostaglandin in the mucosa.

The receptive endometrium involves the action of *SELL*, non-coding mRNAs, *SLC7A11* for maintaining the endometrium in a receptive state. Moreover, endometrium relaxes its immune response specifically with genes that downregulate the *MAPK* pathways as part of the luteinizing hormone/chorionic gonadotropin response. The response was suggested to be maintained through the ion channel *TRPV2* mainly by the endometrium, but there are genes like *GPR32* that are expressed also by the blastoid.

The selection of pathways that promotes embryo development is mediated by *NQO1* and *SLC7A11* regulation. This paves the way for genes like *SCUBE1* that were linked to tissue development pathways that should be promoted over embryo development. *SCUBE1* also contributes to the vascularization of the endometrium and is relevant for placentation. Nonetheless, Genes that have little or no information regarding implantation events were associated with blastoid attachment. Besides, *ARL4C* and *LINC01320* are reference genes for future targeted research with endometrium and blastoid expression.

To conclude, the integration of transcriptomic and genomic variation data enhances the interpretability of *in vitro* implantation models and offers insights into mechanisms underlying

implantation success and failure, with potential implications for improving reproductive outcomes. Additionally, origin assigned genes were related to the embryo implantation to the endometrium and can be targeted for future research.

REFERENCES

Almeida-da-Silva, C. L. C., Savio, L. E. B., Coutinho-Silva, R., & Ojcius, D. M. (2023). The role of NOD-like receptors in innate immunity. *Frontiers in Immunology*, *14*. https://doi.org/10.3389/fimmu.2023.1122586

Altmäe, S., Koel, M., Võsa, U., Adler, P., Suhorutšenko, M., Laisk-Podar, T., Kukushkina, V., Saare, M., Velthut-Meikas, A., Krjutškov, K., Aghajanova, L., Lalitkumar, P. G., Gemzell-Danielsson, K., Giudice, L., Simón, C., & Salumets, A. (2017). Meta-signature of human endometrial receptivity: a meta-analysis and validation study of transcriptomic biomarkers. *Scientific Reports*, *7*(1), 10077. https://doi.org/10.1038/s41598-017-10098-3

Andrews, S. (2023). *FastQC: A quality control tool for high throughput sequence data*. Https://Www.Bioinformatics.Babraham.Ac.Uk/Projects/Fastqc/.

Anoshko, Y., Dons'koi, B., Sudoma, I., Khazhylenko, K., Zabara, D., & Goncharova, Y. (2023). Changes in the immunophenotype of endometrium during implantation window receptivity formation in healthy fertile women. *Placenta*, *143*, 62–68. https://doi.org/10.1016/j.placenta.2023.10.002

Atiomo, W., Shafiee, M. N., Chapman, C., Metzler, V. M., Abouzeid, J., Latif, A., Chadwick, A., Kitson, S., Sivalingam, V. N., Stratford, I. J., Rutland, C. S., Persson, J. L., Ødum, N., Fuentes-Utrilla, P., Jeyapalan, J. N., Heery, D. M., Crosbie, E. J., & Mongan, N. P. (2017). Expression of NAD(P)H quinone dehydrogenase 1 (NQO1) is increased in the endometrium of women with endometrial cancer and women with polycystic ovary syndrome. *Clinical Endocrinology*, *87*(5), 557–565. https://doi.org/10.1111/cen.13436

Betz, D., & Fane, K. (2026). *Human Chorionic Gonadotropin*. StatPearls Publishing LLC.

Buck, V. U., Windoffer, R., Leube, R. E., & Classen-Linke, I. (2012). Redistribution of adhering junctions in human endometrial epithelial cells during the implantation window of the menstrual cycle. *Histochemistry and Cell Biology*, *137*(6), 777–790. https://doi.org/10.1007/s00418-012-0929-0

Bulletti, F. M., Sciorio, R., Conforti, A., De Luca, R., Bulletti, C., Palagiano, A., Berrettini, M., Scaravelli, G., & Pierson, R. A. (2025). Causes of embryo implantation failure: A systematic review and metaanalysis of procedures to increase embryo implantation potential. *Frontiers in Endocrinology*, *15*. https://doi.org/10.3389/fendo.2024.1429193

Capalbo, A., Poli, M., Riera-Escamilla, A., Shukla, V., Kudo Høffding, M., Krausz, C., Hoffmann, E. R., & Simon, C. (2021). Preconception genome medicine: current state and

future perspectives to improve infertility diagnosis and reproductive and health outcomes based on individual genomic data. *Human Reproduction Update*, *27*(2), 254–279. https://doi.org/10.1093/humupd/dmaa044

Chen, H., Li, J., Cai, S., Zeng, S., Yin, C., Kuang, W., Cheng, K., Jiang, Y., Tao, M., Chu, C., Hocher, J.-G., Lin, G., Gong, F., & Hocher, B. (2022). Impact of body mass index (BMI) on the success rate of fresh embryo transfer in women undergoing first in vitro fertilization/intracytoplasmic sperm injection (IVF/ICSI) treatment. *International Journal of Obesity*, *46*(1), 202–210. https://doi.org/10.1038/s41366-021-00978-0

Clark, A. T., Brivanlou, A., Fu, J., Kato, K., Mathews, D., Niakan, K. K., Rivron, N., Saitou, M., Surani, A., Tang, F., & Rossant, J. (2021). Human embryo research, stem cell-derived embryo models and in vitro gametogenesis: Considerations leading to the revised ISSCR guidelines. *Stem Cell Reports*, *16*(6), 1416–1424. https://doi.org/10.1016/j.stemcr.2021.05.008

Conforti, A., Longobardi, S., Carbone, L., Iorio, G. G., Cariati, F., Campitiello, M. R., Strina, I., Palese, M., D'Hooghe, T., & Alviggi, C. (2022). Does Intrauterine Injection of hCG Improve IVF Outcome? A Systematic Review and a Meta-Analysis. *International Journal of Molecular Sciences*, *23*(20), 12193. https://doi.org/10.3390/ijms232012193

Dabbagh Rezaeiye, R., Mehrara, A., Ali Pour, A. M., Fallahi, J., & Forouhari, S. (2022). Impact of Various Parameters as Predictors of The Success Rate of In Vitro Fertilization. *International Journal of Infertility and Sterility*, *61*(2), 76–84. https://doi.org/https://doi.org/10.22074/IJFS.2021.531672.1134

Damario, M. A., Liu, H.-C., Mele, C. A., Horenstein, M. G., & Rosenwaks, Z. (1998). Immunohistochemical Analysis of Insulin-like Growth Factor–Binding Proteins -1, -2, and -3 in Implantation Sites of the Mouse. *Journal of Assisted Reproduction and Genetics*, *15*(8), 513–520. https://doi.org/10.1023/A:1022538621928

Das, S., Forer, L., Schönherr, S., Sidore, C., Locke, A. E., Kwong, A., Vrieze, S. I., Chew, E. Y., Levy, S., McGue, M., Schlessinger, D., Stambolian, D., Loh, P.-R., Iacono, W. G., Swaroop, A., Scott, L. J., Cucca, F., Kronenberg, F., Boehnke, M., … Fuchsberger, C. (2016). Next-generation genotype imputation service and methods. *Nature Genetics*, *48*(10), 1284–1287. https://doi.org/10.1038/ng.3656

David, L., Bruneau, A., Fréour, T., Rivron, N., & Van de Velde, H. (2023). An update on human pre- and peri-implantation development: a blueprint for blastoids. *Current Opinion in Genetics & Development*, *83*, 102125. https://doi.org/10.1016/j.gde.2023.102125

Díaz-Gimeno, P., Horcajadas, J. A., Martínez-Conejero, J. A., Esteban, F. J., Alamá, P., Pellicer, A., & Simón, C. (2011). A genomic diagnostic tool for human endometrial receptivity based on the transcriptomic signature. *Fertility and Sterility*, *95*(1), 50-60.e15. https://doi.org/10.1016/j.fertnstert.2010.04.063

Díaz-Gimeno, P., Ruiz-Alonso, M., Sebastian-Leon, P., Pellicer, A., Valbuena, D., & Simón, C. (2017). Window of implantation transcriptomic stratification reveals different endometrial subsignatures associated with live birth and biochemical pregnancy. *Fertility and Sterility*, *108*(4), 703-710.e3. https://doi.org/10.1016/j.fertnstert.2017.07.007

Dobin, A., Davis, C. A., Schlesinger, F., Drenkow, J., Zaleski, C., Jha, S., Batut, P., Chaisson, M., & Gingeras, T. R. (2013). STAR: ultrafast universal RNA-seq aligner. *Bioinformatics*, *29*(1), 15–21. https://doi.org/10.1093/bioinformatics/bts635

Dong, L., Sun, X., An, S., Xiang, J., Hu, L., Yao, D., Chang, J., Jia, R., Yang, Y., & Wang, S. (2025). Mechanistic Insights Into Recurrent Implantation Failure: The Lactate– H3K18la – SLC7A11 Axis Explored via Endometrial Organoid and Blastoid–Endometrial Cell Implantation Models. *Cell Proliferation*. https://doi.org/10.1111/cpr.70147

Dong, Y., Zhang, T., Li, X., Yu, F., Yu, H., & Shao, S. (2022). Identification of Key Prognostic-Related miRNA-mRNA Pairs in the Progression of Endometrial Carcinoma. *Gynecologic and Obstetric Investigation*, *87*(1), 12–21. https://doi.org/10.1159/000520339

Dutta, S., & Sengupta, P. (2018). Rabbits and men: relating their ages. *Journal of Basic and Clinical Physiology and Pharmacology*, *29*(5), 427–435. https://doi.org/10.1515/jbcpp-2018-0002

Farzizadeh, N., Amoozgar, M., Aminbeidokhti, M., Hariri, A., Khosravi, A., Najmi, Z., & Zarrabi, A. (2026). Non-invasive biomarkers in assisted reproduction: a comprehensive review for predicting IVF success. *Journal of Assisted Reproduction and Genetics*, *43*(1), 35–50. https://doi.org/10.1007/s10815-025-03707-y

Fernando, S. R., Yan, Y., Kumar, M., Lai, H.-L., Lee, Y.-L., Ng, E. H. Y., Yeung, W. S. B., & Lee, K.-F. (2024). Multiomics approaches to uncover endometrial receptivity in embryo implantation: a mini-review. *Reproductive and Developmental Medicine*, *8*(3), 178–185. https://doi.org/10.1097/RD9.0000000000000078

Fischer, B., Chavatte-Palmer, P., Viebahn, C., Navarrete Santos, A., & Duranthon, V. (2012). Rabbit as a reproductive model for human health. *REPRODUCTION*, *144*(1), 1–10. https://doi.org/10.1530/REP-12-0091

Ge, S. X., Jung, D., & Yao, R. (2020). ShinyGO: a graphical gene-set enrichment tool for animals and plants. *Bioinformatics*, *36*(8), 2628–2629. https://doi.org/10.1093/bioinformatics/btz931

Gellersen, B., Brosens, I., & Brosens, J. (2007). Decidualization of the Human Endometrium: Mechanisms, Functions, and Clinical Perspectives. *Seminars in Reproductive Medicine*, *25*(6), 445–453. https://doi.org/10.1055/s-2007-991042

Genbacev, O. D., Prakobphol, A., Foulk, R. A., Krtolica, A. R., Ilic, D., Singer, M. S., Yang, Z.-Q., Kiessling, L. L., Rosen, S. D., & Fisher, S. J. (2003). Trophoblast L-Selectin-Mediated Adhesion at the Maternal-Fetal Interface. *Science*, *299*(5605), 405–408. https://doi.org/10.1126/science.1079546

Gliozheni, O., Hambartsoumian, E., Strohmer, H., Petrovskaya, E., De Neubourg, D., Bogaerts, K., Balic, D., Antonova, I., Cvetkova, E., Ljiljak, D., Rezabek, K., Kirk, J., Sõritsa, D., Gissler, M., Pelkonen, S., Mansouri, I., de Mouzon, J., Chkonia, L., Schneider, A. T., … Goossens, V. (2025). ART in Europe, 2020: results generated from European registries by ESHRE. *Human Reproduction*, *40*(11), 2038–2055. https://doi.org/10.1093/humrep/deaf179

Godakumara, K., Ord, J., Lättekivi, F., Dissanayake, K., Viil, J., Boggavarapu, N. R., Faridani, O. R., Jääger, K., Velthut-Meikas, A., Jaakma, Ü., Salumets, A., & Fazeli, A. (2021). Trophoblast derived extracellular vesicles specifically alter the transcriptome of endometrial cells and may constitute a critical component of embryo-maternal communication. *Reproductive Biology and Endocrinology*, *19*(1), 115. https://doi.org/10.1186/s12958-021-00801-5

Graham, M. E., Jelin, A., Hoon, A. H., Wilms Floet, A. M., Levey, E., & Graham, E. M. (2023). Assisted reproductive technology: Short- and long-term outcomes. *Developmental Medicine & Child Neurology*, *65*(1), 38–49. https://doi.org/10.1111/dmcn.15332

Heidari Khoei, H., Javali, A., Kagawa, H., Sommer, T. M., Sestini, G., David, L., Slovakova, J., Novatchkova, M., Scholte op Reimer, Y., & Rivron, N. (2023). Generating human blastoids modeling blastocyst-stage embryos and implantation. *Nature Protocols*, *18*(5), 1584–1620. https://doi.org/10.1038/s41596-023-00802-1

Hu, S., Yao, G., Wang, Y., Xu, H., Ji, X., He, Y., Zhu, Q., Chen, Z., & Sun, Y. (2014). Transcriptomic Changes During the Pre-Receptive to Receptive Transition in Human Endometrium Detected by RNA-Seq. *The Journal of Clinical Endocrinology & Metabolism*, *99*(12), E2744–E2753. https://doi.org/10.1210/jc.2014-2155

Idelevich, A., & Vilella, F. (2020). Mother and Embryo Cross-Communication. *Genes*, *11*(4), 376. https://doi.org/10.3390/genes11040376

Illumina Inc. (2010). *Interpreting Infinium Assay Data for Whole-Genome Structural Variation*.

Illumina Inc. (2016). *GenomeStudio Genotyping Module v2.0 Software Guide*.

Itriyeva, K. (2022). The normal menstrual cycle. *Current Problems in Pediatric and Adolescent Health Care*, *52*(5), 101183. https://doi.org/10.1016/j.cppeds.2022.101183

Jatan, N., Al-Mashhadani, M., Dsouza, S., Khan, S., Mokhtar, J., Kaddoura, R., & du Plessis, S. S. (2026). Male Infertility and Neurodegenerative Diseases: A Systematic Review of Associations and Molecular Mechanisms. *International Journal of Molecular Sciences*, *27*(7), 3222. https://doi.org/10.3390/ijms27073222

Kagawa, H., Javali, A., Khoei, H. H., Sommer, T. M., Sestini, G., Novatchkova, M., Scholte op Reimer, Y., Castel, G., Bruneau, A., Maenhoudt, N., Lammers, J., Loubersac, S., Freour, T., Vankelecom, H., David, L., & Rivron, N. (2022). Human blastoids model blastocyst development and implantation. *Nature*, *601*(7894), 600–605. https://doi.org/10.1038/s41586-021-04267-8

Keleş, I. D., Günel, T., Özgör, B. Y., Ülgen, E., Gümüşoğlu, E., Hosseini, M. K., Sezerman, U., Buyru, F., Yeh, J., & Baştu, E. (2023). Gene pathway analysis of the endometrium at the start of the window of implantation in women with unexplained infertility and unexplained recurrent pregnancy loss: is unexplained recurrent pregnancy loss a subset of unexplained infertility? *Human Fertility*, *26*(5), 1129–1141. https://doi.org/10.1080/14647273.2022.2143299

Kikas, T., Dutta, A., Inno, R., Pomm, K., Tjagur, S., Poolamets, O., Roomere, H., Punab, M., & Laan, M. (2026). Microdeletion and microduplication syndromes, including recurrent rearrangements at 16p11.2 and 22q11.21, are enriched in unexplained male infertility. *Human Reproduction*, *41*(2), 159–167. https://doi.org/10.1093/humrep/deaf231

Kizildemir, Y. Z., Uyanikoglu, H., Incebiyik, M., Kalir, H., Karsli, S. E., Işik Okuyan, I., Kahveci, B., Civelek, M., & Emral, C. K. (2026). Follicular fluid SCUBE1 as a novel

angiogenesis-associated biomarker in women undergoing ART: a pilot study reflecting the follicular vascular microenvironment. *Journal of Assisted Reproduction and Genetics*, *43*(4), 1179–1191. https://doi.org/10.1007/s10815-026-03811-7

Koel, M., Krjutškov, K., Saare, M., Samuel, K., Lubenets, D., Katayama, S., Einarsdottir, E., Vargas, E., Sola-Leyva, A., Lalitkumar, P. G., Gemzell-Danielsson, K., Blesa, D., Simon, C., Lanner, F., Kere, J., Salumets, A., & Altmäe, S. (2022). Human endometrial cell-type-specific RNA sequencing provides new insights into the embryo–endometrium interplay. *Human Reproduction Open*, *2022*(4). https://doi.org/10.1093/hropen/hoac043

Kuracinova, T., Bollova, M., Kocan, D., Mikus Kuracinova, K., Janegova, A., & Janega, P. (2025). Nitric Oxide Synthase Expression in Endometrium During Physiological Cycle. *Physiological Research*, *74*(Suppl 2), S285. https://doi.org/10.33549/physiolres.935735

Lai, Z.-Z., Wang, Y., Zhou, W.-J., Liang, Z., Shi, J.-W., Yang, H.-L., Xie, F., Chen, W.-D., Zhu, R., Zhang, C., Mei, J., Zhao, J.-Y., Ye, J.-F., Zhang, T., & Li, M.-Q. (2022). Single-cell transcriptome profiling of the human endometrium of patients with recurrent implantation failure. *Theranostics*, *12*(15), 6527–6547. https://doi.org/10.7150/thno.74053

Lavogina, D., Apostolov, A., Risal, S., Iglesias Moreno, P., Pathare, A. D. S., Roop, A., Bergamelli, M., Rooda, I., Hansing, K., Saare, M., Lanner, F., Acharya, G., Adibi, J. J., Damdimopoulou, P., Sola-Leyva, A., Koistinen, H., & Salumets, A. (2026). *Functional profiling of human chorionic gonadotrophin in embryo peri- and post-implantation* in vitro *models*. https://doi.org/10.64898/2026.04.01.26349947

Lee, G.-Y., Ham, S., & Lee, S.-J. V. (2024). Brief guide to RNA sequencing analysis for nonexperts in bioinformatics. *Molecules and Cells*, *47*(5), 100060. https://doi.org/10.1016/j.mocell.2024.100060

Lee, S.-Y., Lee, H.-S., Gil, M., Kim, C. J., Lee, Y.-H., Kim, K.-R., & Park, C.-S. (2014). Differential Expression Patterns of a Disintegrin and Metalloproteinase With Thrombospondin Motifs (ADAMTS) -1, -4, -5, and -14 in Human Placenta and Gestational Trophoblastic Diseases. *Archives of Pathology and Laboratory Medicine*, *138*(5), 643–650. https://doi.org/10.5858/arpa.2012-0227-OA

Li, L., Guo, F., Gao, Y., Ren, Y., Yuan, P., Yan, L., Li, R., Lian, Y., Li, J., Hu, B., Gao, J., Wen, L., Tang, F., & Qiao, J. (2018). Single-cell multi-omics sequencing of human early embryos. *Nature Cell Biology*, *20*(7), 847–858. https://doi.org/10.1038/s41556-018-0123-2

Li, T., Long, S., Ye, Z., Tang, Z., Song, Y., Su, M., Zhou, B., Wang, Y., & Zhang, L. (2026). Distribution and trends of the global burden of female infertility attributable to sexually transmitted infections from 1990 to 2021. *BMC Infectious Diseases*, *26*(1), 492. https://doi.org/10.1186/s12879-026-12733-9

Li, Z., Albrechtsen, A., & Davies, R. W. (2025). Flexible read-aware genotype imputation from sequence using biobank sized reference panels. *Nature Communications*, *17*(1), 524. https://doi.org/10.1038/s41467-025-67218-1

Liu, X., & Polo, J. M. (2024). Human blastoid as an in vitro model of human blastocysts. *Current Opinion in Genetics & Development*, *84*, 102135. https://doi.org/10.1016/j.gde.2023.102135

Lofthouse, E. M., Manousopoulou, A., Cleal, J. K., O'Kelly, I. M., Poore, K. R., Garbis, S. D., & Lewis, R. M. (2021). N-acetylcysteine, xCT and suppression of Maxi-chloride channel activity in human placenta. *Placenta*, *110*, 46–55. https://doi.org/10.1016/j.placenta.2021.05.009

Love, M. I., Huber, W., & Anders, S. (2014). Moderated estimation of fold change and dispersion for RNA-seq data with DESeq2. *Genome Biology*, *15*(12), 550. https://doi.org/10.1186/s13059-014-0550-8

Luijkx, D., Shankar, V., van Blitterswijk, C., Giselbrecht, S., & Vrij, E. (2022). From Mice to Men: Generation of Human Blastocyst-Like Structures In Vitro. *Frontiers in Cell and Developmental Biology*, *10*. https://doi.org/10.3389/fcell.2022.838356

Madjunkov, M., Madjunkova, S., & Librach, C. (2026). The biology and clinical aspects of female infertility. *Systems Biology in Reproductive Medicine*, *72*(1), 23–54. https://doi.org/10.1080/19396368.2025.2593345

Marečková, M., Garcia-Alonso, L., Moullet, M., Lorenzi, V., Petryszak, R., Sancho-Serra, C., Oszlanczi, A., Icoresi Mazzeo, C., Wong, F. C. K., Kelava, I., Hoffman, S., Krassowski, M., Garbutt, K., Gaitskell, K., Yancheva, S., Woon, E. Von, Male, V., Granne, I., Hellner, K., … Vento-Tormo, R. (2024). An integrated single-cell reference atlas of the human endometrium. *Nature Genetics*, *56*(9), 1925–1937. https://doi.org/10.1038/s41588-024-01873-w

Margarit, L., Gonzalez, D., Lewis, P. D., Hopkins, L., Davies, C., Conlan, R. S., Joels, L., & White, J. O. (2009). L-Selectin ligands in human endometrium: comparison of fertile and

infertile subjects. *Human Reproduction*, *24*(11), 2767–2777. https://doi.org/10.1093/humrep/dep247

Metsalu, T., & Vilo, J. (2015). ClustVis: a web tool for visualizing clustering of multivariate data using Principal Component Analysis and heatmap. *Nucleic Acids Research*, *43*(W1), W566–W570. https://doi.org/10.1093/nar/gkv468

Molè, M. A., Elderkin, S., Zorzan, I., Penfold, C., Horsley, N., Pokhilko, A., Polanek, M., Palomar, A., Sinha, M., Wang, Y., Quiñonero, A., Androulidakis, C., Acton, R., Balmanno, K., Jarman, A., Srinivasan, J., Bendall, A., Morales-Álvarez, S., Yagüe-Serrano, R., … Rugg-Gunn, P. J. (2026). Modeling human embryo implantation in vitro. *Cell*, *189*(1), 87-105.e28. https://doi.org/10.1016/j.cell.2025.10.027

Moreno, I., Capalbo, A., Mas, A., Garrido-Gomez, T., Roson, B., Poli, M., Dimitriadis, E., Santamaria, X., Vilella, F., & Simon, C. (2023). The human periconceptional maternal-embryonic space in health and disease. *Physiological Reviews*, *103*(3), 1965–2038. https://doi.org/10.1152/physrev.00050.2021

Nguyen, T. T.-T. N. (2024). *Deciphering the Molecular Mechanisms of Human Platelet Lysate as a Treatment for Recurrent Implantation Failure and a Thin Endometrium* [PhD]. University of Toronto.

Opuchlik, K., Pankiewicz, K., Pierzyński, P., Sierdziński, J., Aleksejeva, E., Salumets, A., Issat, T., & Laudański, P. (2025). Factors influencing endometrial receptivity in women with recurrent implantation failure. *BMC Women's Health*, *25*(1), 15. https://doi.org/10.1186/s12905-024-03531-z

Poh, Q. H., Rai, A., Salamonsen, L. A., & Greening, D. W. (2023). Omics insights into extracellular vesicles in embryo implantation and their therapeutic utility. *PROTEOMICS*, *23*(6). https://doi.org/10.1002/pmic.202200107

Price, T. S., Grosser, T., Plomin, R., & Jaffee, S. R. (2010). Fetal Genotype for the Xenobiotic Metabolizing Enzyme *NQO1* Influences Intrauterine Growth Among Infants Whose Mothers Smoked During Pregnancy. *Child Development*, *81*(1), 101–114. https://doi.org/10.1111/j.1467-8624.2009.01383.x

Radley, A., Corujo-Simon, E., Nichols, J., Smith, A., & Dunn, S.-J. (2023). Entropy sorting of single-cell RNA sequencing data reveals the inner cell mass in the human pre-implantation embryo. *Stem Cell Reports*, *18*(1), 47–63. https://doi.org/10.1016/j.stemcr.2022.09.007

Rodriguez, C., Pozo, M., Nieto, E., Fernandez, M., & Alemany, S. (2006). TRAF6 and Src kinase activity regulates Cot activation by IL-1. *Cellular Signalling*, *18*(9), 1376–1385. https://doi.org/10.1016/j.cellsig.2005.10.016

Rossant, J., & Tam, P. P. L. (2022). Early human embryonic development: Blastocyst formation to gastrulation. *Developmental Cell*, *57*(2), 152–165. https://doi.org/10.1016/j.devcel.2021.12.022

Rubin, S. C., Abdulkadir, M., Lewis, J., Harutyunyan, A., Hirani, R., & Grimes, C. L. (2023). Review of Endometrial Receptivity Array: A Personalized Approach to Embryo Transfer and Its Clinical Applications. *Journal of Personalized Medicine*, *13*(5), 749. https://doi.org/10.3390/jpm13050749

Rugg-Gunn, P. J., Moris, N., & Tam, P. P. L. (2023). Technical challenges of studying early human development. *Development*, *150*(11). https://doi.org/10.1242/dev.201797

Ruiz-Alonso, M., Blesa, D., & Simón, C. (2012). The genomics of the human endometrium. *Biochimica et Biophysica Acta (BBA) - Molecular Basis of Disease*, *1822*(12), 1931–1942. https://doi.org/10.1016/j.bbadis.2012.05.004

Salilew-Wondim, D., Hölker, M., Rings, F., Ghanem, N., Ulas-Cinar, M., Peippo, J., Tholen, E., Looft, C., Schellander, K., & Tesfaye, D. (2010). Bovine pretransfer endometrium and embryo transcriptome fingerprints as predictors of pregnancy success after embryo transfer. *Physiological Genomics*, *42*(2), 201–218. https://doi.org/10.1152/physiolgenomics.00047.2010

Salleh, N. (2014). Diverse roles of prostaglandins in blastocyst implantation. *TheScientificWorldJournal*, *2014*, 968141. https://doi.org/10.1155/2014/968141

Sang, Q., Li, B., Kuang, Y., Wang, X., Zhang, Z., Chen, B., Wu, L., Lyu, Q., Fu, Y., Yan, Z., Mao, X., Xu, Y., Mu, J., Li, Q., Jin, L., He, L., & Wang, L. (2018). Homozygous Mutations in WEE2 Cause Fertilization Failure and Female Infertility. *The American Journal of Human Genetics*, *102*(4), 649–657. https://doi.org/10.1016/j.ajhg.2018.02.015

Shibata, S., Endo, S., Nagai, L. A. E., H. Kobayashi, E., Oike, A., Kobayashi, N., Kitamura, A., Hori, T., Nashimoto, Y., Nakato, R., Hamada, H., Kaji, H., Kikutake, C., Suyama, M., Saito, M., Yaegashi, N., Okae, H., & Arima, T. (2024). Modeling embryo-endometrial interface recapitulating human embryo implantation. *Science Advances*, *10*(8). https://doi.org/10.1126/sciadv.adi4819

Siriwardena, D., & Boroviak, T. E. (2022). Evolutionary divergence of embryo implantation in primates. *Philosophical Transactions of the Royal Society of London. Series B, Biological Sciences*, *377*(1865), 20210256. https://doi.org/10.1098/rstb.2021.0256

Skogler, J., Moberg, T., Tancredi, L., Styrmisdóttir, L., Hedayati, E., Alarcon-Ruiz, C. A., Khamis, A., Persad, E., Iskandarani, G., Hansson, S. R., & Bruschettini, M. (2023). Association between human chorionic gonadotropin (hCG) levels and adverse pregnancy outcomes: A systematic review and meta-analysis. *Pregnancy Hypertension*, *34*, 124–137. https://doi.org/10.1016/j.preghy.2023.11.003

Song, J., Zhao, R., Zhang, Y., Lu, M., Liu, P., Li, T., Li, C., Yu, R., Chen, X., Yang, H., Zhang, X., Su, Y., Han, Y., Sun, D., Zhou, Q., Hou, Z., Liu, W., Gao, X., Tao, W., … Zhao, H. (2026). 3D post-implantation co-culture of human embryo and endometrium. *Cell Stem Cell*, *33*(1), 58-72.e7. https://doi.org/10.1016/j.stem.2025.12.002

Sousa, L. G., Correia-da-Silva, G., Teixeira, N., & Fonseca, B. M. (2025). Specialized pro-resolving mediators: key regulators in placental function and pregnancy complications. *Journal of Molecular Medicine*, *103*(8), 885–897. https://doi.org/10.1007/s00109-025-02561-w

Sponchiado, M. (2019). *Deciphering the embryo-maternal interactome: Embryo-dependent programming of endometrial function during early pregnancy in cattle* [PhD]. University of São Paulo.

Steptoe, P. C., & Edwards, R. G. (1978). Birth After The Reimplantation of a Human Embryo. *The Lancet*, *312*(8085), 366. https://doi.org/10.1016/S0140-6736(78)92957-4

Su, R.-W., & Fazleabas, A. T. (2015). *Implantation and Establishment of Pregnancy in Human and Nonhuman Primates* (pp. 189–213). https://doi.org/10.1007/978-3-319-15856-3_10

Suhorutshenko, M., Kukushkina, V., Velthut-Meikas, A., Altmäe, S., Peters, M., Mägi, R., Krjutškov, K., Koel, M., Codoñer, F. M., Martinez-Blanch, J. F., Vilella, F., Simón, C., Salumets, A., & Laisk, T. (2018). Endometrial receptivity revisited: endometrial transcriptome adjusted for tissue cellular heterogeneity. *Human Reproduction*, *33*(11), 2074–2086. https://doi.org/10.1093/humrep/dey301

Tepekoy, F., Akkoyunlu, G., & Demir, R. (2015). The role of Wnt signaling members in the uterus and embryo during pre-implantation and implantation. *Journal of Assisted Reproduction and Genetics*, *32*(3), 337–346. https://doi.org/10.1007/s10815-014-0409-7

Thiyagarajan, D. K., Basit, H., & Jeanmonod, R. (2026). *Physiology, Menstrual Cycle*.

Thowfeequ, S., Hanna, C. W., & Srinivas, S. (2025). Origin, fate and function of extraembryonic tissues during mammalian development. *Nature Reviews Molecular Cell Biology*, *26*(4), 255–275. https://doi.org/10.1038/s41580-024-00809-w

Tinning, H., Vasconcelos, E. J. R., Wang, D., & Forde, N. (2025). A bovine 3D endometrium-on-a-chip reveals the role of conceptus-derived proteins, CAPG and PDI, in conceptus–endometrial communication. *Biology of Reproduction*, *113*(1), 61–82. https://doi.org/10.1093/biolre/ioaf077

Turco, M. Y., Gardner, L., Hughes, J., Cindrova-Davies, T., Gomez, M. J., Farrell, L., Hollinshead, M., Marsh, S. G. E., Brosens, J. J., Critchley, H. O., Simons, B. D., Hemberger, M., Koo, B.-K., Moffett, A., & Burton, G. J. (2017). Long-term, hormone-responsive organoid cultures of human endometrium in a chemically defined medium. *Nature Cell Biology*, *19*(5), 568–577. https://doi.org/10.1038/ncb3516

Van der Auwera, G. A., & O'Connor, B. D. (2020). *Genomics in the Cloud: Using Docker, GATK, and WDL in Terra* (1st Edition). O'Reilly Media.

van Loendersloot, L. L., van Wely, M., Limpens, J., Bossuyt, P. M. M., Repping, S., & van der Veen, F. (2010). Predictive factors in in vitro fertilization (IVF): a systematic review and meta-analysis. *Human Reproduction Update*, *16*(6), 577–589. https://doi.org/10.1093/humupd/dmq015

Voros, C., Sapantzoglou, I., Mavrogianni, D., Athanasiou, D., Varthaliti, A., Bananis, K., Athanasiou, A., Athanasiou, A., Papahliou, A.-M., Zografos, C. G., Gkirgkinoudis, A., Papapanagiotou, I., Migklis, K., Mazis Kourakos, D., Papadimas, G., Daskalaki, M. A., Antsaklis, P., Loutradis, D., & Daskalakis, G. (2025). Unlocking Implantation: The Role of Nitric Oxide, NO2-NO3, and eNOS in Endometrial Receptivity and IVF Success—A Systematic Review. *International Journal of Molecular Sciences*, *26*(14), 6569. https://doi.org/10.3390/ijms26146569

Wang, W., Vilella, F., Alama, P., Moreno, I., Mignardi, M., Isakova, A., Pan, W., Simon, C., & Quake, S. R. (2020). Single-cell transcriptomic atlas of the human endometrium during the menstrual cycle. *Nature Medicine*, *26*(10), 1644–1653. https://doi.org/10.1038/s41591-020-1040-z

Weimar, C. H. E., Kavelaars, A., Brosens, J. J., Gellersen, B., de Vreeden-Elbertse, J. M. T., Heijnen, C. J., & Macklon, N. S. (2012). Endometrial Stromal Cells of Women with Recurrent Miscarriage Fail to Discriminate between High- and Low-Quality Human Embryos. *PLoS ONE*, *7*(7), e41424. https://doi.org/10.1371/journal.pone.0041424

Xavier, G. M., Sharpe, P. T., & Cobourne, M. T. (2009). Scube1 is expressed during facial development in the mouse. *Journal of Experimental Zoology Part B: Molecular and Developmental Evolution*, *312B*(5), 518–524. https://doi.org/10.1002/jez.b.21260

Yang, H. (2025). Spatiotemporal Frameworks of Morphogenesis and Cell Lineage Specification in Pre- and Peri-Implantation Mammalian Embryogenesis: Insights and Knowledge Gaps from Mouse Embryo. *Biology*, *14*(11), 1596. https://doi.org/10.3390/biology14111596

Yu, L., Logsdon, D., Pinzon-Arteaga, C. A., Duan, J., Ezashi, T., Wei, Y., Ribeiro Orsi, A. E., Oura, S., Liu, L., Wang, L., Liu, K., Ding, X., Zhan, L., Zhang, J., Nahar, A., Stobbe, C., Katz-Jaffe, M., Schoolcraft, W. B., Tan, T., … Wu, J. (2023). Large-scale production of human blastoids amenable to modeling blastocyst development and maternal-fetal cross talk. *Cell Stem Cell*, *30*(9), 1246-1261.e9. https://doi.org/10.1016/j.stem.2023.08.002

Yu, S.-L., Kim, T.-H., Han, Y.-H., Kang, Y., Jeong, D.-U., Lee, D. C., Kang, J., & Park, S.-R. (2021). Transcriptomic analysis and competing endogenous RNA network in the human endometrium between proliferative and mid-secretory phases. *Experimental and Therapeutic Medicine*, *21*(6), 660. https://doi.org/10.3892/etm.2021.10092

Zhuang, J., Deane, J. A., Yang, R. B., Li, J., & Ricardo, S. D. (2010). SCUBE1, a novel developmental gene involved in renal regeneration and repair. *Nephrology Dialysis Transplantation*, *25*(5), 1421–1428. https://doi.org/10.1093/ndt/gfp637

NON-EXCLUSIVE LICENCE TO REPRODUCE THESIS AND MAKE THESIS PUBLIC

I, Brayan Stiveen Rodriguez Morales ,
(author´s name)

1. grant the University of Tartu a free permit (non-exclusive licence) to

   reproduce, for the purpose of preservation, including for adding to the digital archives of the University of Tartu until the expiry of the term of copyright, my thesis

   Molecular Crosstalk at the Endometrium–Embryo Interface ,
   (title of thesis)

   supervised by Alberto Sola Leyva, Amruta Pathare, and Apostol Apostolov ;
   (supervisor´s name)

2. grant the University of Tartu a permit to make the thesis specified in point 1 available to the public via the web environment of the University of Tartu, including via the digital archives, under the Creative Commons licence CC BY NC ND 4.0, which allows, by giving appropriate credit to the author, to reproduce, distribute the work and communicate it to the public, and prohibits the creation of derivative works and any commercial use of the work until the expiry of the term of copyright;

3. am aware of the fact that the author retains the rights specified in points 1 and 2;

4. confirm that granting the non-exclusive licence does not infringe other persons' intellectual property rights or rights arising from the personal data protection legislation.

Brayan Stiveen Rodriguez Morales

20/05/2026

APPENDICES

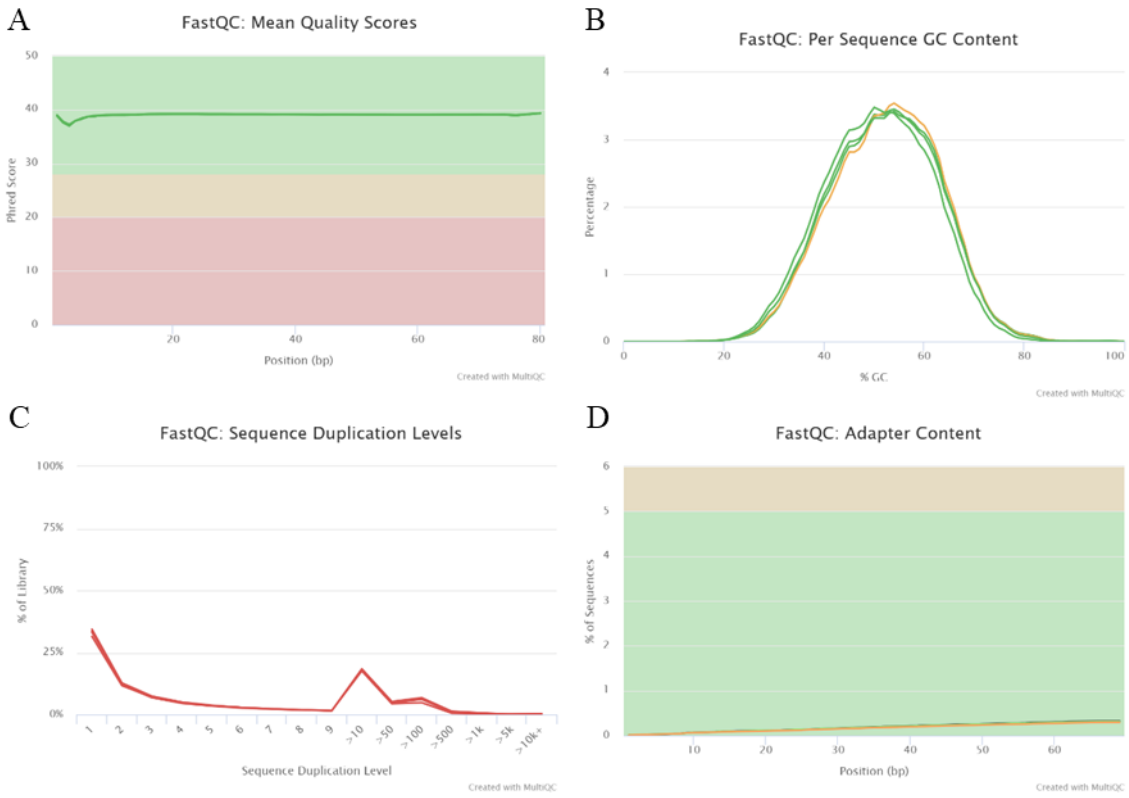

Supplementary figure 1. MultiQC report of aggregated results from FastQC. A. Mean quality Scores of each FASTQ file. Green area shows good quality calls, orange shows reasonable quality and red shows poor quality reads. B. Percentage of GC content across the whole length of each sequence compared to a modelled normal distribution of GC content. C. Relative level of duplication found for every sequence. D. Cumulative percentage count of the proportion of the library which has seen each of the adapter sequences at each position.

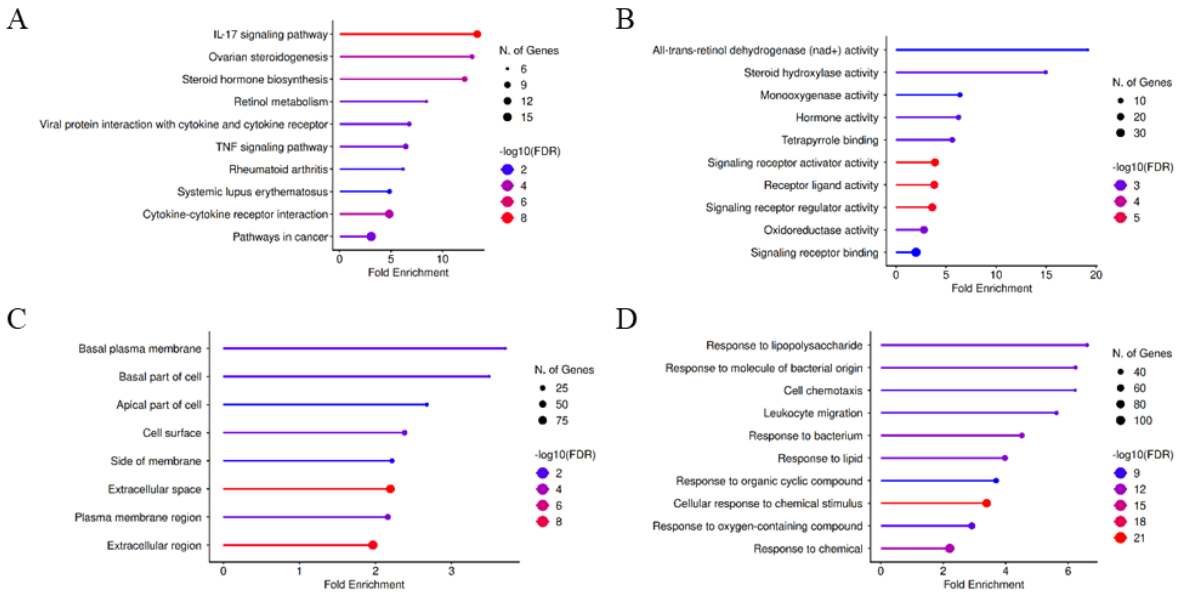

Supplementary figure 2. Functional enrichment analysis of significatively differentially expressed upregulated genes. A. KEGG pathway database. B. Go Molecular Function pathway database. C. Cellular component pathway database. D. Go Biological process pathway database.

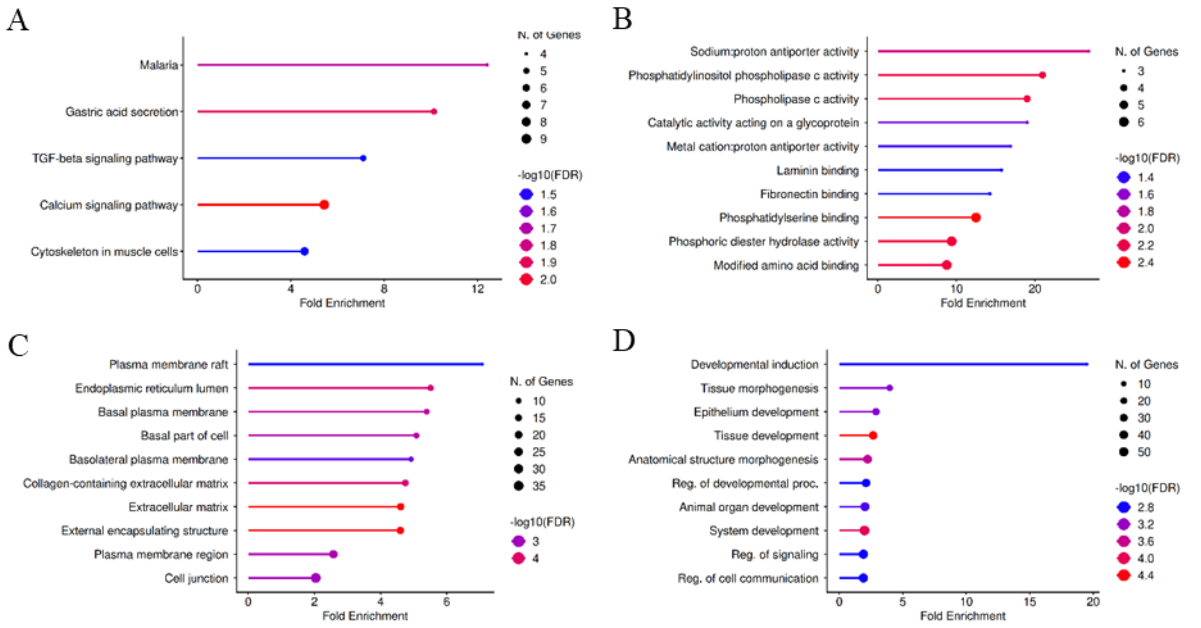

Supplementary figure 3. Functional enrichment analysis of significatively differentially expressed downregulated genes. A. KEGG pathway database. B. Go Molecular Function pathway database. C. Cellular component pathway database. D. Go Biological process pathway database.

Supplementary table 1. Upregulated significatively differentially expressed genes during in-vitro implantation of blastoid to OFEL under hormonal treatment using a Log2 fold change higher than 1 and p-adjusted value below of 0.05.

GeneID	log2(FC)	P-adj
CYP1A1	7.53146617943326	3.5152817494036e-53
CACNA1S	7.10646472360617	5.57189943867618e-08
IL19	6.57282332352109	4.32116624960786e-07
HP	5.64823747664758	3.76194785976228e-05
GPR15	5.48048477916177	0.004592467715505
CYP1B1	5.47259412418066	4.0830734054601306e-52
PGLYRP4	5.4663041737334	0.0029137397988545
IL36A	5.41605127066692	5.26282076967554e-07
CPXM1	5.41323425211745	4.16142411464877e-05
APCDD1L	5.11909126606163	0.0001086557248377
MMP12	5.03144273808389	0.0174501941917868
S100A8	4.95984018885648	0.0031346047566362
PPP1R1A	4.69943161061321	0.0085375402086765
SCUBE1	4.48914913351873	0.0448350135167181
SLC5A5	4.48404872438897	1.12089974894566e-06
CSF3	4.37996490523441	4.4632588395534e-07
DEFB4A	4.28772462959261	0.0028134529785757
PARM1	4.17993138279405	0.0010017287067221
KCND3	4.12995779377686	0.0179915653993745
CEACAM5	3.96707013686988	0.0048646563231441
KIT	3.95955960725663	0.0026708912516291
PRR9	3.94352062951621	1.70484163136597e-06
ADAMTS20	3.89856041714373	1.89574337032539e-06
PHOSPHO1	3.89273454373377	1.03092962722725e-08
ADH1C	3.89243919891456	0.0357947388428491
PLAC4	3.76636996582611	0.0251802823490791
UNC13A	3.67394336609422	1.69814454139389e-07
TNFAIP6	3.66073317204146	0.0035912984344568
CGB5	3.60129953053213	2.12368527718059e-06
CYP1B1-AS1	3.58837896483543	0.0003733760267555
ERVFRD-1	3.58141484647796	0.0045163572452272
TCN1	3.56849087960033	2.54834408172797e-36
CGB8	3.53684127437611	3.10968915406806e-05
ENSG00000267943	3.510498801165	9.8019134041766e-06
IL36G	3.4977373553961	0.0002226741221676
GPR68	3.49263573302254	0.0002091919130181
ERVV-1	3.44962702903394	0.0002091919130181
CGB3	3.42568716270893	2.17152337899474e-07
SRD5A2	3.4236174829345	2.69797281471198e-08
ANGPT4	3.41044092120548	0.0015528954012784
ALDH3A1	3.40314296809071	4.36478934371899e-05
NOS2	3.40242132797154	8.60717980515306e-07
CCR8	3.36960432093585	0.0371223905564229
TNIP3	3.34167328169938	0.0008155847812496

CGA	3.32597106698316	2.48419625642238e-07
SLC22A11	3.30620506597694	0.0330559485604127
ATOH8	3.28178422902505	0.0195848628310554
TREML2	3.27742645157527	1.38093934296799e-08
ERVV-2	3.23971407085288	0.0003619144474439
ENSG00000287059	3.21325956186425	0.045958854946132
FEZ1	3.21145427547992	1.97415344432713e-12
C4orf54	3.20395569889834	3.9741916336626e-05
LGALS16	3.2014343976513	2.6873122645466e-06
HSD17B2	3.17658790671811	0.0110596303817907
LCMT1-AS2	3.12858222231113	3.79578721234528e-07
ENDOU	3.09716230471825	0.0360802788145451
IRAK3	3.07577218181765	2.70768190732249e-05
GCM1	3.06030313327078	3.20074769078745e-07
SERPINB7	3.06011456398703	0.0074411934974529
CYP19A1	3.04110879330077	4.10728082699067e-05
CGB7	3.03660443239732	0.0005350859050371
HOPX	3.01591639956211	0.0174501941917868
ERVW-1	2.98717930149228	6.83481485653608e-05
TREM1	2.98417682659777	0.0025909256990664
ESRG	2.97695216622897	0.0042926103366682
EPB41L3	2.9364174352958	0.0005676367253191
PGF	2.91714509228811	0.0001445222023636
MEGF11	2.83556373012253	1.83085703510361e-05
CCR7	2.83545488813739	0.0001396095543842
SCNN1D	2.83467327637557	0.0237399120660427
FGF4	2.81308213483204	0.02231145295747
CLEC1A	2.8119820107732	0.0058027956170207
GFPT2	2.80728567930225	2.89812657448967e-05
TRPV2	2.79694205728004	0.0029749829326877
SLC16A6	2.78173778602448	0.0388272389315548
WNT10B	2.77475520141928	0.0490741581652775
S100A9	2.74455523472753	0.0025987354164579
SLC38A3	2.72274301833726	8.68922432091665e-05
MUC5AC	2.72037084551511	2.63669833744854e-15
FNDC4	2.70704020841846	0.000503683922174
TBX3	2.69703944208922	1.52524174383121e-06
SLC43A2	2.69232508580706	0.0299816695587964
ECE1-AS1	2.64858492456031	4.65272283290076e-06
SOX2	2.60402497904892	0.0077629974191648
TIPARP	2.59025923389747	2.75253132170002e-43
CYP11A1	2.5679767758897	0.0015843339613178
HS3ST3A1	2.56364021285209	0.0064665268831339
CSF2	2.53661562396871	0.0185091933862198
MUC15	2.5356022162212	1.91767526826358e-05
LYPD5	2.53403252710317	0.0009743061091941
DUOX2	2.5243802430956	7.4923553672902e-05
AQP3	2.52279978302115	0.0001797879927018

ITPRID1	2.50714753143304	0.0046004138389604
SV2B	2.46514530658218	0.0142222085047375
SELL	2.45280846052445	5.38224633553465e-08
MRGPRX1	2.44504897321525	0.0030173812674891
C1S	2.41698930010489	5.97931751816821e-13
IQCD	2.41656224820072	3.35265844963096e-05
PI3	2.36008482957973	0.0127686895022595
SPX	2.35680409187585	0.0062996264992223
RNASE1	2.3400440875967	0.0002721431108845
ADGRA2	2.31407701267112	0.0428210135777537
IL17C	2.31028015069393	0.0002197658971629
TLE1P1	2.2927024919595	0.0105502267900927
KCNK3	2.28580278503739	0.0002334652044818
XDH	2.28285963592798	8.85583001622314e-11
CYP24A1	2.23804536889173	1.78604888208983e-06
GPX2	2.23726996443121	0.0089128965403671
CECR2	2.23539294819849	0.0401224556776706
ENSG00000253400	2.22647554344805	0.0020159141952705
MMP1	2.21874285427965	0.018777646441734
CEBPA	2.21006549560493	0.0046257315365211
CD83	2.20627749721691	0.0208984674941806
GPR32	2.19181402202334	0.0020547358262036
SHISA2	2.17142683709213	3.2952932790965e-33
C1R	2.17128258246096	1.58684588068432e-05
DHRS9	2.17033298005572	3.41845008069776e-05
SP6	2.15816835444976	0.0053897933125039
FBN1	2.14262284163712	0.0133833050125217
ABCA13	2.13063148272204	0.0017517233264585
FOXI3	2.09757771737216	0.0058131324426772
SLC6A14	2.09526172410256	1.75313989374548e-07
FOXA3	2.08068961409462	0.0202774943653524
POU2F3	2.06163183691799	0.0344939140522587
H2BC4	2.05588606077079	0.0203232190506666
RARRES1	2.04907381412691	0.0111586967726198
TNFRSF1B	2.02159380942454	2.78717651414817e-06
SLC16A10	2.01994540982985	0.0240952082395904
GJB2	2.01961872878234	2.31688714853666e-10
STAU2-AS1	2.0145879867555	0.035227436100401
HMGN2P46	2.00396661202016	0.0002316225581603
NXPE2	2.0029093215319	0.0327840285798889
CYP1A2	1.99647862370896	0.0488244358943225
FOXO6	1.99218968723027	0.0033231927792642
LAPTM5	1.95372475579813	0.0001797879927018
LYPD3	1.95159915324643	0.0012187709421242
THBD	1.94753054247266	0.003790641882842
C15orf48	1.9296813333634	0.0142336114354793
GJB6	1.91196376713755	2.2472685746232e-06
CD34	1.90570117270384	3.62815667392607e-07

ZNF750	1.87743776361542	0.0003498603764032
RDH10	1.8719177559507	5.78549974296632e-07
IL1B	1.86237418807715	0.0003260175342968
ENSG00000289866	1.86042099475351	0.0105621747701862
LINC01559	1.84975095688797	0.0045156131845644
TXNRD1	1.83969449464651	3.61693046032595e-08
GPR132	1.82206151158147	0.0271202700474922
ADGRE2	1.8174693675276	0.0412067727629358
FAXDC2	1.81330175153799	0.0085335712952507
SLC28A3	1.80597163134301	1.34809312758019e-05
IGF2BP1	1.79465495045599	0.0129742013224914
BNIP5	1.75988943212205	0.0127686895022595
ENSG00000289223	1.756795062432	0.0084304910376374
GPR78	1.75138723002831	0.0481438677075531
BMF	1.74191561156198	1.09795707240467e-11
EVA1C	1.7276191134994	0.0191052591559099
RNF224	1.71079313140459	0.0291477425676207
XYLT1	1.70415433337288	0.030809445273961
ATP10D	1.70105090594829	0.0009294005143747
GATA2	1.69164231112671	0.0011590971116129
CCL22	1.6845842395792	0.0259950870853553
PRDM1	1.64983568572601	1.27977163741547e-05
HEY1	1.63550252188968	0.0401852486124738
H2BC11	1.63001689480956	0.0192645737546355
ATP10B	1.61047996162468	0.0016124598101291
TCP11L2	1.60176860078915	2.78955258030154e-07
CAPN13	1.59648506640655	0.0498733105256068
KCNJ4	1.59014635155815	0.0278133066837859
BAIAP3	1.58698882584099	0.0107010927113059
TPPP	1.57958839215514	0.030809445273961
SOD2	1.56906957133963	3.42229817168462e-06
CCL20	1.56336164480375	0.0060623507293312
ADCY5	1.56200278567875	0.0211875809775457
TP73	1.55085481633018	0.0184546857895677
NFKBIZ	1.54693354787186	2.30464952585068e-06
CHST6	1.53871874956058	3.43246041361008e-07
SLC46A3	1.5300693559322	0.0461630794527049
ADD2	1.51024305068347	0.034272216305832
ENSG00000288927	1.50089128947237	0.0360375457947076
ENSG00000228509	1.49658588385039	0.0167233527782042
MN1	1.49500147759462	0.0124289893541873
PORCN	1.49303672170955	2.48419625642238e-07
SLC22A4	1.48063708552589	0.0111451473305445
CD69	1.46839347823026	6.24306577701131e-17
SGK1	1.46287936557169	3.37821163236496e-27
H2BC21	1.46256930783534	0.0002676740469424
PTAFR	1.45759122135381	2.03383067928227e-08
GAS7	1.4450432092239	0.0020658841509859

RHOV	1.44082037933911	3.84329998663997e-10
ALPG	1.42753352272361	0.0317442523265033
RRAD	1.42695626876812	0.0035912984344568
SYT7	1.42641014663102	0.0457163193129616
GPR15LG	1.40904366817068	0.0242783242256159
STC2	1.40429615215647	0.0012867839067212
LINC00240	1.39761598770203	0.000130110139239
SRD5A3	1.38779282482991	1.07836309729453e-08
CIITA	1.37819446771226	3.84329998663997e-10
HAVCR1	1.35366685489056	0.0315804852244659
ALPL	1.35190276148173	0.0038243698169168
TMEM45B	1.3451488232918	0.0020290313634171
MMP2	1.34316510051138	0.0105621747701862
IZUMO4	1.3365965621477	0.0287627558452096
RAB31	1.33645619604871	3.12965730163497e-07
ATF3	1.33236058613158	0.0300811888353076
CEACAM6	1.32877022885618	0.0001974437605934
CLDN10	1.32555058775435	8.71652262011065e-13
PLPP3	1.32318201991438	0.001745384896895
PLA2R1	1.31555494857416	6.19244810597795e-08
RIPOR2	1.30153522509405	0.0375167698605499
ECE1	1.30042172899813	1.4524707592326102e-14
SLC26A9	1.29974215463363	0.0126017586427011
DSE	1.29944514069792	2.87163385862629e-06
FAR2	1.29279686744731	0.0371223905564229
EDC3	1.28022235005164	2.05575749889331e-26
RASGRP1	1.28009094335282	1.03888758489681e-09
AIFM2	1.27234170495442	0.0041789576570095
FBXO32	1.27208543625028	2.22915093098403e-12
PLD1	1.2646063666184	0.0012187709421242
H2BC5	1.26263153036013	0.0074504033120029
SNPH	1.26077591014831	0.0003568680337143
RETREG1	1.25358033449992	5.61622969915525e-09
BIRC3	1.23624960366145	1.87973735088296e-11
ERFE	1.23310914175667	6.16050652817002e-06
MAST4	1.20647287752283	1.27977163741547e-05
SOCS1	1.19933174708129	0.0013707999729986
TNFAIP3	1.19192240234384	8.68922432091665e-05
FHDC1	1.19159625779134	1.37444929663529e-07
IFNAR2	1.19044822272556	0.0003038601177667
NFKBID	1.18614237639424	0.0007166117422076
ZC3H12A	1.18465999237592	1.30733748258966e-05
SLC7A11	1.18328787540867	0.0101817510952992
GCNT3	1.18235768176698	0.0009140758254448
RAB3IL1	1.18210061890146	0.0127686895022595
MELTF	1.17983070609262	2.29248545103762e-05
ADGRF1	1.17189916789877	0.0100191537937861
CA2	1.16716722661855	0.0150728083509266

H2AC6	1.16714549445757	0.0049011774905865
MUC5B	1.15142123032577	0.0476948368419028
FUT8-AS1	1.15112874948705	0.0469250882100756
LYN	1.14453384092858	1.20908918352642e-12
FUT2	1.14082368831755	0.0003619144474439
ADAM28	1.13666160000187	0.016237809238247
CXCL2	1.13550920858246	0.0053897933125039
BHLHA15	1.13204929592896	0.0329571279690539
LINC01320	1.11874545875708	0.0499937585671276
MPP1	1.10549482000591	0.0322759623237806
NQO1	1.09183439559459	0.0091876125842794
ENSG00000290032	1.08890951881244	0.0006071478186572
P2RX4	1.08667154755906	0.0023397794624435
TTC39C	1.08404166348906	0.0026708551778155
SDR16C5	1.0828198801954	0.0287854432166704
ENSG00000227619	1.0826381127755	0.033951916376438
ICAM2	1.08151166742922	0.0483267081203204
NDRG2	1.07944668409484	0.0015394305586599
TMC5	1.07919933851018	1.35620786494704e-05
CDHR1	1.06670130355732	7.3378631949652605e-09
SERPINA1	1.06011578174829	1.60692350536748e-06
PACSIN1	1.05529726456897	0.0020547358262036
TNFRSF11A	1.04315298251271	0.0205881995107535
GDA	1.04111604963644	0.0283231171937777
PIK3R1	1.01697965208718	0.0030207615634171
FAM83E	1.01144439999618	2.17514335130666e-06
TFAP2C	1.00121653841479	0.0267659168526515
SPDEF	1.00032614688438	0.0401852486124738

Supplementary table 2. Downregulated significatively differentially expressed genes during in-vitro implantation of blastoid to OFEL under hormonal treatment using a Log2 fold change lower than -1 and p-adjusted value below of 0.05.

GeneID	log2(FC)	P-adj
LIX1	-6.72876814241006	0.0043006480167473
SEMA3E	-5.82885440137721	2.32201013547359e-05
PALMD	-5.45496524630048	0.0006759024017022
ANKRD1	-5.41390852617123	2.7668591376838697e-26
MAMDC2	-4.7081884813599	0.0146807606149437
TMEM255A	-4.23827266948789	0.0420808483863601
DKK1	-4.06417156278104	3.77308495866592e-05
NR2F1-AS1	-3.89381429670265	0.0035912984344568
IGFBP5	-3.66033986160879	4.80315695593877e-06
VIM	-3.49759384137267	4.06538002017864e-07
ALPK2	-3.4499205701528	5.29442066874247e-11
SLC22A2	-3.4303249508098	0.020762506184588
BMP4	-3.23303604169691	2.16792939821054e-09
UPK3B	-3.17387258446128	1.12150547724865e-06
FBN2	-3.16011538837783	3.08505859368981e-07
MSI1	-2.9570052055112	3.50557182384607e-05
WNT2B	-2.94605135462611	8.20114085193352e-08
LINC01618	-2.92589372754661	0.038603667017663
IGDCC4	-2.92053446623378	0.0073817554954307
SERPINB5	-2.85158320574074	0.003127930298891
SH2D5	-2.85084234375666	1.28048108841716e-07
MIR1915HG	-2.83751493256009	0.0031547560009889
SH3GL3	-2.83166740564788	0.0022954871853462
GRPR	-2.77496284906467	0.0048929650931142
DKK3	-2.76630990676707	7.4923553672902e-05
MEOX1	-2.73252214944297	1.68592546810498e-09
NXPH4	-2.71483961094664	0.0046354317953067
THBS1	-2.66047761937901	5.912573134404491e-17
KIAA1549L	-2.56455842542869	0.0161874129451327
GASK1B	-2.56024671021531	3.61573495513994e-13
ST6GALNAC5	-2.55408544052331	0.0450727347547914
NR2F2-AS1	-2.54462439694096	0.0270207051030453
PDE7B	-2.51843217272136	0.0185561098954267
SYT13	-2.51274180021346	0.0407007303177552
AJAP1	-2.4854873734505	0.0234196194710431
ENSG00000291105	-2.4455406911928	0.0161874129451327
SLC9A4	-2.43811714925037	0.003534703425154
LINC02009	-2.40528709466921	0.0029200824429894
LMCD1	-2.37060552151689	8.81576806375017e-06
CCN2	-2.37025634641697	1.50844523941025e-19

IRS1	-2.33945988950418	0.0169788534104395
PLCE1	-2.33624365898659	0.0005308537552128
PPP1R3B-DT	-2.32189352558618	4.04453296520255e-07
MATN3	-2.31667831007721	0.0135310584722192
KLRK1-AS1	-2.31162393252084	3.50557182384607e-05
RBMS3	-2.30854627543	1.37415553040243e-09
PTPRB	-2.29311885572171	0.0002044706235728
PSG4	-2.24927123092544	0.0001928770843136
LINC01091	-2.2473301544836	0.0458646321432713
CCDC80	-2.21332171069465	1.75909695812211e-08
SLIT3	-2.18422992886565	0.0309062218337523
DENND2A	-2.17101865649581	0.0002565130503283
CAVIN2	-2.13214917315941	0.0362829237887326
ENSG00000228613	-2.11432783938611	0.0431216052765217
TNFRSF19	-2.10001365872792	0.0375581163667178
NT5DC3	-2.08297264498681	0.0058027956170207
CNGA1	-2.07646962324833	0.0360802788145451
ARHGDIB	-2.0631015635652	1.58876912391744e-23
MYLK	-2.05804349250663	2.95946858171268e-09
CDH6	-2.02215810838417	0.0056023943019182
KCTD12	-2.02163146001188	0.0001816072153739
RGMA	-1.96685932506452	4.28010240174806e-27
PLEKHG4B	-1.93647095453197	0.0001171812353716
TRIL	-1.91912501746191	0.0171489804241647
IL18	-1.8948427218176	0.0011590971116129
ENC1	-1.84776246356265	0.0012330706723931
ERP27	-1.84047888274039	0.0419521820123712
KCNIP3	-1.83954540189802	0.0025845251786347
SOX9	-1.83674689177918	3.7459935269497203e-17
SYTL2	-1.83379313615728	5.48204722560082e-08
SDC2	-1.82938317466446	2.70768190732249e-05
MGAT5B	-1.82533679704233	1.77860481251246e-08
RHOBTB3	-1.81936562278524	3.14250179521823e-13
GPC1-AS1	-1.81405325507594	1.23734191521611e-05
OXTR	-1.80170445752472	0.000145630465619
HMGA2	-1.78438049650747	6.7263026196693e-08
LINC02672	-1.7780422517955	0.0420808483863601
SLC1A3	-1.75778181073672	0.0014624495017565
PLCXD2	-1.75755422803366	0.0024680786408822
SNHG12	-1.75085952925798	0.0014428341703446
KRT13	-1.75033438279995	0.0339687643918957
PTPRR	-1.75031986080383	0.0140967202900171
HHEX	-1.7351424226679	2.42641271845868e-06
SCD5	-1.72735703116153	6.0815562040286e-06

KRT8P45	-1.72395425184675	0.0340239516728692
ANKRD2	-1.71411272226735	0.0322960715861965
PRSS23	-1.71148397529246	6.60387103702956e-06
COL26A1	-1.69323313017884	0.0150379779318828
B4GALNT4	-1.68710379652457	2.9324161036269e-05
ABTB3	-1.67137614927307	0.023377097674788
EFHD1	-1.6588565500313	0.0030173812674891
CPVL	-1.63733168539623	2.77260907749641e-05
LAYN	-1.62959047585855	0.0002346825305674
CHN2	-1.61612898490833	0.0032209046761286
ARL4C	-1.6086856077001	1.43123194649286e-07
LY6D	-1.60209229433662	0.0422444505178253
KCNJ15	-1.60009305628754	0.0173648965491266
BMPR1B	-1.56666424520011	0.0405263176723137
HMGN3	-1.56373614825513	5.39369048407882e-10
FJX1	-1.5557186493223	1.14324123199482e-07
CDH2	-1.54330558306225	0.0100587386423713
FCHO1	-1.52818836914385	0.0007854602293527
BCAM	-1.50920205006266	0.0322603109857552
SBSPON	-1.50467532017773	0.0034817314004055
IGSF9	-1.49811066079156	0.0313820940259516
LHFPL6	-1.49810124213281	0.0001974717357786
SLC9B2	-1.49382168594363	0.038209534357775
EMP1	-1.49125222811039	7.33255488800461e-21
SLC9A2	-1.47249454264892	0.0014559327344186
ANXA9	-1.46809764350908	0.0006288819356459
TSPAN4	-1.4524456633763	6.4693337171146e-08
ADAMTS14	-1.44845320479339	1.10966740736047e-05
UNC93A	-1.43381483120721	0.0135753027137044
TPM2	-1.42731700852263	0.0011590971116129
DEPDC1B	-1.40251910552778	5.79969863390113e-05
MST1	-1.39237614341084	0.0002573919728976
SNHG15	-1.3839001397892	0.0117251298105723
ARHGAP24	-1.38330233237499	0.0002002753398132
BDNF	-1.36938106609011	0.0251802823490791
KLRG2	-1.35702489345017	0.011874625968832
ELFN2	-1.3559029224243	0.0002908244397867
SLC2A1	-1.34416848224669	0.0311699530058462
EVA1A	-1.34119473025616	3.11382221977475e-07
F2R	-1.33841920869393	9.21242087930962e-06
HAGHL	-1.32648384991675	0.0047657663804452
ZBED2	-1.32027114232776	5.01397265510394e-13
SCARA3	-1.31702381901184	0.0103854055026561
CHRM3	-1.31191730406878	0.001745384896895

AMIGO2	-1.30055249293369	6.319212896933031e-15
CLIC5	-1.29979041319824	0.0002851568320005
CDK18	-1.29886627982415	1.66697652115338e-05
RNF165	-1.29853659726058	0.0107010927113059
LACTB2	-1.26926733691013	0.0001429776558754
PLCB4	-1.25738025762485	0.0105621747701862
SPON2	-1.23982360231668	0.0371223905564229
NFIX	-1.23747927851442	0.0020957017033114
THNSL1	-1.23633614710373	0.0362690830318774
STX2	-1.23256251296522	0.0046004138389604
TACC3	-1.21034745729038	0.0005985090136941
TLL2	-1.20126032821496	8.98082678620856e-05
SCEL	-1.18759305025026	1.54403044609042e-07
DCDC2	-1.18490223507134	1.42251098072897e-08
AP1S3	-1.18302293938741	0.0039044203183096
MAB21L4	-1.17154574879965	6.37381482391556e-07
GCNT4	-1.169159193652	0.0011848856785108
SCIN	-1.16784986439573	0.0479821996010298
GLDC	-1.16184780786634	0.0023708569977441
SPNS2	-1.15942838743445	7.67837824840235e-07
TMEM98	-1.15673145741652	0.0031165687714744
GDPD5	-1.14380643911789	4.97030532241943e-10
RASA3	-1.14260154557368	0.0372020885939172
MIR4435-2HG	-1.14121972519103	0.0054542194464622
NETO2	-1.13493311447702	4.09660547882568e-07
MTARC1	-1.13231760081643	0.014058171483887
TGFB2	-1.12656277723359	0.0105621747701862
ACSF2	-1.11546265076955	1.13197060362866e-06
CDCA7L	-1.11484406860271	3.40248725891871e-05
SERTAD4	-1.11391131241354	0.0208984674941806
ARSJ	-1.10560877180946	3.16270802537353e-07
AMOTL2	-1.10389425514883	5.31582391370218e-14
BHLHE41	-1.08726174784915	8.90634614589562e-07
GADD45B	-1.08320384003991	0.0028715923724701
UAP1L1	-1.07859182033145	5.50575246893399e-05
MALT1	-1.07376934756723	9.45340918019994e-06
ATP10A	-1.05808369704745	0.0078228949990687
ENSG00000275216	-1.04170319457785	0.0198811832306435
BICC1	-1.03251876269875	0.0046439774218734
ADRA1B	-1.0236849107388	0.0420808483863601
TINAGL1	-1.02205974689364	0.0142336114354793
ZFAS1	-1.01862878474719	0.0264642805957806
LTBP4	-1.01220441463523	0.0024304152364788
SPRY1	-1.00366346233617	1.10501088285408e-05

Supplementary table 3. Downregulated and upregulated origin assigned genes associated with functional enrichment analysis. Data base labeling has a initial description for downregulated genes “Down” and upregulated genes “Upp”

Fold Enrichment	**Pathway**	**Data Base**	**Gen**
26.825836216833697	GO:0015385 Sodium:proton antiporter activity	Down_GO-Molecular-Function	SLC9A2
16.890341321717139	GO:0051139 Metal cation:proton antiporter activity	Down_GO-Molecular-Function	SLC9A2
5.347193483758666	GO:0098739 Import across plasma membrane	Down_GO-Biological-Process	SLC9A2
3.152344808891 3	GO:0016324 Apical plasma membrane	Down_GO-Cellular-Component	SLC9A2
2.892181733170 18	GO:0060429 Epithelium development	Down_GO-Biological-Process	SLC9A2
2.668127820797 3	GO:0009888 Tissue development	Down_GO-Biological-Process	SLC9A2
2.660228758169 93	GO:0030855 Epithelial cell differentiation	Down_GO-Biological-Process	SLC9A2
2.574674471058 71	GO:0098590 Plasma membrane region	Down_GO-Cellular-Component	SLC9A2

1.589429860889 01	GO:0030154 Cell differentiation	Down_GO-Biological-Process	SLC9A2
1.589097552743 31	GO:0048869 Cellular developmental process	Down_GO-Biological-Process	SLC9A2
9.402870426521 12	GO:0008081 Phosphoric diester hydrolase activity	Down_GO-Molecular-Function	PDE7B
3.378068264342 77	GO:0042578 Phosphoric ester hydrolase activity	Down_GO-Molecular-Function	PDE7B
2.186489390276 66	GO:0007267 Cell-cell signaling	Down_GO-Biological-Process	PDE7B
2.127842551727 67	GO:0045202 Synapse	Down_GO-Cellular-Component	PDE7B
2.042402117596 88	GO:0030054 Cell junction	Down_GO-Cellular-Component	PDE7B
2.041422548235 92	GO:0141124 Intracellular signaling cassette	Down_GO-Biological-Process	PDE7B
3.662965587841 56	GO:0051056 Regulation of small gtpase mediated signal transduction	Down_GO-Biological-Process	CHN2

2.12784255172767	GO:0045202 Synapse	Down_GO-Cellular-Component	CHN2
2.04240211759688	GO:0030054 Cell junction	Down_GO-Cellular-Component	CHN2
2.04142254823592	GO:0141124 Intracellular signaling cassette	Down_GO-Biological-Process	CHN2
1.90370753506128	GO:0023051 Regulation of signaling	Down_GO-Biological-Process	CHN2
1.90117466181079	GO:0010646 Regulation of cell communication	Down_GO-Biological-Process	CHN2
1.88636075899286	GO:0009966 Regulation of signal transduction	Down_GO-Biological-Process	CHN2
1.58346949891068	GO:0048583 Regulation of response to stimulus	Down_GO-Biological-Process	CHN2
12.409230358810 2	Path:hsa05144 Malaria	Down_KEGG	SDC2
5.511047923701 2	GO:0005788 Endoplasmic reticulum lumen	Down_GO-Cellular-Component	SDC2

4.75040849673203	GO:0062023 Collagen-containing extracellular matrix	Down_GO-Cellular-Component	SDC2
4.606456724103 78	GO:0031012 Extracellular matrix	Down_GO-Cellular-Component	SDC2
4.598714780029 66	GO:0030312 External encapsulating structure	Down_GO-Cellular-Component	SDC2
4.586601307189 54	Path:hsa04820 Cytoskeleton in muscle cells	Down_KEGG	SDC2
2.732819270030 11	GO:0022603 Regulation of anatomical structure morphogenesis	Down_GO-Biological-Process	SDC2
2.487220618115 71	GO:0000902 Cell morphogenesis	Down_GO-Biological-Process	SDC2
2.226132852025 05	GO:0009653 Anatomical structure morphogenesis	Down_GO-Biological-Process	SDC2
2.109708799748 96	GO:0050793 Regulation of developmental process	Down_GO-Biological-Process	SDC2
2.005449497301 12	GO:0030182 Neuron differentiation	Down_GO-Biological-Process	SDC2

1.985708426905 48	GO:0048731 System development	Down_GO-Biological-Process	SDC2
1.962514107310 49	GO:0022008 Neurogenesis	Down_GO-Biological-Process	SDC2
1.928866773295 42	GO:0016477 Cell migration	Down_GO-Biological-Process	SDC2
1.814917283845 52	GO:0007399 Nervous system development	Down_GO-Biological-Process	SDC2
1.642577397691 23	GO:0048468 Cell development	Down_GO-Biological-Process	SDC2
1.589429860889 01	GO:0030154 Cell differentiation	Down_GO-Biological-Process	SDC2
1.589097552743 31	GO:0048869 Cellular developmental process	Down_GO-Biological-Process	SDC2
17.53996983408 75	GO:0032967 Positive regulation of collagen biosynthetic process	Down_GO-Biological-Process	VIM
16.890341321717 39	GO:0010714 Positive regulation of collagen metabolic process	Down_GO-Biological-Process	VIM

13.0296 9187675 07	GO:0032965 Regulation of collagen biosynthetic process	Down_GO-Biological-Process	VIM
11.4009 8039215 69	GO:0010712 Regulation of collagen metabolic process	Down_GO-Biological-Process	VIM
6.53819 6640663 43	GO:0002088 Lens development in camera-type eye	Down_GO-Biological-Process	VIM
4.58660 1307189 54	Path:hsa04820 Cytoskeleton in muscle cells	Down_KEGG	VIM
3.63861 0763454 32	GO:0043010 Camera-type eye development	Down_GO-Biological-Process	VIM
3.18166 8946648 43	GO:0001654 Eye development	Down_GO-Biological-Process	VIM
3.15234 4808891 3	GO:0150063 Visual system development	Down_GO-Biological-Process	VIM
3.06066 5877089 09	GO:0048880 Sensory system development	Down_GO-Biological-Process	VIM
2.89218 1733170 18	GO:0060429 Epithelium development	Down_GO-Biological-Process	VIM

2.668127820797 3	GO:0009888 Tissue development	Down_GO-Biological-Process	VIM
2.660228758169 93	GO:0030855 Epithelial cell differentiation	Down_GO-Biological-Process	VIM
2.169678100202 32	GO:0007417 Central nervous system development	Down_GO-Biological-Process	VIM
2.042402117596 88	GO:0030054 Cell junction	Down_GO-Cellular-Component	VIM
2.024330161506 12	GO:0048513 Animal organ development	Down_GO-Biological-Process	VIM
2.005449497301 12	GO:0030182 Neuron differentiation	Down_GO-Biological-Process	VIM
1.985708426905 48	GO:0048731 System development	Down_GO-Biological-Process	VIM
1.962514107310 49	GO:0022008 Neurogenesis	Down_GO-Biological-Process	VIM
1.814917283845 52	GO:0007399 Nervous system development	Down_GO-Biological-Process	VIM

1.64257739769123	GO:0048468 Cell development	Down_GO-Biological-Process	VIM
1.589429860889 01	GO:0030154 Cell differentiation	Down_GO-Biological-Process	VIM
1.589097552743 31	GO:0048869 Cellular developmental process	Down_GO-Biological-Process	VIM
1.528259760232 08	GO:0005576 Extracellular region	Down_GO-Cellular-Component	VIM
4.606456724103 78	GO:0031012 Extracellular matrix	Down_GO-Cellular-Component	ADAMTS14
4.598714780029 66	GO:0030312 External encapsulating structure	Down_GO-Cellular-Component	ADAMTS14
3.387477925246 24	GO:0030198 Extracellular matrix organization	Down_GO-Biological-Process	ADAMTS14
3.378068264342 77	GO:0043062 Extracellular structure organization	Down_GO-Biological-Process	ADAMTS14
3.359404903766 29	GO:0045229 External encapsulating structure organization	Down_GO-Biological-Process	ADAMTS14

1.52825976023208	GO:0005576 Extracellular region	Down_GO-Cellular-Component	ADAMTS14
3.378068264342 77	GO:0042578 Phosphoric ester hydrolase activity	Down_GO-Molecular-Function	NT5DC3
15.725490196078 4	GO:0043236 Laminin binding	Down_GO-Molecular-Function	BCAM
4.750408496732 03	GO:0062023 Collagen-containing extracellular matrix	Down_GO-Cellular-Component	BCAM
4.606456724103 78	GO:0031012 Extracellular matrix	Down_GO-Cellular-Component	BCAM
4.598714780029 66	GO:0030312 External encapsulating structure	Down_GO-Cellular-Component	BCAM
1.946715285965 91	GO:0007155 Cell adhesion	Down_GO-Biological-Process	BCAM
1.52825976023208	GO:0005576 Extracellular region	Down_GO-Cellular-Component	BCAM
4.606456724103 78	GO:0031012 Extracellular matrix	Down_GO-Cellular-Component	ELFN2

4.59871 4780029 66	GO:0030312 External encapsulating structure	Down_GO-Cellular-Component	ELFN2
2.57467 4471058 71	GO:0098590 Plasma membrane region	Down_GO-Cellular-Component	ELFN2
2.12784 2551727 67	GO:0045202 Synapse	Down_GO-Cellular-Component	ELFN2
2.04240 2117596 88	GO:0030054 Cell junction	Down_GO-Cellular-Component	ELFN2
1.94671 5285965 91	GO:0007155 Cell adhesion	Down_GO-Biological-Process	ELFN2
1.52825 9760232 08	GO:0005576 Extracellular region	Down_GO-Cellular-Component	ELFN2
9.90123 4567901 23	GO:0051861 Glycolipid binding	Upp_GO-Molecular-Function	SELL
5.63011 3773904 62	GO:0050900 Leukocyte migration	Upp_GO-Biological-Process	SELL
3.31897 0537756 33	GO:0034097 Response to cytokine	Upp_GO-Biological-Process	SELL

3.27295893141036	GO:1901652 Response to peptide	Upp_GO-Biological-Process	SELL
3.15533848867182	GO:0007159 Leukocyte cell-cell adhesion	Upp_GO-Biological-Process	SELL
2.60243929730335	GO:0016477 Cell migration	Upp_GO-Biological-Process	SELL
2.49963770753811	GO:0098609 Cell-cell adhesion	Upp_GO-Biological-Process	SELL
2.38177163338454	GO:0009986 Cell surface	Upp_GO-Cellular-Component	SELL
2.29190472212047	GO:0048870 Cell motility	Upp_GO-Biological-Process	SELL
2.23825235777723	GO:0007155 Cell adhesion	Upp_GO-Biological-Process	SELL
2.22585893386927	GO:0005509 Calcium ion binding	Upp_GO-Molecular-Function	SELL
2.21604257693931	GO:0098552 Side of membrane	Upp_GO-Cellular-Component	SELL

2.21023 7102999 91	GO:0042221 Response to chemical	Upp_GO-Biological-Process	SELL
2.19510 6530803 93	GO:0005615 Extracellular space	Upp_GO-Cellular-Component	SELL
2.15632 1736776 33	GO:0002376 Immune system process	Upp_GO-Biological-Process	SELL
1.96542 1535617 61	GO:0005576 Extracellular region	Upp_GO-Cellular-Component	SELL
1.38197 9247307 45	GO:0046872 Metal ion binding	Upp_GO-Molecular-Function	SELL
1.35322 8719641 79	GO:0043169 Cation binding	Upp_GO-Molecular-Function	SELL
5.63011 3773904 62	GO:0050900 Leukocyte migration	Upp_GO-Biological-Process	ADD2
3.15533 8488671 82	GO:0007159 Leukocyte cell-cell adhesion	Upp_GO-Biological-Process	ADD2
2.83782 0150189 12	GO:0046982 Protein heterodimerization activity	Upp_GO-Molecular-Function	ADD2

2.6024392973035	GO:0016477 Cell migration	Upp_GO-Biological-Process	ADD2
2.5116533799237	GO:0030097 Hemopoiesis	Upp_GO-Biological-Process	ADD2
2.4996377075381	GO:0098609 Cell-cell adhesion	Upp_GO-Biological-Process	ADD2
2.2919047221204	GO:0048870 Cell motility	Upp_GO-Biological-Process	ADD2
2.2382523577777	GO:0007155 Cell adhesion	Upp_GO-Biological-Process	ADD2
2.1614551115060	GO:0098590 Plasma membrane region	Upp_GO-Cellular-Component	ADD2
2.1563217367763	GO:0002376 Immune system process	Upp_GO-Biological-Process	ADD2
1.8932030932030	GO:0065008 Regulation of biological quality	Upp_GO-Biological-Process	ADD2
1.8452426534758	GO:0046983 Protein dimerization activity	Upp_GO-Molecular-Function	ADD2

1.78608 6944835 62	GO:0048731 System development	Upp_GO-Biological-Process	ADD2
1.72369 2330910 55	GO:0048468 Cell development	Upp_GO-Biological-Process	ADD2
1.70127 8628877 5	GO:0030154 Cell differentiation	Upp_GO-Biological-Process	ADD2
1.70092 2936084 5	GO:0048869 Cellular developmental process	Upp_GO-Biological-Process	ADD2
1.55826 2314412 82	GO:0007399 Nervous system development	Upp_GO-Biological-Process	ADD2
15.9519 8902606 31	GO:0110075 Regulation of ferroptosis	Upp_GO-Biological-Process	SLC7A11
15.1124 1065627 03	GO:0097707 Ferroptosis	Upp_GO-Biological-Process	SLC7A11
9.20307 0591959 48	GO:0089718 Amino acid import across plasma membrane	Upp_GO-Biological-Process	SLC7A11
8.20388 0070546 74	GO:0072349 Modified amino acid transmembrane transporter activity	Upp_GO-Molecular-Function	SLC7A11

6.836566725455 62	GO:0048286 Lung alveolus development	Upp_GO-Biological-Process	SLC7A11
6.276192403696 96	GO:0019748 Secondary metabolic process	Upp_GO-Biological-Process	SLC7A11
6.276192403696 96	GO:0015804 Neutral amino acid transport	Upp_GO-Biological-Process	SLC7A11
5.685857474636 35	GO:0015171 Amino acid transmembrane transporter activity	Upp_GO-Molecular-Function	SLC7A11
5.630113773904 62	GO:0015179 L-amino acid transmembrane transporter activity	Upp_GO-Molecular-Function	SLC7A11
5.173618062506 95	GO:0072348 Sulfur compound transport	Upp_GO-Biological-Process	SLC7A11
5.082049601223 64	GO:0003333 Amino acid transmembrane transport	Upp_GO-Biological-Process	SLC7A11
4.625483806813 84	GO:0009636 Response to toxic substance	Upp_GO-Biological-Process	SLC7A11
4.518589166180 96	GO:0042180 Cellular ketone metabolic process	Upp_GO-Biological-Process	SLC7A11

4.127738400275 09	GO:0046942 Carboxylic acid transport	Upp_GO-Biological-Process	SLC7A11
4.116642329306 61	GO:0015849 Organic acid transport	Upp_GO-Biological-Process	SLC7A11
4.063242487770 79	GO:0030324 Lung development	Upp_GO-Biological-Process	SLC7A11
4.055590430355 02	GO:0018958 Phenol-containing compound metabolic process	Upp_GO-Biological-Process	SLC7A11
3.987997256515 78	GO:0030323 Respiratory tube development	Upp_GO-Biological-Process	SLC7A11
3.847715945985 07	GO:0098739 Import across plasma membrane	Upp_GO-Biological-Process	SLC7A11
3.828477366255 14	GO:1901615 Organic hydroxy compound metabolic process	Upp_GO-Biological-Process	SLC7A11
3.692744070684 05	GO:0014070 Response to organic cyclic compound	Upp_GO-Biological-Process	SLC7A11
3.604215093754 84	GO:0060541 Respiratory system development	Upp_GO-Biological-Process	SLC7A11

3.54488645023624	GO:0046943 Carboxylic acid transmembrane transporter activity	Upp_GO-Molecular-Function	SLC7A11
3.52622915312974	GO:0005342 Organic acid transmembrane transporter activity	Upp_GO-Molecular-Function	SLC7A11
3.49313628307951	GO:0034599 Cellular response to oxidative stress	Upp_GO-Biological-Process	SLC7A11
3.453523397395 1	GO:0006575 Cellular modified amino acid metabolic process	Upp_GO-Biological-Process	SLC7A11
3.41298369859955	GO:0007423 Sensory organ development	Upp_GO-Biological-Process	SLC7A11
3.39960421866919	GO:0042886 Amide transport	Upp_GO-Biological-Process	SLC7A11
3.39262485541792	GO:0070887 Cellular response to chemical stimulus	Upp_GO-Biological-Process	SLC7A11
3.27780596425954	GO:0006979 Response to oxidative stress	Upp_GO-Biological-Process	SLC7A11
3.14453993121572	GO:0015711 Organic anion transport	Upp_GO-Biological-Process	SLC7A11

3.12784 0985502 57	GO:0015291 Secondary active transmembrane transporter activity	Upp_GO-Molecular-Function	SLC7A11
2.81891 3129263 21	GO:0007267 Cell-cell signaling	Upp_GO-Biological-Process	SLC7A11
2.78232 3667336 59	GO:0062197 Cellular response to chemical stress	Upp_GO-Biological-Process	SLC7A11
2.73897 4268386 03	GO:0009611 Response to wounding	Upp_GO-Biological-Process	SLC7A11
2.67458 4986405 79	GO:0045177 Apical part of cell	Upp_GO-Cellular-Component	SLC7A11
2.65175 9214722 18	GO:0035295 Tube development	Upp_GO-Biological-Process	SLC7A11
2.63207 8189300 41	GO:0030855 Epithelial cell differentiation	Upp_GO-Biological-Process	SLC7A11
2.58680 9031253 48	GO:0042060 Wound healing	Upp_GO-Biological-Process	SLC7A11
2.51873 5109378 38	GO:0019725 Cellular homeostasis	Upp_GO-Biological-Process	SLC7A11

2.49963 7707538 11	GO:0098609 Cell-cell adhesion	Upp_GO-Biological-Process	SLC7A11
2.38965 4072235 47	GO:0055082 Intracellular chemical homeostasis	Upp_GO-Biological-Process	SLC7A11
2.38177 1633384 54	GO:0009986 Cell surface	Upp_GO-Cellular-Component	SLC7A11
2.28702 3516281 45	GO:0043067 Regulation of programmed cell death	Upp_GO-Biological-Process	SLC7A11
2.28111 8589625 71	GO:0043069 Negative regulation of programmed cell death	Upp_GO-Biological-Process	SLC7A11
2.26856 7288130 87	GO:0048871 Multicellular organismal-level homeostasis	Upp_GO-Biological-Process	SLC7A11
2.25804 4108712 13	GO:0060429 Epithelium development	Upp_GO-Biological-Process	SLC7A11
2.23825 2357777 23	GO:0007155 Cell adhesion	Upp_GO-Biological-Process	SLC7A11
2.21023 7102999 91	GO:0042221 Response to chemical	Upp_GO-Biological-Process	SLC7A11

2.19816882273023	GO:0002682 Regulation of immune system process	Upp_GO-Biological-Process	SLC7A11
2.18466475248983	GO:0042981 Regulation of apoptotic process	Upp_GO-Biological-Process	SLC7A11
2.16145511150608	GO:0098590 Plasma membrane region	Upp_GO-Cellular-Component	SLC7A11
2.15632173677633	GO:0002376 Immune system process	Upp_GO-Biological-Process	SLC7A11
2.14993529303013	GO:0009628 Response to abiotic stimulus	Upp_GO-Biological-Process	SLC7A11
2.12201978730077	GO:0009888 Tissue development	Upp_GO-Biological-Process	SLC7A11
2.12003743944437	GO:0042127 Regulation of cell population proliferation	Upp_GO-Biological-Process	SLC7A11
2.09971336357686	GO:0048878 Chemical homeostasis	Upp_GO-Biological-Process	SLC7A11
2.09111189781801	GO:0012501 Programmed cell death	Upp_GO-Biological-Process	SLC7A11

2.08731160359208	GO:0008219 Cell death	Upp_GO-Biological-Process	SLC7A11
2.05879217636146	GO:0008283 Cell population proliferation	Upp_GO-Biological-Process	SLC7A11
2.037919302889 12	GO:0001775 Cell activation	Upp_GO-Biological-Process	SLC7A11
2.03162124388539	GO:0006915 Apoptotic process	Upp_GO-Biological-Process	SLC7A11
2.01444437781909	GO:0042592 Homeostatic process	Upp_GO-Biological-Process	SLC7A11
2.00094635866994	GO:0051049 Regulation of transport	Upp_GO-Biological-Process	SLC7A11
1.95632940672685	GO:0048513 Animal organ development	Upp_GO-Biological-Process	SLC7A11
1.95330477870 16	GO:0005215 Transporter activity	Upp_GO-Molecular-Function	SLC7A11
1.94085613874464	GO:0055085 Transmembrane transport	Upp_GO-Biological-Process	SLC7A11

1.91730637332489	GO:0022857 Transmembrane transporter activity	Upp_GO-Molecular-Function	SLC7A11
1.893203093203 09	GO:0065008 Regulation of biological quality	Upp_GO-Biological-Process	SLC7A11
1.853168362103 7	GO:0006950 Response to stress	Upp_GO-Biological-Process	SLC7A11
1.786086944835 62	GO:0048731 System development	Upp_GO-Biological-Process	SLC7A11
1.761029147311 47	GO:0032879 Regulation of localization	Upp_GO-Biological-Process	SLC7A11
1.701278628877 5	GO:0030154 Cell differentiation	Upp_GO-Biological-Process	SLC7A11
1.700922936084 5	GO:0048869 Cellular developmental process	Upp_GO-Biological-Process	SLC7A11
1.672253731406 41	GO:0044281 Small molecule metabolic process	Upp_GO-Biological-Process	SLC7A11
1.576244068866 77	GO:0006810 Transport	Upp_GO-Biological-Process	SLC7A11

1.55826231441282	GO:0007399 Nervous system development	Upp_GO-Biological-Process	SLC7A11
1.55566959326914	GO:0023051 Regulation of signaling	Upp_GO-Biological-Process	SLC7A11
1.52813093384319	GO:0010646 Regulation of cell communication	Upp_GO-Biological-Process	SLC7A11
1.42428473446992	GO:0048583 Regulation of response to stimulus	Upp_GO-Biological-Process	SLC7A11
7.97599451303155	GO:0050931 Pigment cell differentiation	Upp_GO-Biological-Process	ADAMTS20
4.78559670781893	GO:0004222 Metalloendopeptidase activity	Upp_GO-Molecular-Function	ADAMTS20
3.31675019353787	GO:0008237 Metallopeptidase activity	Upp_GO-Molecular-Function	ADAMTS20
2.80915530018721	GO:0045597 Positive regulation of cell differentiation	Upp_GO-Biological-Process	ADAMTS20
2.41668418598002	GO:0045595 Regulation of cell differentiation	Upp_GO-Biological-Process	ADAMTS20

2.3118824675453838	GO:0051094 Positive regulation of developmental process	Upp_GO-Biological-Process	ADAMTS20
2.2870235162814545	GO:0043067 Regulation of programmed cell death	Upp_GO-Biological-Process	ADAMTS20
2.2811185896257171	GO:0043069 Negative regulation of programmed cell death	Upp_GO-Biological-Process	ADAMTS20
2.1951065308039393	GO:0005615 Extracellular space	Upp_GO-Cellular-Component	ADAMTS20
2.1846647524898383	GO:0042981 Regulation of apoptotic process	Upp_GO-Biological-Process	ADAMTS20
2.0986171937185656	GO:0046914 Transition metal ion binding	Upp_GO-Molecular-Function	ADAMTS20
2.0911118978180101	GO:0012501 Programmed cell death	Upp_GO-Biological-Process	ADAMTS20
2.0873116035920808	GO:0008219 Cell death	Upp_GO-Biological-Process	ADAMTS20
2.0316212438853939	GO:0006915 Apoptotic process	Upp_GO-Biological-Process	ADAMTS20

2.010453230591 6	GO:0050793 Regulation of developmental process	Upp_GO-Biological-Process	ADAMTS20
1.971409560378 55	GO:0043066 Negative regulation of apoptotic process	Upp_GO-Biological-Process	ADAMTS20
1.965421535617 61	GO:0005576 Extracellular region	Upp_GO-Cellular-Component	ADAMTS20
1.827317628372 55	GO:0023056 Positive regulation of signaling	Upp_GO-Biological-Process	ADAMTS20
1.781607874679 23	GO:0010647 Positive regulation of cell communication	Upp_GO-Biological-Process	ADAMTS20
1.777586705167 8	GO:0009967 Positive regulation of signal transduction	Upp_GO-Biological-Process	ADAMTS20
1.701278628877 5	GO:0030154 Cell differentiation	Upp_GO-Biological-Process	ADAMTS20
1.700922936084 5	GO:0048869 Cellular developmental process	Upp_GO-Biological-Process	ADAMTS20
1.584051870922 04	GO:0048584 Positive regulation of response to stimulus	Upp_GO-Biological-Process	ADAMTS20

1.55566 9593269 14	GO:0023051 Regulation of signaling	Upp_GO-Biological-Process	ADAMTS20
1.52813 0933843 19	GO:0010646 Regulation of cell communication	Upp_GO-Biological-Process	ADAMTS20
1.44842 5153698 22	GO:0009966 Regulation of signal transduction	Upp_GO-Biological-Process	ADAMTS20
1.42428 4734469 92	GO:0048583 Regulation of response to stimulus	Upp_GO-Biological-Process	ADAMTS20
1.38197 9247307 45	GO:0046872 Metal ion binding	Upp_GO-Molecular-Function	ADAMTS20
1.35322 8719641 79	GO:0043169 Cation binding	Upp_GO-Molecular-Function	ADAMTS20
8.70108 4923307 15	GO:0034121 Regulation of toll-like receptor signaling pathway	Upp_GO-Biological-Process	IRAK3
6.60082 3045267 49	GO:0032496 Response to lipopolysaccharide	Upp_GO-Biological-Process	IRAK3
6.38079 5610425 24	GO:0002224 Toll-like receptor signaling pathway	Upp_GO-Biological-Process	IRAK3

6.23686788988933	GO:0002237 Response to molecule of bacterial origin	Upp_GO-Biological-Process	IRAK3
5.71983670257243	GO:0071222 Cellular response to lipopolysaccharide	Upp_GO-Biological-Process	IRAK3
5.50068587105624	GO:0071219 Cellular response to molecule of bacterial origin	Upp_GO-Biological-Process	IRAK3
4.98499657064472	GO:0071216 Cellular response to biotic stimulus	Upp_GO-Biological-Process	IRAK3
4.51807887943154	GO:0009617 Response to bacterium	Upp_GO-Biological-Process	IRAK3
4.27144168962351	GO:0019221 Cytokine-mediated signaling pathway	Upp_GO-Biological-Process	IRAK3
3.976163436763 5	GO:0033993 Response to lipid	Upp_GO-Biological-Process	IRAK3
3.69274407068405	GO:0014070 Response to organic cyclic compound	Upp_GO-Biological-Process	IRAK3
3.66496360539889	GO:0071396 Cellular response to lipid	Upp_GO-Biological-Process	IRAK3

3.64121488638397	GO:0032635 Interleukin-6 production	Upp_GO-Biological-Process	IRAK3
3.64121488638397	GO:0032675 Regulation of interleukin-6 production	Upp_GO-Biological-Process	IRAK3
3.46782370131807	GO:0071345 Cellular response to cytokine stimulus	Upp_GO-Biological-Process	IRAK3
3.39262485541792	GO:0070887 Cellular response to chemical stimulus	Upp_GO-Biological-Process	IRAK3
3.31897053775633	GO:0034097 Response to cytokine	Upp_GO-Biological-Process	IRAK3
3.27295893141036	GO:1901652 Response to peptide	Upp_GO-Biological-Process	IRAK3
3.13076420137687	GO:0062207 Regulation of pattern recognition receptor signaling pathway	Upp_GO-Biological-Process	IRAK3
3.05666855589233	GO:0002697 Regulation of immune effector process	Upp_GO-Biological-Process	IRAK3
2.92536475869809	GO:1901701 Cellular response to oxygen-containing compound	Upp_GO-Biological-Process	IRAK3

2.91672 9370453 98	GO:1901700 Response to oxygen-containing compound	Upp_GO-Biological-Process	IRAK3
2.83782 0150189 12	GO:0046982 Protein heterodimerization activity	Upp_GO-Molecular-Function	IRAK3
2.76092 1177587 84	GO:0002221 Pattern recognition receptor signaling pathway	Upp_GO-Biological-Process	IRAK3
2.73462 6690182 25	GO:1901698 Response to nitrogen compound	Upp_GO-Biological-Process	IRAK3
2.67895 9989109 83	GO:0051090 Regulation of dna-binding transcription factor activity	Upp_GO-Biological-Process	IRAK3
2.53442 8163019 37	GO:0002683 Negative regulation of immune system process	Upp_GO-Biological-Process	IRAK3
2.53072 2743426 19	GO:0051707 Response to other organism	Upp_GO-Biological-Process	IRAK3
2.52671 4206873 78	GO:0043207 Response to external biotic stimulus	Upp_GO-Biological-Process	IRAK3
2.52133 7108458 32	GO:0009607 Response to biotic stimulus	Upp_GO-Biological-Process	IRAK3

2.51047696147878	GO:0051241 Negative regulation of multicellular organismal process	Upp_GO-Biological-Process	IRAK3
2.43998677743534	GO:0044419 Biological process involved in interspecies interaction between organisms	Upp_GO-Biological-Process	IRAK3
2.42747659092265	GO:0002684 Positive regulation of immune system process	Upp_GO-Biological-Process	IRAK3
2.42747659092265	GO:0002252 Immune effector process	Upp_GO-Biological-Process	IRAK3
2.39173061702686	GO:0006952 Defense response	Upp_GO-Biological-Process	IRAK3
2.38163444246043	GO:0001819 Positive regulation of cytokine production	Upp_GO-Biological-Process	IRAK3
2.35812011689628	GO:0002253 Activation of immune response	Upp_GO-Biological-Process	IRAK3
2.32765865280485	GO:0009605 Response to external stimulus	Upp_GO-Biological-Process	IRAK3
2.31954942470816	GO:0032103 Positive regulation of response to external stimulus	Upp_GO-Biological-Process	IRAK3

2.25381320619416	GO:0031349 Positive regulation of defense response	Upp_GO-Biological-Process	IRAK3
2.248266909713 59	GO:0002757 Immune response-activating signaling pathway	Upp_GO-Biological-Process	IRAK3
2.239445051471 73	GO:0001817 Regulation of cytokine production	Upp_GO-Biological-Process	IRAK3
2.223610591511 83	GO:0001816 Cytokine production	Upp_GO-Biological-Process	IRAK3
2.210237102999 91	GO:0042221 Response to chemical	Upp_GO-Biological-Process	IRAK3
2.198168822730 23	GO:0002682 Regulation of immune system process	Upp_GO-Biological-Process	IRAK3
2.194668553904 22	GO:0098542 Defense response to other organism	Upp_GO-Biological-Process	IRAK3
2.172279110839 4	GO:0140546 Defense response to symbiont	Upp_GO-Biological-Process	IRAK3
2.156321736776 33	GO:0002376 Immune system process	Upp_GO-Biological-Process	IRAK3

2.14223353827226	GO:0045087 Innate immune response	Upp_GO-Biological-Process	IRAK3
2.13008755540902	GO:0043408 Regulation of mapk cascade	Upp_GO-Biological-Process	IRAK3
2.10521143470432	GO:0032101 Regulation of response to external stimulus	Upp_GO-Biological-Process	IRAK3
2.02549845755675	GO:0051239 Regulation of multicellular organismal process	Upp_GO-Biological-Process	IRAK3
2.01662097898367	GO:0006955 Immune response	Upp_GO-Biological-Process	IRAK3
1.97662593933793	GO:0007166 Cell surface receptor signaling pathway	Upp_GO-Biological-Process	IRAK3
1.95046154030466	GO:0010628 Positive regulation of gene expression	Upp_GO-Biological-Process	IRAK3
1.94734352301889	GO:0031347 Regulation of defense response	Upp_GO-Biological-Process	IRAK3
1.94629531179239	GO:0001932 Regulation of protein phosphorylation	Upp_GO-Biological-Process	IRAK3

1.93307 3760796 87	GO:0051240 Positive regulation of multicellular organismal process	Upp_GO-Biological-Process	IRAK3
1.91615 4837965 54	GO:0050778 Positive regulation of immune response	Upp_GO-Biological-Process	IRAK3
1.85316 8362103 7	GO:0006950 Response to stress	Upp_GO-Biological-Process	IRAK3
1.84524 2653475 87	GO:0046983 Protein dimerization activity	Upp_GO-Molecular-Function	IRAK3
1.78662 2770919 07	GO:0031399 Regulation of protein modification process	Upp_GO-Biological-Process	IRAK3
1.78608 6944835 62	GO:0048731 System development	Upp_GO-Biological-Process	IRAK3
1.58857 9820022 88	GO:0031325 Positive regulation of cellular metabolic process	Upp_GO-Biological-Process	IRAK3
1.58405 1870922 04	GO:0048584 Positive regulation of response to stimulus	Upp_GO-Biological-Process	IRAK3
1.57655 1519047 68	GO:0048585 Negative regulation of response to stimulus	Upp_GO-Biological-Process	IRAK3

1.56947 6919754 77	GO:0010604 Positive regulation of macromolecule metabolic process	Upp_GO-Biological-Process	IRAK3
1.56465 0955382 18	GO:0051246 Regulation of protein metabolic process	Upp_GO-Biological-Process	IRAK3
1.55999 8926821 62	GO:0009893 Positive regulation of metabolic process	Upp_GO-Biological-Process	IRAK3
1.55566 9593269 14	GO:0023051 Regulation of signaling	Upp_GO-Biological-Process	IRAK3
1.54738 0545471 93	GO:0009891 Positive regulation of biosynthetic process	Upp_GO-Biological-Process	IRAK3
1.54321 1288284 66	GO:0031328 Positive regulation of cellular biosynthetic process	Upp_GO-Biological-Process	IRAK3
1.52813 0933843 19	GO:0010646 Regulation of cell communication	Upp_GO-Biological-Process	IRAK3
1.50648 3748526 42	GO:0010557 Positive regulation of macromolecule biosynthetic process	Upp_GO-Biological-Process	IRAK3
1.47658 0286275 51	GO:0035556 Intracellular signal transduction	Upp_GO-Biological-Process	IRAK3

1.4484251536982 2	GO:0009966 Regulation of signal transduction	Upp_GO-Biological-Process	IRAK3
1.4242847344699 2	GO:0048583 Regulation of response to stimulus	Upp_GO-Biological-Process	IRAK3
1.3819792473074 5	GO:0046872 Metal ion binding	Upp_GO-Molecular-Function	IRAK3
1.3532287196417 9	GO:0043169 Cation binding	Upp_GO-Molecular-Function	IRAK3
20.149880875027 1	GO:0016264 Gap junction assembly	Upp_GO-Biological-Process	GJB6
10.182120654939	GO:0051602 Response to electrical stimulus	Upp_GO-Biological-Process	GJB6
9.816608631423 45	GO:0003161 Cardiac conduction system development	Upp_GO-Biological-Process	GJB6
6.600823045267 49	GO:0032496 Response to lipopolysaccharide	Upp_GO-Biological-Process	GJB6
6.236867889889 33	GO:0002237 Response to molecule of bacterial origin	Upp_GO-Biological-Process	GJB6

5.14155018195422	GO:0043583 Ear development	Upp_GO-Biological-Process	GJB6
4.919772316449 37	GO:0048839 Inner ear development	Upp_GO-Biological-Process	GJB6
4.518078879431 54	GO:0009617 Response to bacterium	Upp_GO-Biological-Process	GJB6
3.976163436763 5	GO:0033993 Response to lipid	Upp_GO-Biological-Process	GJB6
3.412983698599 55	GO:0007423 Sensory organ development	Upp_GO-Biological-Process	GJB6
3.392624855417 92	GO:0070887 Cellular response to chemical stimulus	Upp_GO-Biological-Process	GJB6
3.112583224597 68	GO:0009743 Response to carbohydrate	Upp_GO-Biological-Process	GJB6
3.109774033961 76	GO:0001894 Tissue homeostasis	Upp_GO-Biological-Process	GJB6
3.098587796429 52	GO:0060249 Anatomical structure homeostasis	Upp_GO-Biological-Process	GJB6

2.92536475869809	GO:1901701 Cellular response to oxygen-containing compound	Upp_GO-Biological-Process	GJB6
2.91672937045398	GO:1901700 Response to oxygen-containing compound	Upp_GO-Biological-Process	GJB6
2.835909160189	GO:0042593 Glucose homeostasis	Upp_GO-Biological-Process	GJB6
2.825444550741 8	GO:0033500 Carbohydrate homeostasis	Upp_GO-Biological-Process	GJB6
2.818913129263 21	GO:0007267 Cell-cell signaling	Upp_GO-Biological-Process	GJB6
2.751472439813 76	GO:0048568 Embryonic organ development	Upp_GO-Biological-Process	GJB6
2.674584986405 79	GO:0045177 Apical part of cell	Upp_GO-Cellular-Component	GJB6
2.530722743426 19	GO:0051707 Response to other organism	Upp_GO-Biological-Process	GJB6
2.526714206873 78	GO:0043207 Response to external biotic stimulus	Upp_GO-Biological-Process	GJB6

2.52133 7108458 32	GO:0009607 Response to biotic stimulus	Upp_GO-Biological-Process	GJB6
2.51873 5109378 38	GO:0019725 Cellular homeostasis	Upp_GO-Biological-Process	GJB6
2.43998 6777435 34	GO:0044419 Biological process involved in interspecies interaction between organisms	Upp_GO-Biological-Process	GJB6
2.38965 4072235 47	GO:0055082 Intracellular chemical homeostasis	Upp_GO-Biological-Process	GJB6
2.36325 7633490 83	GO:0048598 Embryonic morphogenesis	Upp_GO-Biological-Process	GJB6
2.33443 7418448 26	GO:0008285 Negative regulation of cell population proliferation	Upp_GO-Biological-Process	GJB6
2.32765 8652804 85	GO:0009605 Response to external stimulus	Upp_GO-Biological-Process	GJB6
2.26856 7288130 87	GO:0048871 Multicellular organismal-level homeostasis	Upp_GO-Biological-Process	GJB6
2.21023 7102999 91	GO:0042221 Response to chemical	Upp_GO-Biological-Process	GJB6

2.16797166293811	GO:0072359 Circulatory system development	Upp_GO-Biological-Process	GJB6
2.161455111506 08	GO:0098590 Plasma membrane region	Upp_GO-Cellular-Component	GJB6
2.14993529303013	GO:0009628 Response to abiotic stimulus	Upp_GO-Biological-Process	GJB6
2.12201978730077	GO:0009888 Tissue development	Upp_GO-Biological-Process	GJB6
2.12003743944437	GO:0042127 Regulation of cell population proliferation	Upp_GO-Biological-Process	GJB6
2.11518086533433	GO:0009887 Animal organ morphogenesis	Upp_GO-Biological-Process	GJB6
2.09971336357686	GO:0048878 Chemical homeostasis	Upp_GO-Biological-Process	GJB6
2.05879217636146	GO:0008283 Cell population proliferation	Upp_GO-Biological-Process	GJB6
2.01444437781909	GO:0042592 Homeostatic process	Upp_GO-Biological-Process	GJB6

1.99899611855427	GO:0009790 Embryo development	Upp_GO-Biological-Process	GJB6
1.96896935677348	GO:0009653 Anatomical structure morphogenesis	Upp_GO-Biological-Process	GJB6
1.95632940672685	GO:0048513 Animal organ development	Upp_GO-Biological-Process	GJB6
1.953304778701 6	GO:0005215 Transporter activity	Upp_GO-Molecular-Function	GJB6
1.940856138744 64	GO:0055085 Transmembrane transport	Upp_GO-Biological-Process	GJB6
1.917306373324 89	GO:0022857 Transmembrane transporter activity	Upp_GO-Molecular-Function	GJB6
1.786086944835 62	GO:0048731 System development	Upp_GO-Biological-Process	GJB6
1.576244068866 77	GO:0006810 Transport	Upp_GO-Biological-Process	GJB6
15.95198902606 31	GO:0110075 Regulation of ferroptosis	Upp_GO-Biological-Process	NQO1

15.112410656270303	GO:0097707 Ferroptosis	Upp_GO-Biological-Process	NQO1
10.182120654933939	GO:0051602 Response to electrical stimulus	Upp_GO-Biological-Process	NQO1
8.701084923307015	GO:0006775 Fat-soluble vitamin metabolic process	Upp_GO-Biological-Process	NQO1
8.233284658613021	GO:0046209 Nitric oxide metabolic process	Upp_GO-Biological-Process	NQO1
8.145696523947011	GO:2001057 Reactive nitrogen species metabolic process	Upp_GO-Biological-Process	NQO1
7.975994513031055	GO:0006809 Nitric oxide biosynthetic process	Upp_GO-Biological-Process	NQO1
7.052458306259048	GO:0016209 Antioxidant activity	Upp_GO-Molecular-Function	NQO1
6.600823045267049	GO:0032496 Response to lipopolysaccharide	Upp_GO-Biological-Process	NQO1
6.261528402753074	GO:0098869 Cellular oxidant detoxification	Upp_GO-Biological-Process	NQO1

6.23686 7889889 33	GO:0002237 Response to molecule of bacterial origin	Upp_GO-Biological-Process	NQO1
6.02382 8023828 02	GO:0097237 Cellular response to toxic substance	Upp_GO-Biological-Process	NQO1
5.94819 9297854 04	GO:0007584 Response to nutrient	Upp_GO-Biological-Process	NQO1
5.80072 3282204 76	GO:0042542 Response to hydrogen peroxide	Upp_GO-Biological-Process	NQO1
5.80072 3282204 76	GO:0002931 Response to ischemia	Upp_GO-Biological-Process	NQO1
5.75710 8821436 31	GO:1990748 Cellular detoxification	Upp_GO-Biological-Process	NQO1
5.24448 9542815 27	GO:0006801 Superoxide metabolic process	Upp_GO-Biological-Process	NQO1
5.19367 0845694 96	GO:0006766 Vitamin metabolic process	Upp_GO-Biological-Process	NQO1
4.92936 9999470 14	GO:1901654 Response to ketone	Upp_GO-Biological-Process	NQO1

4.785596707818 93	GO:0098754 Detoxification	Upp_GO-Biological-Process	NQO1
4.687931468883 85	GO:0072593 Reactive oxygen species metabolic process	Upp_GO-Biological-Process	NQO1
4.625483806813 84	GO:0009636 Response to toxic substance	Upp_GO-Biological-Process	NQO1
4.518589166180 96	GO:0042180 Cellular ketone metabolic process	Upp_GO-Biological-Process	NQO1
4.518078879431 54	GO:0009617 Response to bacterium	Upp_GO-Biological-Process	NQO1
4.451717867738 54	GO:0006805 Xenobiotic metabolic process	Upp_GO-Biological-Process	NQO1
4.307037037037 04	GO:0071466 Cellular response to xenobiotic stimulus	Upp_GO-Biological-Process	NQO1
3.976163436763 5	GO:0033993 Response to lipid	Upp_GO-Biological-Process	NQO1
3.828477366255 14	GO:1901615 Organic hydroxy compound metabolic process	Upp_GO-Biological-Process	NQO1

3.70715237929635	GO:0097305 Response to alcohol	Upp_GO-Biological-Process	NQO1
3.69274407068405	GO:0014070 Response to organic cyclic compound	Upp_GO-Biological-Process	NQO1
3.60496927142669	GO:0031667 Response to nutrient levels	Upp_GO-Biological-Process	NQO1
3.49313628307951	GO:0034599 Cellular response to oxidative stress	Upp_GO-Biological-Process	NQO1
3.39262485541792	GO:0070887 Cellular response to chemical stimulus	Upp_GO-Biological-Process	NQO1
3.38055396578821	GO:0009410 Response to xenobiotic stimulus	Upp_GO-Biological-Process	NQO1
3.37310781167854	Path:hsa05208 Chemical carcinogenesis-reactive oxygen species	Upp_KEGG	NQO1
3.27780596425954	GO:0006979 Response to oxidative stress	Upp_GO-Biological-Process	NQO1
3.11258322459768	GO:0043068 Positive regulation of programmed cell death	Upp_GO-Biological-Process	NQO1

3.11258322459768	GO:0009743 Response to carbohydrate	Upp_GO-Biological-Process	NQO1
3.08427230649453	GO:0009725 Response to hormone	Upp_GO-Biological-Process	NQO1
3.07580884812559	Path:hsa05200 Pathways in cancer	Upp_KEGG	NQO1
2.92536475869809	GO:1901701 Cellular response to oxygen-containing compound	Upp_GO-Biological-Process	NQO1
2.91672937045398	GO:1901700 Response to oxygen-containing compound	Upp_GO-Biological-Process	NQO1
2.89062888391747	GO:0043065 Positive regulation of apoptotic process	Upp_GO-Biological-Process	NQO1
2.81891312926321	GO:0007267 Cell-cell signaling	Upp_GO-Biological-Process	NQO1
2.79111351124312	GO:0016491 Oxidoreductase activity	Upp_GO-Molecular-Function	NQO1
2.78232366733659	GO:0062197 Cellular response to chemical stress	Upp_GO-Biological-Process	NQO1

2.7346266901822 5	GO:1901698 Response to nitrogen compound	Upp_GO-Biological-Process	NQO1
2.6439760816679 2	GO:0010038 Response to metal ion	Upp_GO-Biological-Process	NQO1
2.5669867398262 5	GO:0009719 Response to endogenous stimulus	Upp_GO-Biological-Process	NQO1
2.5307227434261 9	GO:0051707 Response to other organism	Upp_GO-Biological-Process	NQO1
2.5267142068737 8	GO:0043207 Response to external biotic stimulus	Upp_GO-Biological-Process	NQO1
2.5213371084583 2	GO:0009607 Response to biotic stimulus	Upp_GO-Biological-Process	NQO1
2.5187351093783 8	GO:0019725 Cellular homeostasis	Upp_GO-Biological-Process	NQO1
2.4399867774353 4	GO:0044419 Biological process involved in interspecies interaction between organisms	Upp_GO-Biological-Process	NQO1
2.3917306170268 6	GO:0006952 Defense response	Upp_GO-Biological-Process	NQO1

2.32765865280485	GO:0009605 Response to external stimulus	Upp_GO-Biological-Process	NQO1
2.28702351628145	GO:0043067 Regulation of programmed cell death	Upp_GO-Biological-Process	NQO1
2.28111858962571	GO:0043069 Negative regulation of programmed cell death	Upp_GO-Biological-Process	NQO1
2.21023710299991	GO:0042221 Response to chemical	Upp_GO-Biological-Process	NQO1
2.19466855390422	GO:0098542 Defense response to other organism	Upp_GO-Biological-Process	NQO1
2.18466475248983	GO:0042981 Regulation of apoptotic process	Upp_GO-Biological-Process	NQO1
2.17227911083394	GO:0140546 Defense response to symbiont	Upp_GO-Biological-Process	NQO1
2.15632173677633	GO:0002376 Immune system process	Upp_GO-Biological-Process	NQO1
2.14993529303013	GO:0009628 Response to abiotic stimulus	Upp_GO-Biological-Process	NQO1

2.14223353827226	GO:0045087 Innate immune response	Upp_GO-Biological-Process	NQO1
2.091111897818 01	GO:0012501 Programmed cell death	Upp_GO-Biological-Process	NQO1
2.08731 1603592 08	GO:0008219 Cell death	Upp_GO-Biological-Process	NQO1
2.03162 1243885 39	GO:0006915 Apoptotic process	Upp_GO-Biological-Process	NQO1
2.01662 0978983 67	GO:0006955 Immune response	Upp_GO-Biological-Process	NQO1
2.01444 4377819 09	GO:0042592 Homeostatic process	Upp_GO-Biological-Process	NQO1
1.97140 9560378 55	GO:0043066 Negative regulation of apoptotic process	Upp_GO-Biological-Process	NQO1
1.85316 8362103 7	GO:0006950 Response to stress	Upp_GO-Biological-Process	NQO1
1.78383 4248415 8	Path:hsa01100 Metabolic pathways	Upp_KEGG	NQO1

1.67225373140641	GO:0044281 Small molecule metabolic process	Upp_GO-Biological-Process	NQO1
1.564650955382 18	GO:0051246 Regulation of protein metabolic process	Upp_GO-Biological-Process	NQO1
3.661112235489 89	Path:hsa04621 NOD-like receptor signaling pathway	Upp_KEGG	TRPV2
2.824286581663 63	GO:0060284 Regulation of cell development	Upp_GO-Biological-Process	TRPV2
2.809155300187 21	GO:0045597 Positive regulation of cell differentiation	Upp_GO-Biological-Process	TRPV2
2.658664837677 18	GO:0010720 Positive regulation of cell development	Upp_GO-Biological-Process	TRPV2
2.438122424623 62	GO:2000026 Regulation of multicellular organismal development	Upp_GO-Biological-Process	TRPV2
2.416684185980 2	GO:0045595 Regulation of cell differentiation	Upp_GO-Biological-Process	TRPV2
2.381771633384 54	GO:0009986 Cell surface	Upp_GO-Cellular-Component	TRPV2

2.37793625233239	GO:0046873 Metal ion transmembrane transporter activity	Upp_GO-Molecular-Function	TRPV2
2.31188246754538	GO:0051094 Positive regulation of developmental process	Upp_GO-Biological-Process	TRPV2
2.26856728813087	GO:0048871 Multicellular organismal-level homeostasis	Upp_GO-Biological-Process	TRPV2
2.21604257693931	GO:0051050 Positive regulation of transport	Upp_GO-Biological-Process	TRPV2
2.14993529303013	GO:0009628 Response to abiotic stimulus	Upp_GO-Biological-Process	TRPV2
2.13370553851799	GO:0030001 Metal ion transport	Upp_GO-Biological-Process	TRPV2
2.02549845755675	GO:0051239 Regulation of multicellular organismal process	Upp_GO-Biological-Process	TRPV2
2.01444437781909	GO:0042592 Homeostatic process	Upp_GO-Biological-Process	TRPV2
2.01045323059116	GO:0050793 Regulation of developmental process	Upp_GO-Biological-Process	TRPV2

2.00094635866994	GO:0051049 Regulation of transport	Upp_GO-Biological-Process	TRPV2
1.968969356773348	GO:0009653 Anatomical structure morphogenesis	Upp_GO-Biological-Process	TRPV2
1.953304778701 6	GO:0005215 Transporter activity	Upp_GO-Molecular-Function	TRPV2
1.940856138744 64	GO:0055085 Transmembrane transport	Upp_GO-Biological-Process	TRPV2
1.933073760796 87	GO:0051240 Positive regulation of multicellular organismal process	Upp_GO-Biological-Process	TRPV2
1.917306373324 89	GO:0022857 Transmembrane transporter activity	Upp_GO-Molecular-Function	TRPV2
1.893203093203 09	GO:0065008 Regulation of biological quality	Upp_GO-Biological-Process	TRPV2
1.855148759671 37	GO:0006811 Monoatomic ion transport	Upp_GO-Biological-Process	TRPV2
1.819933060881 88	GO:0006812 Monoatomic cation transport	Upp_GO-Biological-Process	TRPV2

1.78608694483562	GO:0048731 System development	Upp_GO-Biological-Process	TRPV2
1.761029147311 47	GO:0032879 Regulation of localization	Upp_GO-Biological-Process	TRPV2
1.750514126582 5	GO:0022008 Neurogenesis	Upp_GO-Biological-Process	TRPV2
1.723692330910 55	GO:0048468 Cell development	Upp_GO-Biological-Process	TRPV2
1.701278628877 5	GO:0030154 Cell differentiation	Upp_GO-Biological-Process	TRPV2
1.700922936084 5	GO:0048869 Cellular developmental process	Upp_GO-Biological-Process	TRPV2
1.576244068866 77	GO:0006810 Transport	Upp_GO-Biological-Process	TRPV2
1.559998926821 62	GO:0009893 Positive regulation of metabolic process	Upp_GO-Biological-Process	TRPV2
1.558262314412 82	GO:0007399 Nervous system development	Upp_GO-Biological-Process	TRPV2

19.1423868312757	GO:0032310 Prostaglandin secretion	Upp_GO-Biological-Process	NOS2
15.437408734898	GO:0015732 Prostaglandin transport	Upp_GO-Biological-Process	NOS2
10.938506760729	GO:0002227 Innate immune response in mucosa	Upp_GO-Biological-Process	NOS2
9.383522956507 71	GO:0032309 Icosanoid secretion	Upp_GO-Biological-Process	NOS2
8.701084923307 15	GO:0140353 Lipid export from cell	Upp_GO-Biological-Process	NOS2
8.233284658613 21	GO:0046209 Nitric oxide metabolic process	Upp_GO-Biological-Process	NOS2
8.203880070546 74	GO:0018198 Peptidyl-cysteine modification	Upp_GO-Biological-Process	NOS2
8.203880070546 74	GO:0071715 Icosanoid transport	Upp_GO-Biological-Process	NOS2
8.145696523947 11	GO:2001057 Reactive nitrogen species metabolic process	Upp_GO-Biological-Process	NOS2

7.97599 4513031 55	GO:0002385 Mucosal immune response	Upp_GO-Biological-Process	NOS2
7.97599 4513031 55	GO:0006809 Nitric oxide biosynthetic process	Upp_GO-Biological-Process	NOS2
7.36245 6473567 59	GO:0002251 Organ or tissue specific immune response	Upp_GO-Biological-Process	NOS2
6.78273 5491396 91	GO:0015908 Fatty acid transport	Upp_GO-Biological-Process	NOS2
6.60082 3045267 49	GO:0032496 Response to lipopolysaccharide	Upp_GO-Biological-Process	NOS2
6.38079 5610425 24	GO:0004497 Monooxygenase activity	Upp_GO-Molecular-Function	NOS2
6.23686 7889889 33	GO:0002237 Response to molecule of bacterial origin	Upp_GO-Biological-Process	NOS2
5.71983 6702572 43	GO:0071222 Cellular response to lipopolysaccharide	Upp_GO-Biological-Process	NOS2
5.63011 3773904 62	GO:0046906 Tetrapyrrole binding	Upp_GO-Molecular-Function	NOS2

5.54121724063245	GO:0015718 Monocarboxylic acid transport	Upp_GO-Biological-Process	NOS2
5.500685871056 24	GO:0071219 Cellular response to molecule of bacterial origin	Upp_GO-Biological-Process	NOS2
5.383796296296 3	GO:0020037 Heme binding	Upp_GO-Molecular-Function	NOS2
5.244489542815 27	GO:0006801 Superoxide metabolic process	Upp_GO-Biological-Process	NOS2
4.984996570644 72	GO:0071216 Cellular response to biotic stimulus	Upp_GO-Biological-Process	NOS2
4.691761478253 85	Path:hsa05146 Amoebiasis	Upp_KEGG	NOS2
4.687931468883 85	GO:0072593 Reactive oxygen species metabolic process	Upp_GO-Biological-Process	NOS2
4.518078879431 54	GO:0009617 Response to bacterium	Upp_GO-Biological-Process	NOS2
4.307037037037 04	GO:0071466 Cellular response to xenobiotic stimulus	Upp_GO-Biological-Process	NOS2

4.27144168962351	GO:0010817 Regulation of hormone levels	Upp_GO-Biological-Process	NOS2
4.127738400275 09	GO:0046942 Carboxylic acid transport	Upp_GO-Biological-Process	NOS2
4.116642329306 61	GO:0015849 Organic acid transport	Upp_GO-Biological-Process	NOS2
4.029976175005 42	GO:0008217 Regulation of blood pressure	Upp_GO-Biological-Process	NOS2
3.987997256515 78	GO:0016705 Oxidoreductase activity acting on paired donors with incorporation or reduction of molecular oxygen	Upp_GO-Molecular-Function	NOS2
3.987997256515 78	GO:0042742 Defense response to bacterium	Upp_GO-Biological-Process	NOS2
3.976163436763 5	GO:0033993 Response to lipid	Upp_GO-Biological-Process	NOS2
3.664963605398 89	GO:0071396 Cellular response to lipid	Upp_GO-Biological-Process	NOS2
3.641214886383 97	GO:0032635 Interleukin-6 production	Upp_GO-Biological-Process	NOS2

3.64121488638397	GO:0032675 Regulation of interleukin-6 production	Upp_GO-Biological-Process	NOS2
3.467823701318 07	GO:0071345 Cellular response to cytokine stimulus	Upp_GO-Biological-Process	NOS2
3.399604218669 19	GO:0042886 Amide transport	Upp_GO-Biological-Process	NOS2
3.392624855417 92	GO:0070887 Cellular response to chemical stimulus	Upp_GO-Biological-Process	NOS2
3.380553965788 21	GO:0009410 Response to xenobiotic stimulus	Upp_GO-Biological-Process	NOS2
3.330814494694 85	GO:0006954 Inflammatory response	Upp_GO-Biological-Process	NOS2
3.318970537756 33	GO:0034097 Response to cytokine	Upp_GO-Biological-Process	NOS2
3.272958931410 36	GO:1901652 Response to peptide	Upp_GO-Biological-Process	NOS2
3.144539931215 72	GO:0015711 Organic anion transport	Upp_GO-Biological-Process	NOS2

3.11258322459768	GO:0043068 Positive regulation of programmed cell death	Upp_GO-Biological-Process	NOS2
3.08427230649453	GO:0009725 Response to hormone	Upp_GO-Biological-Process	NOS2
3.07580884812559	Path:hsa05200 Pathways in cancer	Upp_KEGG	NOS2
3.07580884812559	GO:0046903 Secretion	Upp_GO-Biological-Process	NOS2
3.05666855589233	GO:0002697 Regulation of immune effector process	Upp_GO-Biological-Process	NOS2
3.04700913980981	GO:0023061 Signal release	Upp_GO-Biological-Process	NOS2
3.042864958728	GO:0046879 Hormone secretion	Upp_GO-Biological-Process	NOS2
2.97242031541548	GO:0036293 Response to decreased oxygen levels	Upp_GO-Biological-Process	NOS2
2.94910721490242	GO:0009914 Hormone transport	Upp_GO-Biological-Process	NOS2

2.92536475869809	GO:1901701 Cellular response to oxygen-containing compound	Upp_GO-Biological-Process	NOS2
2.91672937045398	GO:1901700 Response to oxygen-containing compound	Upp_GO-Biological-Process	NOS2
2.8940973611	GO:0006869 Lipid transport	Upp_GO-Biological-Process	NOS2
2.830473408786 66	GO:0032940 Secretion by cell	Upp_GO-Biological-Process	NOS2
2.818913129263 21	GO:0007267 Cell-cell signaling	Upp_GO-Biological-Process	NOS2
2.796777296777 3	GO:0001666 Response to hypoxia	Upp_GO-Biological-Process	NOS2
2.791113511243 12	GO:0016491 Oxidoreductase activity	Upp_GO-Molecular-Function	NOS2
2.772144434407 31	GO:0051046 Regulation of secretion	Upp_GO-Biological-Process	NOS2
2.745084153624 63	GO:0010876 Lipid localization	Upp_GO-Biological-Process	NOS2

2.74246 2296744 37	GO:0070482 Response to oxygen levels	Upp_GO-Biological-Process	NOS2
2.70427 2609867 41	GO:0140352 Export from cell	Upp_GO-Biological-Process	NOS2
2.65866 4837677 18	GO:0002443 Leukocyte mediated immunity	Upp_GO-Biological-Process	NOS2
2.56698 6739826 25	GO:0009719 Response to endogenous stimulus	Upp_GO-Biological-Process	NOS2
2.53072 2743426 19	GO:0051707 Response to other organism	Upp_GO-Biological-Process	NOS2
2.52671 4206873 78	GO:0043207 Response to external biotic stimulus	Upp_GO-Biological-Process	NOS2
2.52133 7108458 32	GO:0009607 Response to biotic stimulus	Upp_GO-Biological-Process	NOS2
2.51873 5109378 38	GO:0019725 Cellular homeostasis	Upp_GO-Biological-Process	NOS2
2.43998 6777435 34	GO:0044419 Biological process involved in interspecies interaction between organisms	Upp_GO-Biological-Process	NOS2

2.42747 6590922 65	GO:0002684 Positive regulation of immune system process	Upp_GO-Biological-Process	NOS2
2.42747 6590922 65	GO:0002252 Immune effector process	Upp_GO-Biological-Process	NOS2
2.39279 8353909 46	GO:1903530 Regulation of secretion by cell	Upp_GO-Biological-Process	NOS2
2.39173 0617026 86	GO:0006952 Defense response	Upp_GO-Biological-Process	NOS2
2.38163 4442460 43	GO:0001819 Positive regulation of cytokine production	Upp_GO-Biological-Process	NOS2
2.32765 8652804 85	GO:0009605 Response to external stimulus	Upp_GO-Biological-Process	NOS2
2.28702 3516281 45	GO:0043067 Regulation of programmed cell death	Upp_GO-Biological-Process	NOS2
2.23944 5051471 73	GO:0001817 Regulation of cytokine production	Upp_GO-Biological-Process	NOS2
2.22361 0591511 83	GO:0001816 Cytokine production	Upp_GO-Biological-Process	NOS2

2.21023710299991	GO:0042221 Response to chemical	Upp_GO-Biological-Process	NOS2
2.198168822730 23	GO:0002682 Regulation of immune system process	Upp_GO-Biological-Process	NOS2
2.194668553904 22	GO:0098542 Defense response to other organism	Upp_GO-Biological-Process	NOS2
2.172279110839 4	GO:0140546 Defense response to symbiont	Upp_GO-Biological-Process	NOS2
2.156321736776 33	GO:0002376 Immune system process	Upp_GO-Biological-Process	NOS2
2.149935293030 13	GO:0009628 Response to abiotic stimulus	Upp_GO-Biological-Process	NOS2
2.143947325102 88	GO:0003013 Circulatory system process	Upp_GO-Biological-Process	NOS2
2.142233538272 26	GO:0045087 Innate immune response	Upp_GO-Biological-Process	NOS2
2.120037439444 37	GO:0042127 Regulation of cell population proliferation	Upp_GO-Biological-Process	NOS2

2.0911118978181	GO:0012501 Programmed cell death	Upp_GO-Biological-Process	NOS2
2.0873116035920	GO:0008219 Cell death	Upp_GO-Biological-Process	NOS2
2.0587921763614	GO:0008283 Cell population proliferation	Upp_GO-Biological-Process	NOS2
2.0254984575567	GO:0051239 Regulation of multicellular organismal process	Upp_GO-Biological-Process	NOS2
2.0166209789836	GO:0006955 Immune response	Upp_GO-Biological-Process	NOS2
2.0144443778190	GO:0042592 Homeostatic process	Upp_GO-Biological-Process	NOS2
2.0009463586694	GO:0051049 Regulation of transport	Upp_GO-Biological-Process	NOS2
1.9504615403046	GO:0010628 Positive regulation of gene expression	Upp_GO-Biological-Process	NOS2
1.9330737607968	GO:0051240 Positive regulation of multicellular organismal process	Upp_GO-Biological-Process	NOS2

1.8932030932030 9	GO:0065008 Regulation of biological quality	Upp_GO-Biological-Process	NOS2
1.8531683621037	GO:0006950 Response to stress	Upp_GO-Biological-Process	NOS2
1.8452426534758 7	GO:0046983 Protein dimerization activity	Upp_GO-Molecular-Function	NOS2
1.7838342484158	Path:hsa01100 Metabolic pathways	Upp_KEGG	NOS2
1.7610291473114 7	GO:0032879 Regulation of localization	Upp_GO-Biological-Process	NOS2
1.6722537314064 1	GO:0044281 Small molecule metabolic process	Upp_GO-Biological-Process	NOS2
1.5885798200228 8	GO:0031325 Positive regulation of cellular metabolic process	Upp_GO-Biological-Process	NOS2
1.5762440688667 7	GO:0006810 Transport	Upp_GO-Biological-Process	NOS2
1.5694769197547 7	GO:0010604 Positive regulation of macromolecule metabolic process	Upp_GO-Biological-Process	NOS2

1.56465095538218	GO:0051246 Regulation of protein metabolic process	Upp_GO-Biological-Process	NOS2
1.559998926821 62	GO:0009893 Positive regulation of metabolic process	Upp_GO-Biological-Process	NOS2
1.555669593269 14	GO:0023051 Regulation of signaling	Upp_GO-Biological-Process	NOS2
1.547380545471 93	GO:0009891 Positive regulation of biosynthetic process	Upp_GO-Biological-Process	NOS2
1.543211288284 66	GO:0031328 Positive regulation of cellular biosynthetic process	Upp_GO-Biological-Process	NOS2
1.528130933843 19	GO:0010646 Regulation of cell communication	Upp_GO-Biological-Process	NOS2
1.506483748526 42	GO:0010557 Positive regulation of macromolecule biosynthetic process	Upp_GO-Biological-Process	NOS2
1.476580286275 51	GO:0035556 Intracellular signal transduction	Upp_GO-Biological-Process	NOS2
1.381979247307 45	GO:0046872 Metal ion binding	Upp_GO-Molecular-Function	NOS2

1.353228719641 79	GO:0043169 Cation binding	Upp_GO-Molecular-Function	NOS2
3.918032392366 38	GO:0007204 Positive regulation of cytosolic calcium ion concentration	Upp_GO-Biological-Process	GPR32
3.330814494694 85	GO:0006954 Inflammatory response	Upp_GO-Biological-Process	GPR32
2.559142624502 1	GO:0002429 Immune response-activating cell surface receptor signaling pathway	Upp_GO-Biological-Process	GPR32
2.427476590922 65	GO:0002684 Positive regulation of immune system process	Upp_GO-Biological-Process	GPR32
2.391730617026 86	GO:0006952 Defense response	Upp_GO-Biological-Process	GPR32
2.358120116896 28	GO:0002253 Activation of immune response	Upp_GO-Biological-Process	GPR32
2.248266909713 59	GO:0002757 Immune response-activating signaling pathway	Upp_GO-Biological-Process	GPR32
2.198168822730 23	GO:0002682 Regulation of immune system process	Upp_GO-Biological-Process	GPR32

2.15632 1736776 33	GO:0002376 Immune system process	Upp_GO-Biological-Process	GPR32
2.01662 0978983 67	GO:0006955 Immune response	Upp_GO-Biological-Process	GPR32
1.97662 5939337 93	GO:0007166 Cell surface receptor signaling pathway	Upp_GO-Biological-Process	GPR32
1.91615 4837965 54	GO:0050778 Positive regulation of immune response	Upp_GO-Biological-Process	GPR32
1.89320 3093203 09	GO:0065008 Regulation of biological quality	Upp_GO-Biological-Process	GPR32
1.85316 8362103 7	GO:0006950 Response to stress	Upp_GO-Biological-Process	GPR32
1.69508 8017949 78	GO:0007186 G protein-coupled receptor signaling pathway	Upp_GO-Biological-Process	GPR32
1.58405 1870922 04	GO:0048584 Positive regulation of response to stimulus	Upp_GO-Biological-Process	GPR32
1.42428 4734469 92	GO:0048583 Regulation of response to stimulus	Upp_GO-Biological-Process	GPR32

5.14580291163326	GO:0009791 Post-embryonic development	Upp_GO-Biological-Process	SCUBE1
3.681228236783 79	GO:0003158 Endothelium development	Upp_GO-Biological-Process	SCUBE1
3.330814494694 85	GO:0006954 Inflammatory response	Upp_GO-Biological-Process	SCUBE1
2.738974268386 03	GO:0009611 Response to wounding	Upp_GO-Biological-Process	SCUBE1
2.632078189300 41	GO:0030855 Epithelial cell differentiation	Upp_GO-Biological-Process	SCUBE1
2.586809031253 48	GO:0042060 Wound healing	Upp_GO-Biological-Process	SCUBE1
2.391730617026 86	GO:0006952 Defense response	Upp_GO-Biological-Process	SCUBE1
2.381771633384 54	GO:0009986 Cell surface	Upp_GO-Cellular-Component	SCUBE1
2.258044108712 13	GO:0060429 Epithelium development	Upp_GO-Biological-Process	SCUBE1

2.225858933869 27	GO:0005509 Calcium ion binding	Upp_GO-Molecular-Function	SCUBE1
2.216042576939 31	GO:0098552 Side of membrane	Upp_GO-Cellular-Component	SCUBE1
2.195106530803 93	GO:0005615 Extracellular space	Upp_GO-Cellular-Component	SCUBE1
2.167971662938 11	GO:0072359 Circulatory system development	Upp_GO-Biological-Process	SCUBE1
2.122019787300 77	GO:0009888 Tissue development	Upp_GO-Biological-Process	SCUBE1
1.976625939337 93	GO:0007166 Cell surface receptor signaling pathway	Upp_GO-Biological-Process	SCUBE1
1.965421535617 61	GO:0005576 Extracellular region	Upp_GO-Cellular-Component	SCUBE1
1.956329406726 85	GO:0048513 Animal organ development	Upp_GO-Biological-Process	SCUBE1
1.893203093203 09	GO:0065008 Regulation of biological quality	Upp_GO-Biological-Process	SCUBE1

1.853168362103 7	GO:0006950 Response to stress	Upp_GO-Biological-Process	SCUBE1
1.827317628372 55	GO:0023056 Positive regulation of signaling	Upp_GO-Biological-Process	SCUBE1
1.786086944835 62	GO:0048731 System development	Upp_GO-Biological-Process	SCUBE1
1.781607874679 23	GO:0010647 Positive regulation of cell communication	Upp_GO-Biological-Process	SCUBE1
1.777586705167 8	GO:0009967 Positive regulation of signal transduction	Upp_GO-Biological-Process	SCUBE1
1.701278628877 5	GO:0030154 Cell differentiation	Upp_GO-Biological-Process	SCUBE1
1.700922936084 5	GO:0048869 Cellular developmental process	Upp_GO-Biological-Process	SCUBE1
1.584051870922 04	GO:0048584 Positive regulation of response to stimulus	Upp_GO-Biological-Process	SCUBE1
1.555669593269 14	GO:0023051 Regulation of signaling	Upp_GO-Biological-Process	SCUBE1

1.52813093384319	GO:0010646 Regulation of cell communication	Upp_GO-Biological-Process	SCUBE1
1.448425153698 22	GO:0009966 Regulation of signal transduction	Upp_GO-Biological-Process	SCUBE1
1.424284734469 92	GO:0048583 Regulation of response to stimulus	Upp_GO-Biological-Process	SCUBE1
1.381979247307 45	GO:0046872 Metal ion binding	Upp_GO-Molecular-Function	SCUBE1
1.353228719641 79	GO:0043169 Cation binding	Upp_GO-Molecular-Function	SCUBE1